EFFECTS OF LONG-TERM FOREST FIRE RETARDANTS ON FIRE INTENSITY, HEAT OF COMBUSTION OF THE FUEL AND FLAME EMISSIVITY

by

Alba Àgueda Costafreda

A dissertation submitted in partial fulfillment
of the requirements for the degree
of
DOCTOR OF PHILOSOPHY
in
Chemical Engineering

Thesis supervisors:
Dra. Elsa Pastor Ferrer and Dra. Eulàlia Planas Cuchi

Barcelona, September 2009
Centre d'Estudis del Risc Tecnològic
Department of Chemical Engineering
Universitat Politècnica de Catalunya

A la meva família

Agraïments

Fer una Tesi Doctoral (i recerca en general) no és tan senzill com agafar un mapa, fixar un punt de partida i una destinació, i seguir el camí que hi apareix fins arribar-hi. Sovint el camí que es veu al mapa resulta ser un corriol i a vegades un se sent perdut i no sap cap on tirar. És aleshores quan un, mirant de nou el mapa i les referències que li dóna el paisatge, es pot tornar a situar i seguir endavant.

Arribar fins aquí, poder presentar la memòria de Tesi Doctoral, és quelcom que m'ha costat. Per fer una Tesi es requereix una capacitat de resistència mental important però feliçment també representa una experiència vital molt enriquidora a nivell intel·lectual i social. Durant aquests anys he tingut l'oportunitat de trobar pel corriol molta gent. A tots ells els vull agrair la seva participació, directa o indirecta, en l'elaboració d'aquesta Tesi.

Primerament, voldria expressar la meva gratitud cap a en Joaquim Casal, director del Centre d'Estudis del Risc Tecnològic (CERTEC), per donar-me l'oportunitat de dur a terme aquesta Tesi en aquest grup del Departament d'Enginyeria Química de la UPC.

Pels bons moments que hem compartit junts, també m'agradaria donar les gràcies als professors, doctorands i estudiants del CERTEC amb qui he coincidit al llarg d'aquesta etapa: en Joaquim (novament), en Josep, en Juan Antonio, en

Miguel, l'Andrea, en Fabio, en Luís, l'Anna, en Pau, la Rosa Mari, la Míriam, la Laia, la Mercedes, en Jordi, la Isabel, l'Adriana, l'Héctor, l'Ariadna, l'Eduard, la Carol, en Marcos, en Miki i, finalment, la Yolanda i la Rut. Gràcies Yolanda per ser una companya de 'grup forestals' i d'estada extraordinària! I gràcies Rut per l'energia transmesa durant la recta final!

Mil gràcies a la Clàudia i la Mar, del grup CEPIMA del Departament d'Enginyeria Química, per les hores dedicades al funcionament de la termobalança.

Part del treball que es presenta en aquesta Tesi es va realitzar durant una estada a l'Associação para o Desenvolvimento da Aerodinâmica Industrial (Universitat de Coimbra). Voldria agrair al Prof. Viegas, director d'aquest centre, que ens hagi donat l'oportunitat de fer proves en les seves instal·lacions. També voldria agrair l'ajuda desinteressada rebuda per part de tot el personal del centre. Gràcies pel càlid acolliment a en Carlos, en Pedro, en Luís Mário, en Luís Paulo, en Nuno, l'Ana Rosa, la Fátima i tota la resta.

Una altra part de la Tesi es va desenvolupar al Laboratori de Química Inorgànica i Analítica de la Universitat Tècnica d'Atenes. És un plaer agrair al Prof. Liodakis, director del grup, la seva hospitalitat. He après moltes coses treballant al seu costat. D'aquesta estada he de mencionar l'optimista i extravertit Yannis, gràcies al seu bon nivell de castellà vaig poder entendre millor la vida d'Atenes. Tampoc voldria oblidar l'alegria, l'ajuda i la companyia rebuda per part d'en Tilemachos, la Magda, la Sophia, la Vasso, l'Iraklis, en Kostas i tots els altres companys de laboratori. També voldria recordar aquí la familiaritat amb què em van acollir a casa seva en Georgos i l'Andy. Barcelona us espera!

A més a més, voldria prendre aquesta oportunitat per agrair a la gent de 'Les Corts Power' l'amistat dipositada. Gràcies per la vostra energia! També, un agraïment especial per als 'físics' doctorands/doctors, perquè amb ells he compartit molts bons moments entre muntanyes reals, per a en Sam, perquè gràcies al seu anglès (i català) impecable m'ha ajudat a redactar correus formals, i per a la Laia (la neboda), perquè sense ser-ne conscient és una font de vida immesurable.

També agraeixo a la Direcció General de Recerca de la Generalitat de Catalunya l'ajuda econòmica rebuda durant els anys en què vaig gaudir d'una Beca de Formació d'Investigadors.

Aquesta Tesi està dedicada a la meva família més propera, els meus pares, les meves germanes i en Jorge. Gràcies pares per l'esperit diligent que m'heu

transmès i pel suport que m'heu donat al llarg dels anys. Gràcies Anna i Neus per ser dues de les muntanyes més característiques del paisatge i servir-me de referència. Gràcies Jorge per acompanyar-me amb molta estima durant aquests anys.

Finalment, la meva gratitud a l'Elsa Pastor i l'Eulàlia Planas, les directores d'aquesta Tesi, només es pot expressar amb pobresa en aquestes línies. Gràcies Elsa i Eulàlia per la vostra dedicació i entrega a aquesta Tesi. Al vostre costat he practicat el rigor, la decisió, la prudència, l'organització i l'enginy, i m'he format com a investigadora i com a persona. Heu estat també muntanyes característiques del paisatge i, a la vegada, companyes de viatge. Aquesta Tesi continua la línia de recerca que vàreu iniciar juntes ara fa gairebé deu anys, és per mi un orgull que així sigui.

Abstract

Effects of long-term forest fire retardants on fire intensity, heat of combustion of the fuel and flame emissivity

by

Alba Àgueda Costafreda

Universitat Politècnica de Catalunya, 2009

Every year, thousands of hectares of forest are destroyed by wildland fires. It is necessary to investigate the mechanisms that influence the ignition and propagation of wildland fires in order to successfully devise strategies for fighting wildland fires and to establish plans for managing forest areas or grasslands. Researchers have been formulating models to describe surface fires and, to a lesser extent, crown fires, for more than sixty years. However, these models have a significant shortcoming: none of them has been developed for use as a tool to predict fire behavior after indirect attack operations with long-term retardants. Furthermore, most of the work done to date on long-term retardants has been with the goal of evaluating these products for commercial purposes.

The goal of the present study was to improve knowledge of the effects of long-term retardants on the spread of forest fires. Retardants' effects on fire intensity were quantified for varying fire situations (no-slope/no-wind, upslope, upwind), together with retardants' effects on the heat of combustion of the fuel and flame emissivity. Assessing how these last two parameters change due to the presence of retardants on the fuel is a first step towards including the effects of indirect attack operations with long-term retardants in propagation models.

We found that the presence of retardants reduced fire intensity by a factor of 0.8 under the experimental conditions tested in this study. The amount of heat effectively released during flaming combustion under the presence of retardants was observed to decrease by a factor of 0.18 in comparison with untreated samples and flame emissivity was observed to be unaffected by the presence of retardants. These results indicated that the presence of retardants reduces fire intensity primarily by reducing the amount of heat effectively released per unit mass of fuel, rather than by affecting the radiation properties of the flames.

Table of contents

CHAPTER 1

Introduction

Every year, thousands of hectares are destroyed by wildland fires. These fires have dramatic effects on the ecosystems and the socioeconomic activity of the affected regions, and very often lead directly to loss of life.

Over the last decades, the number of fires has increased due to urban demand for forest areas, which leads to greater human presence in such areas and the construction of infrastructure such as electric lines and roads. The risk of forest fire propagation has increased due to a decline in agricultural activities and the consequent rise in the volume of available fuel [1]. These phenomena, and the presence of critical climatological conditions (recurrent in the Mediterranean context and exacerbated by climate change), account for the recent occurrence of large forest fires (> 500 ha).

Large forest fires are a relatively common problem in Catalonia. Figure 1.1 shows that the firefighting force of the *Generalitat de Catalunya* (the autonomous Catalan government) dealt successfully with 47.8% of the fires recorded in the period 1982-1991, based on their containment to an area of less

than 1 ha. Nevertheless, 0.8% of the fires could not be controlled (i.e. they affected areas of more than 500 ha) and caused 70.2% of the total burned area recorded over the period. A similar trend is observed for the period 1992-2007, although it can be seen in Figure 1.1 that fire extinction was more effective during this period (78.5% of the fires were contained to an area of less than 1 ha). During the same period, 0.4% of the fires could not be controlled and caused 77% of the total burned area. The latter period is also notable for the devastating fires in Berguedà (almost 17,000 hectares of forest burned) and Bages (almost 14,000 hectares) in 1994, and those in Bages in 1998 and Alt Empordà in 2000, where 18,000 and 6000 hectares of forest were burned, respectively.

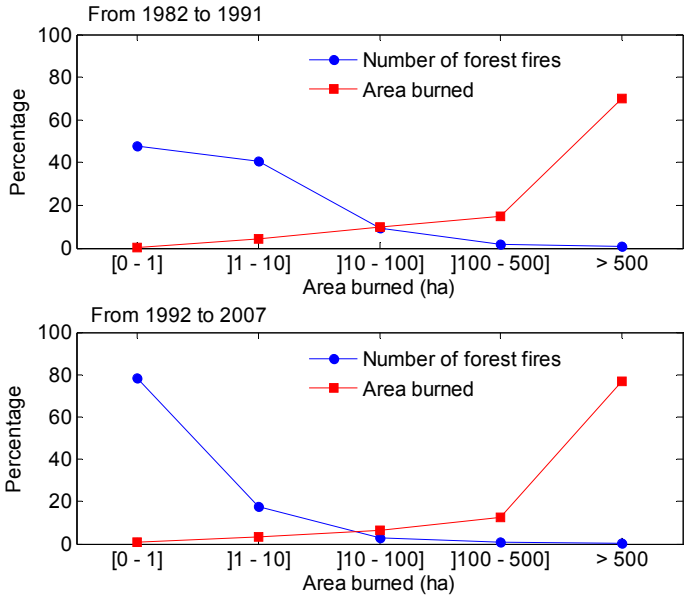

Figure 1.1 Number of forest fires and area burned (period 1982-1991 and 1992-2007). Source: [1].

Given that fire is a natural element in Mediterranean ecosystems, prevention and extinction measures are aimed at reducing risk and vulnerability to tolerable levels for society [2]. For example, a measure recently introduced in Catalonia for the prevention of forest fires consists in carrying out controlled burns in forests, one of the principal aims being to manage the growth of vegetation to prevent excessive accumulation.

Forest fires are a highly complex phenomenon; various factors are involved in the causal framework and several variables influence their propagation and the regeneration of burned fuel (topographical factors, fuel characteristics,

meteorological conditions, availability of means of extinction, performance strategy, etc). This complexity means that the issue should be dealt with from a multidisciplinary perspective, with the intervention of both public institutions and the research community. The fundamental aim of the research community is to understand the behavior of forest fires and to develop tools and resources that the civil service and firefighters can use to tackle forest fires effectively and at a suitable speed.

In this chapter we define the basic terms used by the research community to characterize the phenomena and variables associated with forest fires.

1.1 Important characteristics of forest fires

1.1.1 Combustion in forest fires

Combustion is defined as a chemical reaction in which, with the simultaneous presence of reagents (fuel and oxygen) and an initial external heat contribution, new substances are generated (combustion products) and energy is released. The conditions under which combustion occurs often prevent the complete reaction from taking place. In this case, other compounds derived from the partial decomposition of the fuel may be obtained, in addition to carbon dioxide and water. In forest fires the combustion reaction is normally incomplete.

The combustion reaction in forest fires generally produces a flame and can be broken down into three stages:

- Ignition: This is generically defined as the phase in which an external heat supply initiates the combustion reaction. First, the moisture content of the fuel evaporates at a temperature close to 373K. Next, the pyrolysis phase begins, during which the contributed heat causes thermal decomposition of the fuel and evaporation of volatile compounds. This process begins at approximately 473K. Finally, when the appropriate amount of gaseous phase is mixed with oxygen, ignition can occur. The heat contribution activates the combustion reaction at a temperature of approximately 600K [3-5].

- Combustion: This stage corresponds exactly to the interval in which the combustion reaction takes place continuously, consuming fuel and oxygen.

- Extinction: The combustion phase continues for as long as both reagents are present and the heat released is sufficient to sustain the evaporation

of fuel. If either of these conditions is not met, the combustion reaction stops and the extinction phase occurs.

When the combustion reaction with presence of flame stops, and if suitable conditions exist, glowing combustion can occur. This is the residual reaction that takes place during the final stages of forest fires. In this case the residue, which is rich in carbon and contains no volatile compounds, continues to burn slowly. Smoldering combustion, another type of combustion without flame, can occur in porous material that has not been converted into char. This type of combustion takes place slowly at low temperatures and is typical of ground fires (see the following section).

1.1.2 Types of forest fires

Forest fires are classified generically according to the type of fuel that promotes propagation and sustains burning. Forest fires involving different strata are: ground fires, surface fires and crown fires. These fires may occur jointly or successively during the course of a forest fire because multiple factors take part in the appearance of one or another type of fire. Some authors [6] use the concept of 'integral fire' to refer to fires involving all vegetation strata. Below, we define the specific features of ground, surface and crown fires.

Ground fires

In this type of fire the organic material between the surface litter and the mineral soil (including duff, tree or shrub roots, peat and sawdust) is consumed. Ground fires support glowing combustion, so they are usually detected when smoke is emitted. They propagate slowly due to the limited presence of oxygen, but the combustion reaction is maintained for days or even weeks, even if the organic material has a high moisture content, causing severe ecological damage.

Surface fires

In this type of fire loose surface debris (including dead branches and leaves) and low vegetation are burned. The behavior of a surface fire varies greatly depending on the type of vegetation involved. This category includes fires burning in vegetation consisting predominantly of shrubs, brush and scrub.

Crown fires

Crown fires advance in the tree crowns. Surface and crown phases may propagate as a linked unit (active crown fire) or independently (independent crown fire). Consequently, the intensity of the fire depends on the vertical

continuity of the different strata, the volume and arrangement of the aerial fuel, and the percentage of fine fuel present at the tree crown [7].

1.1.3 Characteristics of forest fuels

Forest fuels can be characterized microscopically and macroscopically. Microscopic analysis refers mainly to the intrinsic characteristics of the fuel particles, i.e. thermal, geometrical and chemical properties. The macroscopic description refers to the arrangement of the fuel within a natural setting. Below, we define the main microscopic and macroscopic characteristics of forest fuels and include a section on their relative moisture content.

Fuel moisture content

The moisture content of a fuel (%) is defined as the amount of water per unit mass of oven-dried fuel (dry basis). It can also be expressed per unit mass of total moist fuel.

Live fuel moisture content depends on the vegetative conditions of plants, which vary greatly between species and within seasons. In contrast, dead fuel moisture content depends mainly on environmental conditions: rainfall, wind, temperature, air humidity, solar radiation and topography. Moreover, changes in moisture content due to meteorological alterations are faster as the size of the fuel particles is smaller.

Forest fuel moisture content is a very important variable when considering the propagation of forest fires, because a fraction of the energy released during combustion is used to evaporate the water content of the vegetation adjacent to the fire front. If the energy release is not sufficient to evaporate this water content, ignition does not take place and the combustion reaction stops.

Chemical composition of forest fuel

Forest fuels have an approximate content of carbon, oxygen and hydrogen of 50, 44 and 5%, respectively (% in mass). Plants cell walls consist mainly of-long chain organic molecules (polymers), the most quantitatively important of which are as follows:

- Cellulose: Polysaccharide consisting of parallel unbranched chains of β-D-glucose units cross-linked in a stable structure. The combustion reaction of this carbohydrate takes place at 573-673K [8].

- Hemicellulose: Branched polymer consisting of shorter chains than cellulose that mostly contain pentoses and hexoses. The combustion reaction of this carbohydrate takes place at 523K and its complete degradation is at 773K.

- Lignin: Aromatic carbohydrate polymer consisting of various monomers of phenylpropane. It is thermally stable and slowly volatilizes as temperature increases. Only a loss of 50% of its weight is normally observed at 773K [8].

Forest fuels contain other types of compounds that are less quantitatively important than the above but which play an important role in determining a plant's flammability. These compounds include the following:

- Extractives: A complex mixture of compounds (inositols, amino acids, simple fats, carboxylic acids, terpenes, phenolic compounds, etc.) which can be removed from the plant by solvents (ether, benzene, acetone, ethanol, water, etc.). They are not part of the cell wall structure but have important functions, such as mediating in metabolic processes or protecting agents against parasites. Wood contains about 1 and 5% of extractives, but this percentage may vary depending on species and their location in wood. Some compounds, such as terpenes, have relatively low boiling points and therefore volatilize easily.

- Minerals: Wood usually contains less than 2% of mineral ashes, whereas vegetation leaves may have a percentage in the range 5-10%. Silica-free minerals act as pyrolysis catalysts, promoting char formation at the expense of volatile inflammable compounds. Thus, species with a high silica-free mineral content form smaller flames than those produced by species with a lower mineral content.

Table 1.1 shows the composition of two species. The figures in this table cannot be taken as absolute values, since they can vary considerably depending on the geographic area in which the vegetation sample was collected, the time of the year, species age, etc. However, the table can be used to establish general comparisons between the two species shown. Straw and pine needles of various species are commonly used in laboratory simulations of forest fires. The figures in Table 1.1 show that straw has a higher mineral content than pine needles, whereas pine needles contain larger amounts of lignin and extractives. The percentages do not total 100% because forest fuel contains other, less abundant

compounds in addition to those shown in the table (starch, proteins, monosaccharids, etc.).

Table 1.1 Biochemical composition of two plant species. Figures are based on dry weight and presented as units of % mass. Data for *Triticum turgidum* straw and *Pinus pinaster* needles are taken from [9] and [10], respectively. Extractives percentage corresponds to those compounds that can be removed by ethanol and benzene.

Species	**Cellulose**	**Hemicellulose**	**Lignin**	**Extractives**	**Minerals**
T. turgidum straw	34.78	17.88	20.11	7.04	6.52
P. pinaster needles	28.75	16.16	24.36	15.82	3.08

Thermal conductivity

Thermal conductivity (W m^{-1} K^{-1}) is a measure of the ability of a substance to conduct heat. Several variables may change the value of this property, such as fuel density, fuel moisture content, heat flux direction (e.g. longitudinal or radial with respect to growth rings), and imperfections such as knots and temperature. In general, this variable increases with density, moisture and temperature. Thermal conductivity is a useful variable for calculating heat transfer by conduction.

Specific heat, heat of pyrolysis and heat of ignition

The specific heat (J kg^{-1} $°C^{-1}$ or J kg^{-1} K^{-1}) is the amount of heat required to raise the temperature of a unit mass of substance by one degree, without transforming the substance from one thermodynamic state to another. In wood, the value of this variable depends mainly on temperature and is largely independent of fuel density and species. The equation most commonly used to calculate the specific heat of forest fuels was formulated by Dunlap [11] and is shown below as Eq. [1.1]:

$$c_s = 1110 + 4.86\,T_c \qquad [1.1]$$

The specific heat term has been used by several authors [12-14] to determine the heat required to ignite an elemental fuel particle positioned in front of a flame front. This is calculated using Eq. [1.2], below:

$$Q_{ig} = c_s\left(T_{ig} - T_a\right) + M_w[c_w(T_{eb} - T_a) + L_w] \qquad [1.2]$$

However, Wilson [15] showed that the first term on the right-hand side of Eq. [1.2] could be determined more exactly if the concept of heat of pyrolysis was used. This term represents the heat required to pyrolize a unit mass of fuel. It can be calculated by integrating differential scanning calorimetry curves obtained under pyrolytic conditions, from 25°C to 400°C. Forest fuel decomposition takes place at 200-400°C. In this temperature range, both the specific heat and the reaction enthalpy associated with the production of pyrolysis gases contribute to the heat needed to produce enough gaseous phase to support flaming combustion. This is why Wilson considered that Eq. [1.2] estimates only a "heat of preignition". According to Wilson [15] and Catchpole et al. [16], the heat of ignition is more accurately defined using Eq. [1.3], below:

$$Q_{ig} = Q_p + M_w[c_w(T_{eb} - T_a) + L_w] \quad [1.3]$$

Heat of combustion

The heat of combustion (kJ kg^{-1}) is the amount of energy released when a given mass of a substance is burned completely to form incombustible products (e.g. water and carbon dioxide). This energy may vary depending on species, location in wood and fuel moisture content. The heat of combustion of forest fuels must be determined experimentally because the exact formula of all of the molecules in forest species is unknown. Heat of combustion of forest fuels is a crucial variable in quantifying the exact calorific power released by a flame front. Distinctions are made between high heat of combustion, low heat of combustion, and heat of combustion of the volatiles.

The high heat of combustion is the heat released per unit mass of dried fuel under complete combustion conditions in a bomb calorimeter. The water of reaction is collected as a liquid in the bomb calorimeter.

The low heat of combustion is the heat released per unit mass of dried fuel under complete combustion conditions in a bomb calorimeter after correcting the experimental value to take into account that the water of reaction is released as vapor.

The heat of combustion of the volatiles is the heat released per unit mass of dried fuel due to combustion of the volatiles generated during pyrolysis of the forest species. This value is usually calculated indirectly, by subtracting the product of the char fraction and the low heat of combustion of the charred residue from the low heat of combustion of the forest species.

Fuel loading

Fuel loading is defined as the amount of fuel present expressed quantitatively in terms of weight of fuel (in a dry basis) per unit area. This variable is usually expressed in kg m^{-2} or tn ha^{-1}; however, in wooded areas it is more commonly expressed as stems ha^{-1}.

Size and shape of forest fuels

The size and shape of forest fuels are usually expressed in terms of surface area-to-volume ratio. The smaller the particle, the more quickly it can become wet, dry out or become heated to combustion temperature during a fire. Consequently, fine fuels (those which are less than 6 mm in diameter and have a comparatively high surface area-to-volume ratio) ignite readily and have a significant influence on fire propagation.

Bulk density and packing ratio

The bulk density (kg m^{-3}) is the weight of dry fuel per unit volume of fuel bed, considering the fuel bed as an array of fuels. Bulk density is always lower than fuel density because part of the volume considered when calculating bulk density is occupied by air.

The packing ratio (%) is the fraction of a fuel bed occupied by fuels, or the ratio between bulk density and fuel density. The packing ratio is a measure of the empty space in the fuel bed. Fire propagation is generally more difficult as the packing ratio increases, because it becomes harder for air to penetrate the fuel bed.

Forest fuel arrangement

The arrangement of vegetation over the terrain has an enormous influence on fire behavior. Two generic arrangements are distinguished according to orientation: vertical and horizontal. Grass, shrubs and trees are arranged vertically, while branches and debris have a horizontal arrangement.

Horizontally arranged fuels determine fire propagation; when they are dispersed fire propagation is difficult, whereas when they are distributed continuously and uniformly fire propagation is assured. The vertical arrangement of fuels determines which part will be involved in the fire; when there is vertical continuity between strata, the fire may start by affecting litter and then progress to crowning. This type of situation could alter the fire behavior significantly.

Flammability of forest species

The flammability of forest species derives from a combination of ignitability, sustainability and combustibility. Ignitability determines how easily a fuel ignites. Sustainability is a measure of how well a fire burns with or without a heat source. Combustibility reflects how easily a fuel is consumed.

Combustibility of natural fuel arrays can be characterized by classifying fuel arrangements according to the values of those variables that are most sensitive to propagation. The most well-known modeling system was developed by Anderson [17], who sorted natural settings into 13 categories according to fuel loading, size, shape and height, and bulk density.

1.1.4 Heat transfer mechanisms involved in forest fire propagation

Forest fires are characterized by heat transfer. The type and amount of heat transferred affects the propagation rate of forest fires, and combustion cannot be maintained without a continuous heat transfer. Heat is transferred through conduction, convection and radiation, which occur simultaneously during fires. However, the relative importance of each of these transfer mechanisms varies according to the intensity of the fire and the configuration of the system in which propagation takes place.

Conduction

When a solid fuel burns, the mechanism by which heat is transferred through the internal parts of the fuel is called conduction. In forest fire propagation, the heat contribution of conduction is generally minimal [18]. However, behind the zone of an advancing fire, conduction is responsible for the continued burning of trunks, branches and other combustible fuel that has initiated the combustion process. Consequently, conduction is responsible for residual combustion, which can reactivate fires.

Convection

In forest fires, a large proportion of the heat generated is transferred by convection. Air is heated through contact with the flames' front surface, and smoke produced during combustion constitute a hot mass of fluid that leaves the flame front surface at a given velocity, which depends on ambient wind and fire intensity. The hot mass of fluid enters in direct contact with other surfaces, such as leaves, branches and tree trunks, which are heated and can ignite. This heat transfer mechanism is predominantly vertical, so in a surface fire the hot mass of fluid contributes greatly to the heating of crowns.

Radiation

Radiation, together with convection, is the principal means of energy transfer in forest fires. Radiation heats fuel before the arrival of the flame front and is considered to be the most important mechanism in preheating fuels. Thermal radiation is the emission of energy by electromagnetic waves from a substance which is at a certain temperature. Flame radiation comes from the mixture of gases (CO_2 and H_2O) and soot, although in forest fires flames are soot-dominated.

1.1.5 Geometric and physical characteristics of forest fires

Geometric and physical characteristics are essential in describing and understanding forest fire behavior. This section presents the principal terminology used to describe the dimensions of forest fires, and the main physical variables used to characterize forest fire behavior.

Morphology and geometry of forest fires

Forest fires generally have irregular shapes. A forest fire can be separated into the following main areas:

- Head: The most rapidly spreading portion of a fire's perimeter, usually to the leeward or up slope.
- Rear: The portion of a fire edge opposite to the head.
- Flanks: The part of a fire's perimeter that is roughly parallel to the main direction of spread. It is located between the head and the rear.

Irregularities in forest fires can be seen in the formation of fingers (long narrow extensions projecting from the main body of the fire), islands (unburned areas within a fire's perimeter) and spot fires.

The principal geometric variables used to characterize forest fires are flame height, depth, length and angle. Flame length and angle can be defined according to several references; Figure 1.2 illustrates the geometric characteristics of flames, including the different options for defining flame length and angle. Anderson et al. [19] proposed the following definitions as possible standard measurements:

- Flame height (m): The average maximum extension of flames, perpendicular to the ground surface, measured from the tip of the flame to the ground surface (H).

- Flame depth (m): This is the distance from the front to the rear of the flame front within which flame combustion takes place continuously (D).

- Flame length (m): Considering as reference the leading edge of the flame front, the distance between the flame tip and the ground surface (L_e).

- Flame angle (radians or degrees): Angle between the flame at the leading edge of the fire front and the ground surface (β_e).

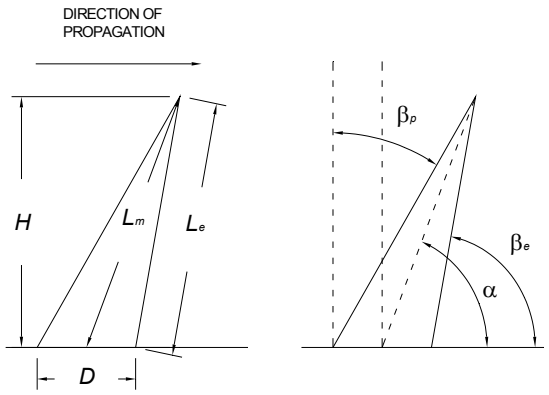

Figure 1.2 Flame measurements (based on [19]).

Knowledge of flame characteristics in free-burning fires is important in determining many aspects of fire behavior and effects. Flame length gives an estimation of fire intensity and, by extension, of fire effects. Flame height is important in determining crowning potential and estimating scorch height, which gives an indication of the possible fire effects. In addition, knowledge of flame height and flame angle is needed to determine the amount of radiative heat transfer. Finally, flame characteristics provide complementary information that is useful in determining an overall suppression strategy.

Combustion rate

The combustion rate is rate of fuel consumption per unit of time per unit of burning area (kg s^{-1} m^{-2}) or per unit of front length (kg s^{-1} m^{-1}). Some authors use the term rate of mass loss. This variable is related to the rate of heat release.

Fuel consumption ratio

The fuel consumption ratio is the ratio between the fuel loading of consumed fuel and the initial fuel loading. It is often expressed as a percentage. This variable gives an idea of the quality and completeness of the combustion reaction. It is generally accepted that fuels of less than 6 mm in diameter will be completely consumed in forest fires.

Rate of spread

The rate of spread is the extension covered by the flame front per unit of time (m s^{-1}). It is one of the most common variables for describing forest fire behavior.

Calorific power, fireline intensity, emissive power and irradiance

Calorific power is defined as the amount of energy released by the flame front per unit time. If it is expressed per unit length of fire front, it is called fireline intensity.

The fireline intensity (kW m^{-1}) is a variable commonly used to measure the calorific power of forest fires. Byram [20] developed the following equation, which is generally used to determine this variable (Eq. [1.4]):

$$I_B = (HHC - 1263 - 24M_w)\, w_a\, R \qquad [1.4]$$

The heat transfer mechanism behind the calorific power can also be differentiated. Radiant calorific power is the energy emitted through radiation per unit time from a flame front. If this power is expressed per unit area of radiant surface, the emissive power of the flame front is obtained (kW m^{-2}). The emissive power is essential in the development of propagation models because, as stated above, radiation is one of the most important heat transfer mechanisms. The emissive power of flames is generally expressed using the Stefan-Boltzmann law, although it can also be estimated using Eq. [1.5] if it is considered that the flame front behaves like a body with a given geometry which emits radiation uniformly from its surface.

$$E_f = \varepsilon_f\, \sigma\, T^4 \qquad [1.5]$$

Finally, thermal irradiance (kW m^{-2}) is the heat flux transferred through radiation to a surface or body located at a given distance and height. It can be estimated using Eq. [1.6], below:

$$q''_{rt} = E_f \, \tau_a \, F \qquad [1.6]$$

1.1.6 Factors influencing forest fire behavior, other than fuel characteristics

The magnitude of forest fires can be determined from physical parameters (rate of spread or fireline intensity) or calculated from the direct consequences of these parameters (number of hectares burned, fatalities, public expenditure on prevention and extinction, etc.). Forest fire behavior is influenced by many variables and by the complex interactions between them. Factors such as rainfall and wind patterns, prevention activities, relief, arrangement and chemical composition of fuels, or the organization of staff and equipment in fire suppression, are directly or indirectly related to the causes, evolution and effects of forest fires.

This section focuses on the most important factors that influence the evolution of forest fires, and groups them in the following categories: meteorological and topographic. Factors related to fuel characteristics are presented in Section 1.1.3; they represent only a small proportion of the many variables that interact in forest fires, but are essential to understanding the development of this phenomenon from a scientific perspective.

Meteorological factors

Climate and meteorological conditions encompass a set of variables that exert an important influence on the development of forest fires. For example, solar radiation and air temperature affect the flammability of forest fuels, air humidity influences ignition and propagation, atmospheric stability partly determines fireline intensity and fire behavior, and wind velocity and direction alter the general fire behavior. Wind is probably the most influential factor. Wind tilts flame fronts, which increases heat transfer through radiation. In addition, in the presence of wind, unburned fuel is also heated to a greater extent through convection and through conduction due to the direct contact between flames and fuel. Wind guarantees a higher oxygen contribution, thus increasing the efficiency of the combustion reaction, and contributes to the drying of unburned fuel, which promotes ignition. In combination, these effects lead directly to an increase in the rate of spread of the flame front.

In addition to the rate of spread, wind affects several other aspects of forest fires, in particular the morphology of the fire perimeter and the appearance of spotting behavior (embers carried out of the main fire by the wind start new fires outside the area of direct ignition).

Topographic factors

Topographic factors influence forest fire behavior through their direct correlation with the propagation of flame fronts and due to their connection with certain vegetation characteristics and meteorological factors. For a given period of time, topographic factors are more constant than meteorological factors, which make their influence on fire behavior easier to predict. Topographic elements which can exert a significant influence on the development of a forest fire include slope, orientation, relief configuration and elevation. Slope is the most influential variable; its effect is similar to that of wind [3,7,21], in that slope also causes tilting and extension of the flames and the convection column, which increase the rate of spread. The main difference between the influence of wind and slope lies in the magnitude of the effect. For example, a forest fire propagating under strong wind extends its horizontal dimensions 100 times faster than under calm conditions. However, the equivalent effect of slope is an increase that does not exceed a factor of 20 [22].

1.2 Methods of forest fire suppression

Two levels of action can be taken against wildfires: prevention and extinction. Measures aimed at reducing the incidence of fires (prevention level) include public education, law enforcement, fuel management, risk prediction, and management of preventive infrastructures (roads, water sources). Extinction encompasses all fire suppression work carried out with a selection of the most effective resources available (staff, aircrafts and fire engines).

Extinction also includes the approval of an attack plan, which details the selected course of action and the organization of staff and equipment. Three important aspects have to be considered when planning extinction operations: strategy, tactics and operational period. Strategy refers to the general plan or direction selected to accomplish the incident objectives. Deployment and direction of resources to accomplish the strategic objectives fall under the category of tactics. The operational period is the time scheduled for the execution of a given set of tactical actions. Two extinction methods are used to fight wildfires: direct attack and indirect attack.

Direct attack

Direct attack refers to any treatment applied directly to burning fuel, such as wetting (with water) or smothering (with fire beaters). The first firefighting staff to arrive at a wildfire are likely to use direct approaches, because at this stage the characteristics of the fire make it more feasible to carry out this type of

action. Water mixed with chemical products (see Section 1.3) can also be applied directly to burning fuel. However, depending on the type of product, more effective use is made by applying the mixture at a reasonable distance from the flame front.

Indirect attack

Indirect attack refers to suppression methods in which the control line is located at a considerable distance from the active edge of the fire. This type of approach uses natural or constructed firebreaks or fuel breaks and favorable breaks in the topography and is generally applied to fast-spreading or high-intensity fires.

The basic indirect attack methods are as follows:

- Scratch line and cat line:

  The scratch line is a narrow line quickly cut in the fuel to temporarily stop the spread of fire. Cat lines are constructed using bulldozers or tractor-plows. Both types of lines can be widened later to be used as final control lines.

- Chemical firebreaks (wet and retardant lines):

  Chemical firebreaks are lines constructed using chemical products, such as short-term or long-term retardants (see Section 1.3). If the line is constructed using foams, it is normally referred to as a ‘wet line’. The term used to characterize lines constructed using long-term retardants is ‘retardant line’. Chemical firebreaks are not considered as final control lines, since these must be cut through the fuel to mineral soil.

- Control line:

  The control line is projected in the extinction plan as the perimeter of the fire. Control lines are normally constructed close to natural or constructed firebreaks.

- Burning-out:

  Burning-out is the use of fire to remove the unburned fuels between the fire perimeter and the control line. It is used to clean up and straighten lines, and widen natural or existing barriers.

- Backfire:

  Backfiring is a special technique requiring extensive planning. It is used to control high-intensity fire fronts that would overrun firelines if they could not be slowed or stopped. It is essential for the main fire to draw the backfire towards it for this technique to work.

1.3 Chemical products used in forest fire suppression

Three types of chemical products are commonly used in wildland fire management: foams, gels (or water enhancers) and long-term retardants.

Foams and gels are also known as short-term retardants because their effectiveness is dependent on the water they contain, and once all of the water has evaporated they are no longer effective. They can be applied using aerial or ground equipment to the fire area to slow or stop combustion.

Foam concentrates are added to water to create a foam solution that can be used as a wetting agent or to create foam when aerated. Foams insulate, envelope and penetrate fuels, act as heat sinkers, exclude air, raise humidity at the fuel's surface, isolate and dilute volatiles, increase the amount of available water and, because they break down in a controlled manner, further wet the fuels they encase [3]. Foams are a highly versatile and universally popular fire suppression material. In Catalonia, they are mainly applied from helicopters during wildfire management operations.

The action mechanism of gels is similar to that of foams, the main difference being that gels have higher viscosities and, as a result, adhere better to fuel surfaces. Thickeners can be added to enhanced water mixtures to improve aerial application, minimize drift and enhance adherence to fuels. Gels consist of macromolecular compounds, known as superabsorbent polymers (SAPs) that can absorb thousands of times their own weight in water. The polymers are formed by three-dimensional cross-linked polymeric structures. Swelling of SAPs is induced by electrostatic repulsion of the ionic charges of their network, which is caused by dissociation of the carboxylic groups (–COONa or –COOK) in solution and allows water to enter the matrix [23]. SAPs are already used to great effect in agriculture, but the potential benefits of their application in wildfire management have yet to be fully harnessed.

Long-term retardants can also be applied using aerial or ground equipment. The retardant is mixed with water in a prescribed ratio and then applied to slow the

spread and reduce the intensity of the fire. These products continue to be effective after their water content has evaporated. Wildland fire retardant mixtures change the preignition pathway from hot, fast pyrolysis to cooler, slow pyrolysis, promoting the production of char and noncombustible gases (CO_2 and H_2O) rather than combustible gases. The chemicals most responsible for retardation are phosphate and sulfate salts. Commercial products commonly contain: (1) retardant salt; (2) colorant; (3) corrosion inhibitor; (4) thickening agent (gum or clay). The last three components prevent the corrosion of aircraft interiors and improve aerial application.

There is no conclusive work on the toxicity of these chemicals to terrestrial plants and animals, since studies usually cover short periods (one or two years) but responses to the burning of terrestrial vegetation are more appropriately measured over the course of several years or even decades. However, some results can be highlighted to illustrate the findings to date. Larson and Duncan [24] found that in the first year after the application of a retardant treatment, fuel loading in treated areas was double that recorded in the untreated area. This is because fire retardants are composed largely of nitrogen and phosphorus fertilizers. It has also been observed that species richness and the number of stems per square meter return to control levels by the end of a one-year study [25]. These results suggested that the effects of treatment with long-term retardants were likely to be transitory. With regard to the toxicity of retardants to aquatic organisms, it is generally accepted that, when dumped into waterways, phosphates can encourage eutrophication, and that sodium ferrocyanide, a corrosion inhibitor still used in some commercial formulations, may contribute to fish kill upon exposure to sunlight [26].

When applying short- and long-term retardants, the concentration of the mixture and the coverage level (liters of solution per m^2) must be established. Manufacturers usually provide information on the ideal mix ratio and coverage level. Vélez [27] collected data on the values used in Spain for these two variables (see Table 1.2 and Table 1.3). The type of fuel is distinguished for coverage levels. The application equipment (ground or aerial) is distinguished for the mix ratio.

Table 1.2 Chemical product and coverage level for different fuel types (LTR: long-term retardants; F: foams).

Type of fuel	**Chemical product**	**Coverage level (l m^{-2})**
Chaparral and shrub fields	LTR/F	1 - 3
Timber litter	LTR	2
Grass and grass-dominated areas	F	0.5 – 1.5
Slash	F	> 2

Table 1.3 Dilution mix ratio for different chemical products and application equipment (n.a.: not applied in Spain).

Application equipment	**Mix ratio (% v/v)**	
	Long-term retardants	Foams
Aerial	20	0.4 – 0.6
Ground	n.a.	0.5 – 1.0

References

1. Department of Environment and Housing, Autonomous Government of Catalonia. Nombre d'incendis per estrats. Source: http://www.mediambient.gencat.cat/cat/el_medi/incendis/doc/estadistiques/estrat.pdf. Last modified: -. Visiting date: 09/06/09.

2. Plana E. Anàlisi d'escenaris de prevenció i extinció d'incendis des de la perspectiva socioambiental. In: Incendis forestals, dimensió socioambiental, gestió del risc i ecologia del foc (Ed. Plana E) Xarxa ALINFO XCT 2001-00061, Solsona, Spain; 2004.

3. Pyne SJ, Andrews PL, Laven RD. Introduction to Wildland Fire. John Wiley and Sons, New York, 1996; 769 pages.

4. Dupuy, JL. Mieux comprendre et prédire la propagation des feux de forêts: expérimentation, test et proposition de modèles. PhD Thesis, Université Claude Bernard – Lyon I, France; 1997.

5. Mercer GN, Weber RO. Fire Plumes. In: Forest Fires: Behaviour and Ecological Effects (Eds. Johnson E, Miyanishi K) Academic Press, London; 2001.

6. Panareda JM, Arola J. Els incendis forestals. EUMO editorial, Vic, Spain, 1999; 136 pages.

7. Trabaud, L. Les feux des forêts. Mécanismes, comportement et environnement. France-Selection Publishers, Aubervilliers, France; 1992.

8. Philpot W. Influence of mineral content on the pyrolysis of plant material. Forest Sci 1970;16(4):461-71.

9. Antolín G, Irusta R. Caracterización de combustibles lignocelulósicos: aplicación a la paja de cereal. Secretariado de Publicaciones, University of Valladolid, Valladolid, Spain; 1989.

10. Vázquez G, Antorrena G, González J, Freire S. Studies on the composition of *Pinus pinaster* foliage. Bioresource Technol 1995;51(1):83-7.

11. Dunlap F. The specific heat of wood. USDA Forest Service Bulletin nº110, 1912; 7-18.

12. Rothermel, R. A mathematical model for predicting fire spread in wildland fuels. USDA Forest Service Research Paper INT-115; 1972.

13. Frandsen W. Effective heating of fuel ahead of spreading fire. USDA Forest Service Research Paper INT-140; 1973.

14. Albini FA. A model for fire spread in wildland fuels by radiation. Combust Sci Technol 1985;42:229-58.

15. Wilson R. Observations of extinction and marginal burning states in free burning porous fuel beds. Combust Sci Technol 1985;44(3-4):179-93.

16. Catchpole W, Catchpole E, Butler B, Rothermel R, Morris G, Latham J. Rate of spread of free-burning fires in woody fuels in a wind tunnel. Combust Sci Technol 1998;131:1-37.

17. Anderson HE. Aids to determining fuel models for estimating fire behavior. USDA Forest Service General Technical Report INT-122; 1982.

18. Chandler C, Cheney P, Thomas P, Trabaud L, Williams D. Fire in Forestry. In: Forest Fire Behavior and Effects vol. 1. John Wiley and Sons, New York, 1983; 450 pages.

19. Anderson W, Pastor E, Butler B, Catchpole E, Dupuy JL, Fernandes P, Guijarro M, Mendes-Lopes JM, Ventura J. Evaluating models to estimate flame characteristics for free-burning fires using laboratory and field data. In: 'Proceedings of the 5th International Conference on Forest Fire Research' 27–30 November, Figueira da Foz, Portugal; 2006.

20. Byram GM. Combustion of forest fuels. In: Forest Fire Control and Use (Ed. Davis KP) McGraw-Hill, New York, 1959; 61-89.

21. Nelson R. An effective wind speed for models of fires spread. Int J Wildland Fire 2002;11(2):153-61.

22. Viegas, DX. Forest fire propagation. Philos T R Soc A 1998;356(1748):2907-28.

23. Davies LC, Novais JM, Martins-Dias S. Influence of salts and phenolic compounds on olive mill wastewater detoxification using superabsorbent polymers. Bioresource Technol 2004;95(3):259-68.

24. Larson JR, Duncan DA. Annual grassland response to fire retardant and wildfire. J Range Manag 1982;35(6):700-3.

25. Larson DL, Newton WE, Anderson P, Stein SJ. Effects of fire retardant chemical and fire suppressant foam on shrub steppe vegetation in northern Nevada. Int J Wildland Fire 1999;9(2):115-27.

26. Little EE, Calfee, RD. The effects of UVB radiation on the toxicity of fire-fighting chemicals. Final Report. US Geological Service, Columbia Environmental Research Center, Columbia; 2000.

27. Vélez R (coordinator). Métodos y medios para la modificacions de los combustibles. In: La Defensa contra Incendios Forestales. Fundamentos y Experiencias (Ed. Grace AG) McGraw-Hill, Madrid; 2000.

A la meva família

Agraïments

Fer una Tesi Doctoral (i recerca en general) no és tan senzill com agafar un mapa, fixar un punt de partida i una destinació, i seguir el camí que hi apareix fins arribar-hi. Sovint el camí que es veu al mapa resulta ser un corriol i a vegades un se sent perdut i no sap cap on tirar. És aleshores quan un, mirant de nou el mapa i les referències que li dóna el paisatge, es pot tornar a situar i seguir endavant.

Arribar fins aquí, poder presentar la memòria de Tesi Doctoral, és quelcom que m'ha costat. Per fer una Tesi es requereix una capacitat de resistència mental important però feliçment també representa una experiència vital molt enriquidora a nivell intel·lectual i social. Durant aquests anys he tingut l'oportunitat de trobar pel corriol molta gent. A tots ells els vull agrair la seva participació, directa o indirecta, en l'elaboració d'aquesta Tesi.

Primerament, voldria expressar la meva gratitud cap a en Joaquim Casal, director del Centre d'Estudis del Risc Tecnològic (CERTEC), per donar-me l'oportunitat de dur a terme aquesta Tesi en aquest grup del Departament d'Enginyeria Química de la UPC.

Pels bons moments que hem compartit junts, també m'agradaria donar les gràcies als professors, doctorands i estudiants del CERTEC amb qui he coincidit al llarg d'aquesta etapa: en Joaquim (novament), en Josep, en Juan Antonio, en

Miguel, l'Andrea, en Fabio, en Luís, l'Anna, en Pau, la Rosa Mari, la Míriam, la Laia, la Mercedes, en Jordi, la Isabel, l'Adriana, l'Héctor, l'Ariadna, l'Eduard, la Carol, en Marcos, en Miki i, finalment, la Yolanda i la Rut. Gràcies Yolanda per ser una companya de 'grup forestals' i d'estada extraordinària! I gràcies Rut per l'energia transmesa durant la recta final!

Mil gràcies a la Clàudia i la Mar, del grup CEPIMA del Departament d'Enginyeria Química, per les hores dedicades al funcionament de la termobalança.

Part del treball que es presenta en aquesta Tesi es va realitzar durant una estada a l'Associação para o Desenvolvimento da Aerodinâmica Industrial (Universitat de Coimbra). Voldria agrair al Prof. Viegas, director d'aquest centre, que ens hagi donat l'oportunitat de fer proves en les seves instal·lacions. També voldria agrair l'ajuda desinteressada rebuda per part de tot el personal del centre. Gràcies pel càlid acolliment a en Carlos, en Pedro, en Luís Mário, en Luís Paulo, en Nuno, l'Ana Rosa, la Fátima i tota la resta.

Una altra part de la Tesi es va desenvolupar al Laboratori de Química Inorgànica i Analítica de la Universitat Tècnica d'Atenes. És un plaer agrair al Prof. Liodakis, director del grup, la seva hospitalitat. He après moltes coses treballant al seu costat. D'aquesta estada he de mencionar l'optimista i extravertit Yannis, gràcies al seu bon nivell de castellà vaig poder entendre millor la vida d'Atenes. Tampoc voldria oblidar l'alegria, l'ajuda i la companyia rebuda per part d'en Tilemachos, la Magda, la Sophia, la Vasso, l'Iraklis, en Kostas i tots els altres companys de laboratori. També voldria recordar aquí la familiaritat amb què em van acollir a casa seva en Georgos i l'Andy. Barcelona us espera!

A més a més, voldria prendre aquesta oportunitat per agrair a la gent de 'Les Corts Power' l'amistat dipositada. Gràcies per la vostra energia! També, un agraïment especial per als 'físics' doctorands/doctors, perquè amb ells he compartit molts bons moments entre muntanyes reals, per a en Sam, perquè gràcies al seu anglès (i català) impecable m'ha ajudat a redactar correus formals, i per a la Laia (la neboda), perquè sense ser-ne conscient és una font de vida immesurable.

També agraeixo a la Direcció General de Recerca de la Generalitat de Catalunya l'ajuda econòmica rebuda durant els anys en què vaig gaudir d'una Beca de Formació d'Investigadors.

Aquesta Tesi està dedicada a la meva família més propera, els meus pares, les meves germanes i en Jorge. Gràcies pares per l'esperit diligent que m'heu

transmès i pel suport que m'heu donat al llarg dels anys. Gràcies Anna i Neus per ser dues de les muntanyes més característiques del paisatge i servir-me de referència. Gràcies Jorge per acompanyar-me amb molta estima durant aquests anys.

Finalment, la meva gratitud a l'Elsa Pastor i l'Eulàlia Planas, les directores d'aquesta Tesi, només es pot expressar amb pobresa en aquestes línies. Gràcies Elsa i Eulàlia per la vostra dedicació i entrega a aquesta Tesi. Al vostre costat he practicat el rigor, la decisió, la prudència, l'organització i l'enginy, i m'he format com a investigadora i com a persona. Heu estat també muntanyes característiques del paisatge i, a la vegada, companyes de viatge. Aquesta Tesi continua la línia de recerca que vàreu iniciar juntes ara fa gairebé deu anys, és per mi un orgull que així sigui.

Abstract

Effects of long-term forest fire retardants on fire intensity, heat of combustion of the fuel and flame emissivity

by

Alba Àgueda Costafreda

Universitat Politècnica de Catalunya, 2009

Every year, thousands of hectares of forest are destroyed by wildland fires. It is necessary to investigate the mechanisms that influence the ignition and propagation of wildland fires in order to successfully devise strategies for fighting wildland fires and to establish plans for managing forest areas or grasslands. Researchers have been formulating models to describe surface fires and, to a lesser extent, crown fires, for more than sixty years. However, these models have a significant shortcoming: none of them has been developed for use as a tool to predict fire behavior after indirect attack operations with long-term retardants. Furthermore, most of the work done to date on long-term retardants has been with the goal of evaluating these products for commercial purposes.

The goal of the present study was to improve knowledge of the effects of long-term retardants on the spread of forest fires. Retardants' effects on fire intensity were quantified for varying fire situations (no-slope/no-wind, upslope, upwind), together with retardants' effects on the heat of combustion of the fuel and flame emissivity. Assessing how these last two parameters change due to the presence of retardants on the fuel is a first step towards including the effects of indirect attack operations with long-term retardants in propagation models.

We found that the presence of retardants reduced fire intensity by a factor of 0.8 under the experimental conditions tested in this study. The amount of heat effectively released during flaming combustion under the presence of retardants was observed to decrease by a factor of 0.18 in comparison with untreated samples and flame emissivity was observed to be unaffected by the presence of retardants. These results indicated that the presence of retardants reduces fire intensity primarily by reducing the amount of heat effectively released per unit mass of fuel, rather than by affecting the radiation properties of the flames.

Table of contents

CHAPTER 1

Introduction

Every year, thousands of hectares are destroyed by wildland fires. These fires have dramatic effects on the ecosystems and the socioeconomic activity of the affected regions, and very often lead directly to loss of life.

Over the last decades, the number of fires has increased due to urban demand for forest areas, which leads to greater human presence in such areas and the construction of infrastructure such as electric lines and roads. The risk of forest fire propagation has increased due to a decline in agricultural activities and the consequent rise in the volume of available fuel [1]. These phenomena, and the presence of critical climatological conditions (recurrent in the Mediterranean context and exacerbated by climate change), account for the recent occurrence of large forest fires (> 500 ha).

Large forest fires are a relatively common problem in Catalonia. Figure 1.1 shows that the firefighting force of the *Generalitat de Catalunya* (the autonomous Catalan government) dealt successfully with 47.8% of the fires recorded in the period 1982-1991, based on their containment to an area of less

than 1 ha. Nevertheless, 0.8% of the fires could not be controlled (i.e. they affected areas of more than 500 ha) and caused 70.2% of the total burned area recorded over the period. A similar trend is observed for the period 1992-2007, although it can be seen in Figure 1.1 that fire extinction was more effective during this period (78.5% of the fires were contained to an area of less than 1 ha). During the same period, 0.4% of the fires could not be controlled and caused 77% of the total burned area. The latter period is also notable for the devastating fires in Berguedà (almost 17,000 hectares of forest burned) and Bages (almost 14,000 hectares) in 1994, and those in Bages in 1998 and Alt Empordà in 2000, where 18,000 and 6000 hectares of forest were burned, respectively.

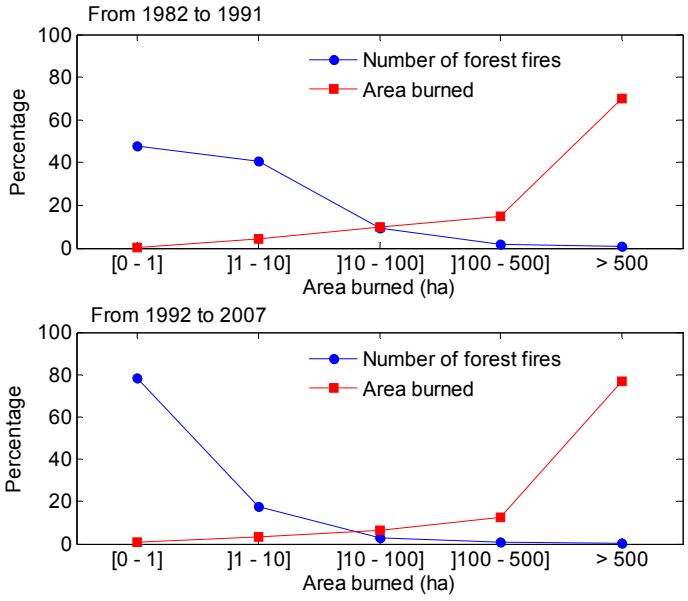

Figure 1.1 Number of forest fires and area burned (period 1982-1991 and 1992-2007). Source: [1].

Given that fire is a natural element in Mediterranean ecosystems, prevention and extinction measures are aimed at reducing risk and vulnerability to tolerable levels for society [2]. For example, a measure recently introduced in Catalonia for the prevention of forest fires consists in carrying out controlled burns in forests, one of the principal aims being to manage the growth of vegetation to prevent excessive accumulation.

Forest fires are a highly complex phenomenon; various factors are involved in the causal framework and several variables influence their propagation and the regeneration of burned fuel (topographical factors, fuel characteristics,

meteorological conditions, availability of means of extinction, performance strategy, etc). This complexity means that the issue should be dealt with from a multidisciplinary perspective, with the intervention of both public institutions and the research community. The fundamental aim of the research community is to understand the behavior of forest fires and to develop tools and resources that the civil service and firefighters can use to tackle forest fires effectively and at a suitable speed.

In this chapter we define the basic terms used by the research community to characterize the phenomena and variables associated with forest fires.

1.1 Important characteristics of forest fires

1.1.1 Combustion in forest fires

Combustion is defined as a chemical reaction in which, with the simultaneous presence of reagents (fuel and oxygen) and an initial external heat contribution, new substances are generated (combustion products) and energy is released. The conditions under which combustion occurs often prevent the complete reaction from taking place. In this case, other compounds derived from the partial decomposition of the fuel may be obtained, in addition to carbon dioxide and water. In forest fires the combustion reaction is normally incomplete.

The combustion reaction in forest fires generally produces a flame and can be broken down into three stages:

- Ignition: This is generically defined as the phase in which an external heat supply initiates the combustion reaction. First, the moisture content of the fuel evaporates at a temperature close to 373K. Next, the pyrolysis phase begins, during which the contributed heat causes thermal decomposition of the fuel and evaporation of volatile compounds. This process begins at approximately 473K. Finally, when the appropriate amount of gaseous phase is mixed with oxygen, ignition can occur. The heat contribution activates the combustion reaction at a temperature of approximately 600K [3-5].

- Combustion: This stage corresponds exactly to the interval in which the combustion reaction takes place continuously, consuming fuel and oxygen.

- Extinction: The combustion phase continues for as long as both reagents are present and the heat released is sufficient to sustain the evaporation

of fuel. If either of these conditions is not met, the combustion reaction stops and the extinction phase occurs.

When the combustion reaction with presence of flame stops, and if suitable conditions exist, glowing combustion can occur. This is the residual reaction that takes place during the final stages of forest fires. In this case the residue, which is rich in carbon and contains no volatile compounds, continues to burn slowly. Smoldering combustion, another type of combustion without flame, can occur in porous material that has not been converted into char. This type of combustion takes place slowly at low temperatures and is typical of ground fires (see the following section).

1.1.2 Types of forest fires

Forest fires are classified generically according to the type of fuel that promotes propagation and sustains burning. Forest fires involving different strata are: ground fires, surface fires and crown fires. These fires may occur jointly or successively during the course of a forest fire because multiple factors take part in the appearance of one or another type of fire. Some authors [6] use the concept of 'integral fire' to refer to fires involving all vegetation strata. Below, we define the specific features of ground, surface and crown fires.

Ground fires

In this type of fire the organic material between the surface litter and the mineral soil (including duff, tree or shrub roots, peat and sawdust) is consumed. Ground fires support glowing combustion, so they are usually detected when smoke is emitted. They propagate slowly due to the limited presence of oxygen, but the combustion reaction is maintained for days or even weeks, even if the organic material has a high moisture content, causing severe ecological damage.

Surface fires

In this type of fire loose surface debris (including dead branches and leaves) and low vegetation are burned. The behavior of a surface fire varies greatly depending on the type of vegetation involved. This category includes fires burning in vegetation consisting predominantly of shrubs, brush and scrub.

Crown fires

Crown fires advance in the tree crowns. Surface and crown phases may propagate as a linked unit (active crown fire) or independently (independent crown fire). Consequently, the intensity of the fire depends on the vertical

continuity of the different strata, the volume and arrangement of the aerial fuel, and the percentage of fine fuel present at the tree crown [7].

1.1.3 Characteristics of forest fuels

Forest fuels can be characterized microscopically and macroscopically. Microscopic analysis refers mainly to the intrinsic characteristics of the fuel particles, i.e. thermal, geometrical and chemical properties. The macroscopic description refers to the arrangement of the fuel within a natural setting. Below, we define the main microscopic and macroscopic characteristics of forest fuels and include a section on their relative moisture content.

Fuel moisture content

The moisture content of a fuel (%) is defined as the amount of water per unit mass of oven-dried fuel (dry basis). It can also be expressed per unit mass of total moist fuel.

Live fuel moisture content depends on the vegetative conditions of plants, which vary greatly between species and within seasons. In contrast, dead fuel moisture content depends mainly on environmental conditions: rainfall, wind, temperature, air humidity, solar radiation and topography. Moreover, changes in moisture content due to meteorological alterations are faster as the size of the fuel particles is smaller.

Forest fuel moisture content is a very important variable when considering the propagation of forest fires, because a fraction of the energy released during combustion is used to evaporate the water content of the vegetation adjacent to the fire front. If the energy release is not sufficient to evaporate this water content, ignition does not take place and the combustion reaction stops.

Chemical composition of forest fuel

Forest fuels have an approximate content of carbon, oxygen and hydrogen of 50, 44 and 5%, respectively (% in mass). Plants cell walls consist mainly of-long chain organic molecules (polymers), the most quantitatively important of which are as follows:

- Cellulose: Polysaccharide consisting of parallel unbranched chains of β-D-glucose units cross-linked in a stable structure. The combustion reaction of this carbohydrate takes place at 573-673K [8].

- Hemicellulose: Branched polymer consisting of shorter chains than cellulose that mostly contain pentoses and hexoses. The combustion reaction of this carbohydrate takes place at 523K and its complete degradation is at 773K.

- Lignin: Aromatic carbohydrate polymer consisting of various monomers of phenylpropane. It is thermally stable and slowly volatilizes as temperature increases. Only a loss of 50% of its weight is normally observed at 773K [8].

Forest fuels contain other types of compounds that are less quantitatively important than the above but which play an important role in determining a plant's flammability. These compounds include the following:

- Extractives: A complex mixture of compounds (inositols, amino acids, simple fats, carboxylic acids, terpenes, phenolic compounds, etc.) which can be removed from the plant by solvents (ether, benzene, acetone, ethanol, water, etc.). They are not part of the cell wall structure but have important functions, such as mediating in metabolic processes or protecting agents against parasites. Wood contains about 1 and 5% of extractives, but this percentage may vary depending on species and their location in wood. Some compounds, such as terpenes, have relatively low boiling points and therefore volatilize easily.

- Minerals: Wood usually contains less than 2% of mineral ashes, whereas vegetation leaves may have a percentage in the range 5-10%. Silica-free minerals act as pyrolysis catalysts, promoting char formation at the expense of volatile inflammable compounds. Thus, species with a high silica-free mineral content form smaller flames than those produced by species with a lower mineral content.

Table 1.1 shows the composition of two species. The figures in this table cannot be taken as absolute values, since they can vary considerably depending on the geographic area in which the vegetation sample was collected, the time of the year, species age, etc. However, the table can be used to establish general comparisons between the two species shown. Straw and pine needles of various species are commonly used in laboratory simulations of forest fires. The figures in Table 1.1 show that straw has a higher mineral content than pine needles, whereas pine needles contain larger amounts of lignin and extractives. The percentages do not total 100% because forest fuel contains other, less abundant

compounds in addition to those shown in the table (starch, proteins, monosaccharids, etc.).

Table 1.1 Biochemical composition of two plant species. Figures are based on dry weight and presented as units of % mass. Data for *Triticum turgidum* straw and *Pinus pinaster* needles are taken from [9] and [10], respectively. Extractives percentage corresponds to those compounds that can be removed by ethanol and benzene.

Species	**Cellulose**	**Hemicellulose**	**Lignin**	**Extractives**	**Minerals**
T. turgidum straw	34.78	17.88	20.11	7.04	6.52
P. pinaster needles	28.75	16.16	24.36	15.82	3.08

Thermal conductivity

Thermal conductivity (W m^{-1} K^{-1}) is a measure of the ability of a substance to conduct heat. Several variables may change the value of this property, such as fuel density, fuel moisture content, heat flux direction (e.g. longitudinal or radial with respect to growth rings), and imperfections such as knots and temperature. In general, this variable increases with density, moisture and temperature. Thermal conductivity is a useful variable for calculating heat transfer by conduction.

Specific heat, heat of pyrolysis and heat of ignition

The specific heat (J kg^{-1} $°C^{-1}$ or J kg^{-1} K^{-1}) is the amount of heat required to raise the temperature of a unit mass of substance by one degree, without transforming the substance from one thermodynamic state to another. In wood, the value of this variable depends mainly on temperature and is largely independent of fuel density and species. The equation most commonly used to calculate the specific heat of forest fuels was formulated by Dunlap [11] and is shown below as Eq. [1.1]:

$$c_s = 1110 + 4.86\,T_c \qquad [1.1]$$

The specific heat term has been used by several authors [12-14] to determine the heat required to ignite an elemental fuel particle positioned in front of a flame front. This is calculated using Eq. [1.2], below:

$$Q_{ig} = c_s\left(T_{ig} - T_a\right) + M_w[c_w(T_{eb} - T_a) + L_w] \qquad [1.2]$$

However, Wilson [15] showed that the first term on the right-hand side of Eq. [1.2] could be determined more exactly if the concept of heat of pyrolysis was used. This term represents the heat required to pyrolize a unit mass of fuel. It can be calculated by integrating differential scanning calorimetry curves obtained under pyrolytic conditions, from 25°C to 400°C. Forest fuel decomposition takes place at 200-400°C. In this temperature range, both the specific heat and the reaction enthalpy associated with the production of pyrolysis gases contribute to the heat needed to produce enough gaseous phase to support flaming combustion. This is why Wilson considered that Eq. [1.2] estimates only a "heat of preignition". According to Wilson [15] and Catchpole et al. [16], the heat of ignition is more accurately defined using Eq. [1.3], below:

$$Q_{ig} = Q_p + M_w[c_w(T_{eb} - T_a) + L_w] \quad [1.3]$$

Heat of combustion

The heat of combustion (kJ kg^{-1}) is the amount of energy released when a given mass of a substance is burned completely to form incombustible products (e.g. water and carbon dioxide). This energy may vary depending on species, location in wood and fuel moisture content. The heat of combustion of forest fuels must be determined experimentally because the exact formula of all of the molecules in forest species is unknown. Heat of combustion of forest fuels is a crucial variable in quantifying the exact calorific power released by a flame front. Distinctions are made between high heat of combustion, low heat of combustion, and heat of combustion of the volatiles.

The high heat of combustion is the heat released per unit mass of dried fuel under complete combustion conditions in a bomb calorimeter. The water of reaction is collected as a liquid in the bomb calorimeter.

The low heat of combustion is the heat released per unit mass of dried fuel under complete combustion conditions in a bomb calorimeter after correcting the experimental value to take into account that the water of reaction is released as vapor.

The heat of combustion of the volatiles is the heat released per unit mass of dried fuel due to combustion of the volatiles generated during pyrolysis of the forest species. This value is usually calculated indirectly, by subtracting the product of the char fraction and the low heat of combustion of the charred residue from the low heat of combustion of the forest species.

Fuel loading

Fuel loading is defined as the amount of fuel present expressed quantitatively in terms of weight of fuel (in a dry basis) per unit area. This variable is usually expressed in kg m^{-2} or tn ha^{-1}; however, in wooded areas it is more commonly expressed as stems ha^{-1}.

Size and shape of forest fuels

The size and shape of forest fuels are usually expressed in terms of surface area-to-volume ratio. The smaller the particle, the more quickly it can become wet, dry out or become heated to combustion temperature during a fire. Consequently, fine fuels (those which are less than 6 mm in diameter and have a comparatively high surface area-to-volume ratio) ignite readily and have a significant influence on fire propagation.

Bulk density and packing ratio

The bulk density (kg m^{-3}) is the weight of dry fuel per unit volume of fuel bed, considering the fuel bed as an array of fuels. Bulk density is always lower than fuel density because part of the volume considered when calculating bulk density is occupied by air.

The packing ratio (%) is the fraction of a fuel bed occupied by fuels, or the ratio between bulk density and fuel density. The packing ratio is a measure of the empty space in the fuel bed. Fire propagation is generally more difficult as the packing ratio increases, because it becomes harder for air to penetrate the fuel bed.

Forest fuel arrangement

The arrangement of vegetation over the terrain has an enormous influence on fire behavior. Two generic arrangements are distinguished according to orientation: vertical and horizontal. Grass, shrubs and trees are arranged vertically, while branches and debris have a horizontal arrangement.

Horizontally arranged fuels determine fire propagation; when they are dispersed fire propagation is difficult, whereas when they are distributed continuously and uniformly fire propagation is assured. The vertical arrangement of fuels determines which part will be involved in the fire; when there is vertical continuity between strata, the fire may start by affecting litter and then progress to crowning. This type of situation could alter the fire behavior significantly.

Flammability of forest species

The flammability of forest species derives from a combination of ignitability, sustainability and combustibility. Ignitability determines how easily a fuel ignites. Sustainability is a measure of how well a fire burns with or without a heat source. Combustibility reflects how easily a fuel is consumed.

Combustibility of natural fuel arrays can be characterized by classifying fuel arrangements according to the values of those variables that are most sensitive to propagation. The most well-known modeling system was developed by Anderson [17], who sorted natural settings into 13 categories according to fuel loading, size, shape and height, and bulk density.

1.1.4 Heat transfer mechanisms involved in forest fire propagation

Forest fires are characterized by heat transfer. The type and amount of heat transferred affects the propagation rate of forest fires, and combustion cannot be maintained without a continuous heat transfer. Heat is transferred through conduction, convection and radiation, which occur simultaneously during fires. However, the relative importance of each of these transfer mechanisms varies according to the intensity of the fire and the configuration of the system in which propagation takes place.

Conduction

When a solid fuel burns, the mechanism by which heat is transferred through the internal parts of the fuel is called conduction. In forest fire propagation, the heat contribution of conduction is generally minimal [18]. However, behind the zone of an advancing fire, conduction is responsible for the continued burning of trunks, branches and other combustible fuel that has initiated the combustion process. Consequently, conduction is responsible for residual combustion, which can reactivate fires.

Convection

In forest fires, a large proportion of the heat generated is transferred by convection. Air is heated through contact with the flames' front surface, and smoke produced during combustion constitute a hot mass of fluid that leaves the flame front surface at a given velocity, which depends on ambient wind and fire intensity. The hot mass of fluid enters in direct contact with other surfaces, such as leaves, branches and tree trunks, which are heated and can ignite. This heat transfer mechanism is predominantly vertical, so in a surface fire the hot mass of fluid contributes greatly to the heating of crowns.

Radiation

Radiation, together with convection, is the principal means of energy transfer in forest fires. Radiation heats fuel before the arrival of the flame front and is considered to be the most important mechanism in preheating fuels. Thermal radiation is the emission of energy by electromagnetic waves from a substance which is at a certain temperature. Flame radiation comes from the mixture of gases (CO_2 and H_2O) and soot, although in forest fires flames are soot-dominated.

1.1.5 Geometric and physical characteristics of forest fires

Geometric and physical characteristics are essential in describing and understanding forest fire behavior. This section presents the principal terminology used to describe the dimensions of forest fires, and the main physical variables used to characterize forest fire behavior.

Morphology and geometry of forest fires

Forest fires generally have irregular shapes. A forest fire can be separated into the following main areas:

- Head: The most rapidly spreading portion of a fire's perimeter, usually to the leeward or up slope.
- Rear: The portion of a fire edge opposite to the head.
- Flanks: The part of a fire's perimeter that is roughly parallel to the main direction of spread. It is located between the head and the rear.

Irregularities in forest fires can be seen in the formation of fingers (long narrow extensions projecting from the main body of the fire), islands (unburned areas within a fire's perimeter) and spot fires.

The principal geometric variables used to characterize forest fires are flame height, depth, length and angle. Flame length and angle can be defined according to several references; Figure 1.2 illustrates the geometric characteristics of flames, including the different options for defining flame length and angle. Anderson et al. [19] proposed the following definitions as possible standard measurements:

- Flame height (m): The average maximum extension of flames, perpendicular to the ground surface, measured from the tip of the flame to the ground surface (H).

- Flame depth (m): This is the distance from the front to the rear of the flame front within which flame combustion takes place continuously (D).

- Flame length (m): Considering as reference the leading edge of the flame front, the distance between the flame tip and the ground surface (L_e).

- Flame angle (radians or degrees): Angle between the flame at the leading edge of the fire front and the ground surface (β_e).

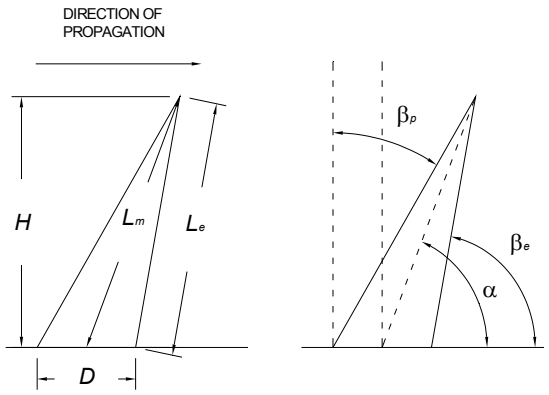

Figure 1.2 Flame measurements (based on [19]).

Knowledge of flame characteristics in free-burning fires is important in determining many aspects of fire behavior and effects. Flame length gives an estimation of fire intensity and, by extension, of fire effects. Flame height is important in determining crowning potential and estimating scorch height, which gives an indication of the possible fire effects. In addition, knowledge of flame height and flame angle is needed to determine the amount of radiative heat transfer. Finally, flame characteristics provide complementary information that is useful in determining an overall suppression strategy.

Combustion rate

The combustion rate is rate of fuel consumption per unit of time per unit of burning area (kg s^{-1} m^{-2}) or per unit of front length (kg s^{-1} m^{-1}). Some authors use the term rate of mass loss. This variable is related to the rate of heat release.

Fuel consumption ratio

The fuel consumption ratio is the ratio between the fuel loading of consumed fuel and the initial fuel loading. It is often expressed as a percentage. This variable gives an idea of the quality and completeness of the combustion reaction. It is generally accepted that fuels of less than 6 mm in diameter will be completely consumed in forest fires.

Rate of spread

The rate of spread is the extension covered by the flame front per unit of time (m s^{-1}). It is one of the most common variables for describing forest fire behavior.

Calorific power, fireline intensity, emissive power and irradiance

Calorific power is defined as the amount of energy released by the flame front per unit time. If it is expressed per unit length of fire front, it is called fireline intensity.

The fireline intensity (kW m^{-1}) is a variable commonly used to measure the calorific power of forest fires. Byram [20] developed the following equation, which is generally used to determine this variable (Eq. [1.4]):

$$I_B = (HHC - 1263 - 24M_w)\, w_a\, R \qquad [1.4]$$

The heat transfer mechanism behind the calorific power can also be differentiated. Radiant calorific power is the energy emitted through radiation per unit time from a flame front. If this power is expressed per unit area of radiant surface, the emissive power of the flame front is obtained (kW m^{-2}). The emissive power is essential in the development of propagation models because, as stated above, radiation is one of the most important heat transfer mechanisms. The emissive power of flames is generally expressed using the Stefan-Boltzmann law, although it can also be estimated using Eq. [1.5] if it is considered that the flame front behaves like a body with a given geometry which emits radiation uniformly from its surface.

$$E_f = \varepsilon_f\, \sigma\, T^4 \qquad [1.5]$$

Finally, thermal irradiance (kW m^{-2}) is the heat flux transferred through radiation to a surface or body located at a given distance and height. It can be estimated using Eq. [1.6], below:

$$q''_{rt} = E_f \, \tau_a \, F \qquad [1.6]$$

1.1.6 Factors influencing forest fire behavior, other than fuel characteristics

The magnitude of forest fires can be determined from physical parameters (rate of spread or fireline intensity) or calculated from the direct consequences of these parameters (number of hectares burned, fatalities, public expenditure on prevention and extinction, etc.). Forest fire behavior is influenced by many variables and by the complex interactions between them. Factors such as rainfall and wind patterns, prevention activities, relief, arrangement and chemical composition of fuels, or the organization of staff and equipment in fire suppression, are directly or indirectly related to the causes, evolution and effects of forest fires.

This section focuses on the most important factors that influence the evolution of forest fires, and groups them in the following categories: meteorological and topographic. Factors related to fuel characteristics are presented in Section 1.1.3; they represent only a small proportion of the many variables that interact in forest fires, but are essential to understanding the development of this phenomenon from a scientific perspective.

Meteorological factors

Climate and meteorological conditions encompass a set of variables that exert an important influence on the development of forest fires. For example, solar radiation and air temperature affect the flammability of forest fuels, air humidity influences ignition and propagation, atmospheric stability partly determines fireline intensity and fire behavior, and wind velocity and direction alter the general fire behavior. Wind is probably the most influential factor. Wind tilts flame fronts, which increases heat transfer through radiation. In addition, in the presence of wind, unburned fuel is also heated to a greater extent through convection and through conduction due to the direct contact between flames and fuel. Wind guarantees a higher oxygen contribution, thus increasing the efficiency of the combustion reaction, and contributes to the drying of unburned fuel, which promotes ignition. In combination, these effects lead directly to an increase in the rate of spread of the flame front.

In addition to the rate of spread, wind affects several other aspects of forest fires, in particular the morphology of the fire perimeter and the appearance of spotting behavior (embers carried out of the main fire by the wind start new fires outside the area of direct ignition).

Topographic factors

Topographic factors influence forest fire behavior through their direct correlation with the propagation of flame fronts and due to their connection with certain vegetation characteristics and meteorological factors. For a given period of time, topographic factors are more constant than meteorological factors, which make their influence on fire behavior easier to predict. Topographic elements which can exert a significant influence on the development of a forest fire include slope, orientation, relief configuration and elevation. Slope is the most influential variable; its effect is similar to that of wind [3,7,21], in that slope also causes tilting and extension of the flames and the convection column, which increase the rate of spread. The main difference between the influence of wind and slope lies in the magnitude of the effect. For example, a forest fire propagating under strong wind extends its horizontal dimensions 100 times faster than under calm conditions. However, the equivalent effect of slope is an increase that does not exceed a factor of 20 [22].

1.2 Methods of forest fire suppression

Two levels of action can be taken against wildfires: prevention and extinction. Measures aimed at reducing the incidence of fires (prevention level) include public education, law enforcement, fuel management, risk prediction, and management of preventive infrastructures (roads, water sources). Extinction encompasses all fire suppression work carried out with a selection of the most effective resources available (staff, aircrafts and fire engines).

Extinction also includes the approval of an attack plan, which details the selected course of action and the organization of staff and equipment. Three important aspects have to be considered when planning extinction operations: strategy, tactics and operational period. Strategy refers to the general plan or direction selected to accomplish the incident objectives. Deployment and direction of resources to accomplish the strategic objectives fall under the category of tactics. The operational period is the time scheduled for the execution of a given set of tactical actions. Two extinction methods are used to fight wildfires: direct attack and indirect attack.

Direct attack

Direct attack refers to any treatment applied directly to burning fuel, such as wetting (with water) or smothering (with fire beaters). The first firefighting staff to arrive at a wildfire are likely to use direct approaches, because at this stage the characteristics of the fire make it more feasible to carry out this type of

action. Water mixed with chemical products (see Section 1.3) can also be applied directly to burning fuel. However, depending on the type of product, more effective use is made by applying the mixture at a reasonable distance from the flame front.

Indirect attack

Indirect attack refers to suppression methods in which the control line is located at a considerable distance from the active edge of the fire. This type of approach uses natural or constructed firebreaks or fuel breaks and favorable breaks in the topography and is generally applied to fast-spreading or high-intensity fires.

The basic indirect attack methods are as follows:

- Scratch line and cat line:

  The scratch line is a narrow line quickly cut in the fuel to temporarily stop the spread of fire. Cat lines are constructed using bulldozers or tractor-plows. Both types of lines can be widened later to be used as final control lines.

- Chemical firebreaks (wet and retardant lines):

  Chemical firebreaks are lines constructed using chemical products, such as short-term or long-term retardants (see Section 1.3). If the line is constructed using foams, it is normally referred to as a ‘wet line’. The term used to characterize lines constructed using long-term retardants is ‘retardant line’. Chemical firebreaks are not considered as final control lines, since these must be cut through the fuel to mineral soil.

- Control line:

  The control line is projected in the extinction plan as the perimeter of the fire. Control lines are normally constructed close to natural or constructed firebreaks.

- Burning-out:

  Burning-out is the use of fire to remove the unburned fuels between the fire perimeter and the control line. It is used to clean up and straighten lines, and widen natural or existing barriers.

- Backfire:

  Backfiring is a special technique requiring extensive planning. It is used to control high-intensity fire fronts that would overrun firelines if they could not be slowed or stopped. It is essential for the main fire to draw the backfire towards it for this technique to work.

1.3 Chemical products used in forest fire suppression

Three types of chemical products are commonly used in wildland fire management: foams, gels (or water enhancers) and long-term retardants.

Foams and gels are also known as short-term retardants because their effectiveness is dependent on the water they contain, and once all of the water has evaporated they are no longer effective. They can be applied using aerial or ground equipment to the fire area to slow or stop combustion.

Foam concentrates are added to water to create a foam solution that can be used as a wetting agent or to create foam when aerated. Foams insulate, envelope and penetrate fuels, act as heat sinkers, exclude air, raise humidity at the fuel's surface, isolate and dilute volatiles, increase the amount of available water and, because they break down in a controlled manner, further wet the fuels they encase [3]. Foams are a highly versatile and universally popular fire suppression material. In Catalonia, they are mainly applied from helicopters during wildfire management operations.

The action mechanism of gels is similar to that of foams, the main difference being that gels have higher viscosities and, as a result, adhere better to fuel surfaces. Thickeners can be added to enhanced water mixtures to improve aerial application, minimize drift and enhance adherence to fuels. Gels consist of macromolecular compounds, known as superabsorbent polymers (SAPs) that can absorb thousands of times their own weight in water. The polymers are formed by three-dimensional cross-linked polymeric structures. Swelling of SAPs is induced by electrostatic repulsion of the ionic charges of their network, which is caused by dissociation of the carboxylic groups (–COONa or –COOK) in solution and allows water to enter the matrix [23]. SAPs are already used to great effect in agriculture, but the potential benefits of their application in wildfire management have yet to be fully harnessed.

Long-term retardants can also be applied using aerial or ground equipment. The retardant is mixed with water in a prescribed ratio and then applied to slow the

spread and reduce the intensity of the fire. These products continue to be effective after their water content has evaporated. Wildland fire retardant mixtures change the preignition pathway from hot, fast pyrolysis to cooler, slow pyrolysis, promoting the production of char and noncombustible gases (CO_2 and H_2O) rather than combustible gases. The chemicals most responsible for retardation are phosphate and sulfate salts. Commercial products commonly contain: (1) retardant salt; (2) colorant; (3) corrosion inhibitor; (4) thickening agent (gum or clay). The last three components prevent the corrosion of aircraft interiors and improve aerial application.

There is no conclusive work on the toxicity of these chemicals to terrestrial plants and animals, since studies usually cover short periods (one or two years) but responses to the burning of terrestrial vegetation are more appropriately measured over the course of several years or even decades. However, some results can be highlighted to illustrate the findings to date. Larson and Duncan [24] found that in the first year after the application of a retardant treatment, fuel loading in treated areas was double that recorded in the untreated area. This is because fire retardants are composed largely of nitrogen and phosphorus fertilizers. It has also been observed that species richness and the number of stems per square meter return to control levels by the end of a one-year study [25]. These results suggested that the effects of treatment with long-term retardants were likely to be transitory. With regard to the toxicity of retardants to aquatic organisms, it is generally accepted that, when dumped into waterways, phosphates can encourage eutrophication, and that sodium ferrocyanide, a corrosion inhibitor still used in some commercial formulations, may contribute to fish kill upon exposure to sunlight [26].

When applying short- and long-term retardants, the concentration of the mixture and the coverage level (liters of solution per m^2) must be established. Manufacturers usually provide information on the ideal mix ratio and coverage level. Vélez [27] collected data on the values used in Spain for these two variables (see Table 1.2 and Table 1.3). The type of fuel is distinguished for coverage levels. The application equipment (ground or aerial) is distinguished for the mix ratio.

Table 1.2 Chemical product and coverage level for different fuel types (LTR: long-term retardants; F: foams).

Type of fuel	**Chemical product**	**Coverage level (l m^{-2})**
Chaparral and shrub fields	LTR/F	1 - 3
Timber litter	LTR	2
Grass and grass-dominated areas	F	0.5 – 1.5
Slash	F	> 2

Table 1.3 Dilution mix ratio for different chemical products and application equipment (n.a.: not applied in Spain).

Application equipment	**Mix ratio (% v/v)**	
	Long-term retardants	Foams
Aerial	20	0.4 – 0.6
Ground	n.a.	0.5 – 1.0

References

1. Department of Environment and Housing, Autonomous Government of Catalonia. Nombre d'incendis per estrats. Source: http://www.mediambient.gencat.cat/cat/el_medi/incendis/doc/estadistiques/estrat.pdf. Last modified: -. Visiting date: 09/06/09.

2. Plana E. Anàlisi d'escenaris de prevenció i extinció d'incendis des de la perspectiva socioambiental. In: Incendis forestals, dimensió socioambiental, gestió del risc i ecologia del foc (Ed. Plana E) Xarxa ALINFO XCT 2001-00061, Solsona, Spain; 2004.

3. Pyne SJ, Andrews PL, Laven RD. Introduction to Wildland Fire. John Wiley and Sons, New York, 1996; 769 pages.

4. Dupuy, JL. Mieux comprendre et prédire la propagation des feux de forêts: expérimentation, test et proposition de modèles. PhD Thesis, Université Claude Bernard – Lyon I, France; 1997.

5. Mercer GN, Weber RO. Fire Plumes. In: Forest Fires: Behaviour and Ecological Effects (Eds. Johnson E, Miyanishi K) Academic Press, London; 2001.

6. Panareda JM, Arola J. Els incendis forestals. EUMO editorial, Vic, Spain, 1999; 136 pages.

7. Trabaud, L. Les feux des forêts. Mécanismes, comportement et environnement. France-Selection Publishers, Aubervilliers, France; 1992.

8. Philpot W. Influence of mineral content on the pyrolysis of plant material. Forest Sci 1970;16(4):461-71.

9. Antolín G, Irusta R. Caracterización de combustibles lignocelulósicos: aplicación a la paja de cereal. Secretariado de Publicaciones, University of Valladolid, Valladolid, Spain; 1989.

10. Vázquez G, Antorrena G, González J, Freire S. Studies on the composition of *Pinus pinaster* foliage. Bioresource Technol 1995;51(1):83-7.

11. Dunlap F. The specific heat of wood. USDA Forest Service Bulletin nº110, 1912; 7-18.

12. Rothermel, R. A mathematical model for predicting fire spread in wildland fuels. USDA Forest Service Research Paper INT-115; 1972.

13. Frandsen W. Effective heating of fuel ahead of spreading fire. USDA Forest Service Research Paper INT-140; 1973.

14. Albini FA. A model for fire spread in wildland fuels by radiation. Combust Sci Technol 1985;42:229-58.

15. Wilson R. Observations of extinction and marginal burning states in free burning porous fuel beds. Combust Sci Technol 1985;44(3-4):179-93.

16. Catchpole W, Catchpole E, Butler B, Rothermel R, Morris G, Latham J. Rate of spread of free-burning fires in woody fuels in a wind tunnel. Combust Sci Technol 1998;131:1-37.

17. Anderson HE. Aids to determining fuel models for estimating fire behavior. USDA Forest Service General Technical Report INT-122; 1982.

18. Chandler C, Cheney P, Thomas P, Trabaud L, Williams D. Fire in Forestry. In: Forest Fire Behavior and Effects vol. 1. John Wiley and Sons, New York, 1983; 450 pages.

19. Anderson W, Pastor E, Butler B, Catchpole E, Dupuy JL, Fernandes P, Guijarro M, Mendes-Lopes JM, Ventura J. Evaluating models to estimate flame characteristics for free-burning fires using laboratory and field data. In: 'Proceedings of the 5th International Conference on Forest Fire Research' 27–30 November, Figueira da Foz, Portugal; 2006.

20. Byram GM. Combustion of forest fuels. In: Forest Fire Control and Use (Ed. Davis KP) McGraw-Hill, New York, 1959; 61-89.

21. Nelson R. An effective wind speed for models of fires spread. Int J Wildland Fire 2002;11(2):153-61.

22. Viegas, DX. Forest fire propagation. Philos T R Soc A 1998;356(1748):2907-28.

23. Davies LC, Novais JM, Martins-Dias S. Influence of salts and phenolic compounds on olive mill wastewater detoxification using superabsorbent polymers. Bioresource Technol 2004;95(3):259-68.

24. Larson JR, Duncan DA. Annual grassland response to fire retardant and wildfire. J Range Manag 1982;35(6):700-3.

25. Larson DL, Newton WE, Anderson P, Stein SJ. Effects of fire retardant chemical and fire suppressant foam on shrub steppe vegetation in northern Nevada. Int J Wildland Fire 1999;9(2):115-27.

26. Little EE, Calfee, RD. The effects of UVB radiation on the toxicity of fire-fighting chemicals. Final Report. US Geological Service, Columbia Environmental Research Center, Columbia; 2000.

27. Vélez R (coordinator). Métodos y medios para la modificacions de los combustibles. In: La Defensa contra Incendios Forestales. Fundamentos y Experiencias (Ed. Grace AG) McGraw-Hill, Madrid; 2000.

CHAPTER 2

General scope and objectives

Over these last decades the problem of forest fires has become more apparent, especially in Mediterranean fire-prone areas. This situation has shown that decision making related to fire management is often handled with little guidance, sub-optimum criteria or unscientific procedures. This issue has also enhanced research and development activities aiming at improving the capability of forest agencies for wildland fire response, particularly getting better decision-making assistance systems for fire management, both at prevention and suppression levels. This PhD Thesis has the final aim of contributing to the decision process knowledge, specifically for long-term retardants use policies.

To efficiently draw up strategies for fighting wildland fires and to establish plans for managing forest areas or grasslands it is necessary to investigate which mechanisms control ignition and propagation of wildland fires. Researchers have been formulating models to describe surface fires and, to a lesser extent, crown fires, for more than sixty years. Mathematical models of wildland fires are generally based on a collection of equations whose solution

provides the spatial/temporal evolution of one or more variables, such as rate of spread, flame height, ignition risk or fuel consumption. In this way, a more or less detailed description of the system behavior is obtained. Wildland fire mathematical models may be classified according to the nature of the equations as physical, quasi-physical, empirical and quasi-empirical models [1].

Physical and quasi-physical models are generated from the laws that govern fluid dynamics, combustion and heat transfer. Physical models (e.g. [2-8]) attempt to represent both the physics and the chemistry of fire spread. They study the behavior of wildfires based on the resolution of balance equations (mass, momentum, energy) governing the evolution of the state of the vegetation and try to describe physical and chemical phenomena involved in wildfires (drying, pyrolysis, combustion, turbulence, radiation, etc.). Quasi-physical models (e.g. [9-16]) attempt to represent only the physics of the phenomenon. They are based on a single equation deduced from a global energy balance set in the fuel medium, i.e., they concentrate on the heat transfer (almost all authors take radiation as the dominant process) between the combusting elements (characteristics describing flames and the solid burning phase are experimentally evaluated) and the unburned vegetation placed at a given distance from the flame front. Sullivan [1] reviewed comprehensively models published in the literature from 1990 to 2007 and discussed several key aspects involved in the design, formulation and implementation of physical and quasi-physical models of fire spread. These are summarized in Table 2.1.

Table 2.1 Key issues involved in the design, formulation and implementation of physical and quasi-physical models of fire spread (based on [1]).

Key issue	**Physical models**	**Quasi-physical models**
Formulation	Formulated as partial or ordinary differential equations which must be solved by numerical methods.	Often in the form of linear differential equations which need to be solved by iterative methods.
Combustion chemistry	Several combustion reactant and product species are considered or an idealized fuel which undergoes direct oxidation is used.	None
Turbulence	Turbulence is increasingly included in a simplified form.	Turbulence is not explicitly included in their formulations.
Radiation	The radiation transfer equation is solved (discrete ordinates method, differential approximation method, surface to surface model).	Surface emission; often a simplified uniform isothermal flame sheet is used as the radiation source.
Input parameters	Large number of input parameters.	Moderate number of input parameters.

Empirical models are composed of statistical correlations extracted from experiments or historical wildland fire studies, and physical and chemical mechanisms involved in the fire spread phenomenon are not taken into account. Quasi-empirical models, the most representative one being the model of Rothermel [17], are proposed from simple, general and theoretical expressions, and they are completed through experimentation. They are based on the principle of energy conservation but heat transfer mechanisms involved in fire propagation are not distinguished.

Although wildland fire spread modeling has expanded to include physical approaches, current operational fire spread models utilize pre-existing empirical or quasi-empirical approaches to simulate the spread of fire across the landscape. In other words, both empirical and quasi-empirical models provide the basis for all current operational fire spread prediction systems used around the world. This is due to the fact that these models have a relatively straightforward implementation and a direct relation to the behavior of fires. As Sullivan [18] reported, most of the simulation models published in the literature from 1990 to 2007 contain the quasi-empirical model of Rothermel [17] as the primary surface spread model.

This research work tries to improve knowledge of the effect of long-term retardants on wildfires spread. Long-term retardants (henceforth referred to as retardants and long-term retardants without distinction) are a significant tool for forest firefighting. The need to predict the effects of these products on fire behavior is longstanding. Many interacting phenomena associated with retardants (type of product, effective coverage level), fuels (type and arrangement) and fire spread (wind- or slope-aided) make this a complex task. Most of the work done to date has actually been on retardant evaluation for commercial purposes, i.e., on the development of procedures to compare one product with another and classify retardant effectiveness, and fewer attempts have been developed to quantify retardants effects for varying fire situations.

Physical, quasi-physical, empirical and quasi-empirical models previously described have a significant shortcoming: none of them has been implemented to predict fire behavior after indirect attack operations with long-term retardants. Moreover, existing simulation models use oversimplified representations of the fire containment and they do not envisage attack with chemicals, except for the widely used simulation model FARSITE [19]. In the simulation model FARSITE this type of operation is implemented but it simulates a chemical drop as a line of specified length/coverage level that is

impermeable to a fire for a specified duration and, after the effectiveness expires, fire may burn across the drop pattern as if the chemical was never applied. This approach applies to short-term retardants operations but is inadequate for the case of long-term retardants.

All mathematical models regardless of the type require some input parameters. These are experimentally set or estimated based on certain relationships and are assumed to keep constant for the situation depicted. These parameters are thermophysical properties related to the arrangement and dimensions of the fuel (fuel loading, fuel density, surface area-to-volume ratio, etc.) or to the thermodynamic system which forest fires represent (heat of pyrolysis, heat of combustion, char yield, specific heat, ignition temperature, chemical kinetic parameters, etc.). Assessing how these input parameters change due to the presence of retardants on the fuel is a first step towards including into spread models indirect attack operations with long-term retardants.

On the basis of the information given in the previous paragraphs, specific objectives established for this work are:

1. To evaluate the use of long-term retardants in Catalonia.

   The analysis of how long-term retardants are used in suppression operations in Catalonia can contribute to identify opportunities for improvement in this area.

2. To study the fire behavior of flame fronts propagating on fuel beds with a retardant-treated strip under the effect of slope or wind.

   Experimental methodologies used to date to characterize retardants effectiveness need to be reviewed before performing propagation tests with long-term retardants. This first step gives an overview of the different type of available data on retardants and helps fixing the experimental methodology to be followed.

   In the literature there are some works in which fire behavior under the presence of retardants has been evaluated, but most of them have been conducted under no-slope/no-wind conditions. These conditions rarely occur in real fire situations, thus in this work the key characteristics used to

describe the behavior of forest fires, i.e., rate of spread, fuel consumption, fire intensity, flame length and flame angle, are estimated for flame fronts propagating on fuel beds with a retardant-treated strip under the effect of slope or wind.

3. To estimate the effect of long-term retardants on the heat of combustion of the fuel.

   Among all the thermophysical properties required a priori to model the propagation of forest fires, those related to fuel structure are not affected due to the presence of retardants. However, on the basis of the action mechanism of long-term retardants, those properties related to the combustion chemistry are certainly affected by the presence of retardants. The heat of combustion, an input parameter required in a great number of propagation models, is a parameter which gives some idea of the type of combustion. Here we try to establish how this parameter varies due to the presence of retardants.

4. To evaluate the effect of long-term retardants on flame emissivity.

   A great part of the calorific energy contributing to the propagation of forest fires is transferred by the mechanism of radiation. In quasi-physical models, the mathematical formulation of the radiation heat transfer corresponding to flames contains a coefficient which corresponds to the emissivity of the flames. Retardants promote CO_2, H_2O and char formation at the expense of volatile compounds. Thus, due to the presence of these products, flame composition is modified. Emissivity values depend on the composition of the flame and for this reason it is reasonable to expect that flame emissivity will be modified due to the presence of retardants. This hypothesis is tested in this work.

References

1. Sullivan A. Wildland surface fire spread modeling, 1990-2007. 1. Physical and quasi-physical models. Int J Wildland Fire 2009;18(4):349-68.

2. Grishin AM. Mathematical modeling of forest fires and new methods of fighting them. Publishing House of Tomsk State University, Tomsk, Russia (Russian translation) 1997.

3. Larini M, Giroud F, Porterie B, Loraud JC. A multiphase formulation for fire propagation in heterogeneous combustible media. Int J Heat Mass Tran 1997;41(6-7):881-97.

4. Linn R. A transport model for prediction of wildfire behavior. Los Alamos National Laboratory, Scientific Report LA 13334-T; 1997.

5. Morvan D, Dupuy JL. Modeling the propagation of a wildfire through a Mediterranean shrub using a multiphase formulation. Combust Flame 2004;138(3):199-210.

6. Morvan D, Méradji S, Accary G. Physical modelling of fire spread in grasslands. Fire Safety J 2009;44(1):50-61.

7. Mell W, Jenkins MA, Gould J, Cheney P. A physics based approach to modeling grassland fires. Int J Wildland Fire 2007;16(1):1-22.

8. Séro-Guillaume O, Marguerit J. Modeling forest fires. Part I: A complete set of equations derived by extended irreversible thermodynamics. Int J Heat Mass Tran 2002;45(8):1705-22.

9. Albini FA. A model for fire spread in wildland fuels by radiation. Combust Sci Technol 1985;42:229-58.

10. Albini FA. Wildland fire spread by radiation, a model including fuel cooling by convection. Combust Sci Technol 1986;45:101-13.

11. De Mestre N, Catchpole E, Anderson D, Rothermel R. Uniform propagation of a planar fire front without wind. Combustion Sci Technol 1989;65:231-44.

12. Balbi JH, Santoni PA, Dupuy JL. Dynamic modelling of fire spread across a fuel bed. Int J Wildland Fire 1999;9(4):275-84.

13. Catchpole WR, Catchpole EA. The second generation US firespread model. Final report of RMRS-94962-RJVA, 2000. Joint research venture of the US Forest Service and ADFA.

14. Vaz G. Modelação de propagação de uma frente de chamas em linha num leito sólido poroso na ausência de declive ou vento. PhD Thesis, Universidade de Coimbra, Portugal; 2001.

15. Simeoni A, Santoni PA, Larini M, Balbi JH. Reduction of a multiphase formulation to include a simplified flow in a semi-physical model of fire spread across a fuel bed. Int J Therm Sci 2003;42(1):95-105.

16. Simeoni A, Santoni PA, Larini M, Balbi JH. Proposal of theoretical improvement of semi-physical forest fire spread models thanks to a multiphase approach: Application to a fire spread model across a fuel bed. Combust Sci Technol 2001;162(1):59-83.

17. Rothermel, R. A mathematical model for predicting fire spread in wildland fuels. USDA Forest Service Research Paper INT-115; 1972.

18. Sullivan A. Wildland surface fire spread modeling, 1990-2007. 3. Simulation and mathematical analogue models. Int J Wildland Fire 2009;18(4):387-403.

19. Finney MA. FARSITE 3.0 Help. FARSITE Fire Area Simulator, Version 3.0.91; 1999.

CHAPTER 3

Fighting fires with chemicals in Catalonia

Both foams and long-term retardants are currently used in Catalonia for the suppression of wildland fires. Foams are generally applied from helicopters or trucks, whereas long-term retardants are only dropped from fixed-wing aircraft.

This section is used to present data on the volume of water, foam and long-term retardant dropped from aircrafts between June and September in the period 2000-2005. Only the period from June to September is considered in this case because wildfire risk is generally higher during these months. Data on retardant drops are related to the number and type of fires, and the situation of the ignition point at the territory.

Fire suppression coordination staff were consulted about their opinion on the use of long-term retardants, and their responses are evaluated for application tactics, effectiveness and logistics.

The aim of these two analyses is to characterize quantitatively the use of chemical products – particularly long-term retardants – in Catalonia.

3.1 Wildland fire occurrence and volume of water, foam and long-term retardant dropped from aircrafts during the period 2000-2005

The period 2000-2005 was characterized by clearly differentiated forest fire campaigns, which can be used to characterize the application of chemical products in fire suppression operations in Catalonia. On the one hand, as in Figure 3.1, in 2000, 2003 and 2005 more than 4000 ha of grassland and forest were burned between June and September. The highest value was recorded in 2003, when 9000 ha of grassland and forest were burned. In 2002 and 2004, less than 1000 ha of grassland and forest were burned and approximately 300 fires broke out, which are the lowest figures for the overall study period. In 2001, although a relatively high number of forest fires were recorded (more than 450), the total burned area was less than 3000 ha, and approximately 58% of this area was burned during a single forest fire in the municipal district of Cadaquès in June.

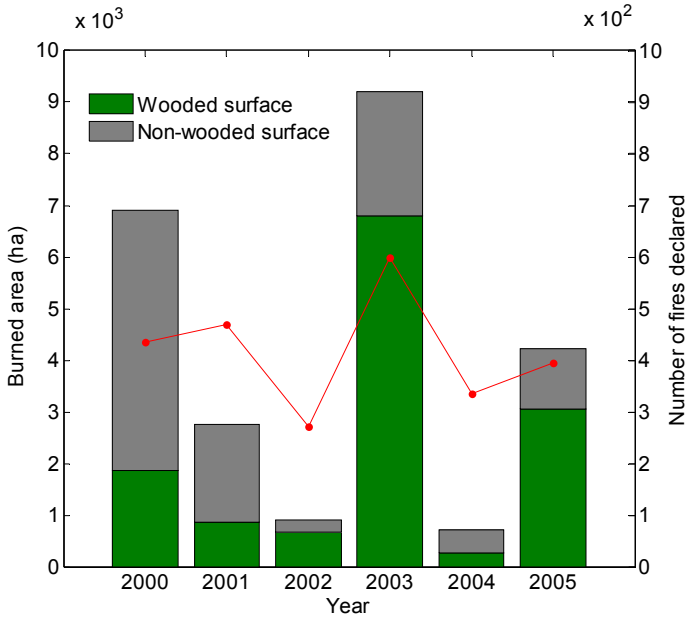

Figure 3.1 Burned area and number of forest fires declared during the period 2000-2005 (months: June, July, August and September). Source: [1].

Figure 3.2 contains six maps of Catalonia showing boundaries between municipal districts. Each map corresponds to a year in the study period. Municipal districts are colored according to the number of hectares burned (see legends) by fires that broke out in the district during the period June-September. The size of the colored areas bears no relation to the number of

hectares burned and simply indicates the geographical limits of each district. The maps were generated using data from the Catalan government's database on forest fires [2]. Figure 3.2 differentiates forest fires according to burned area and also shows the distribution of fires across Catalonia during the study period. The maps shown and the data from which they are generated can be used to make several observations about the locations of forest fires.

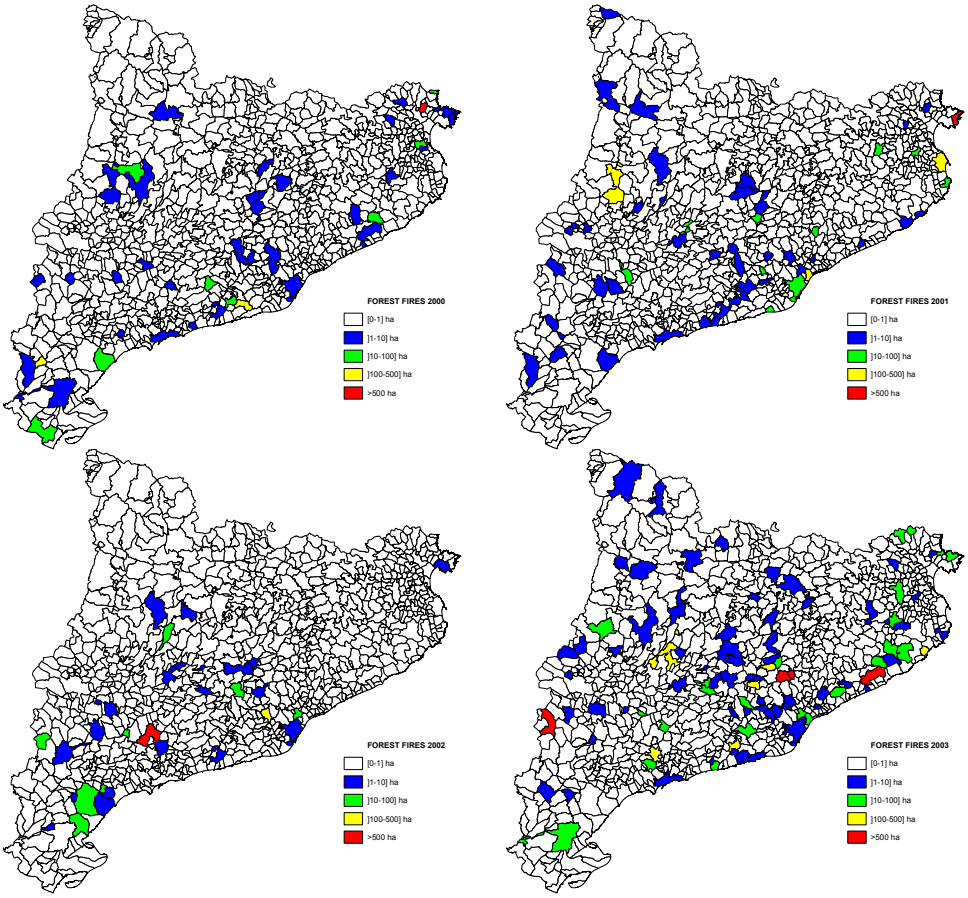

Figure 3.2 Area burned (hectares) in fires that broke out in the municipal districts of Catalonia. Period: 2000-2005 (months: June, July, August and September).

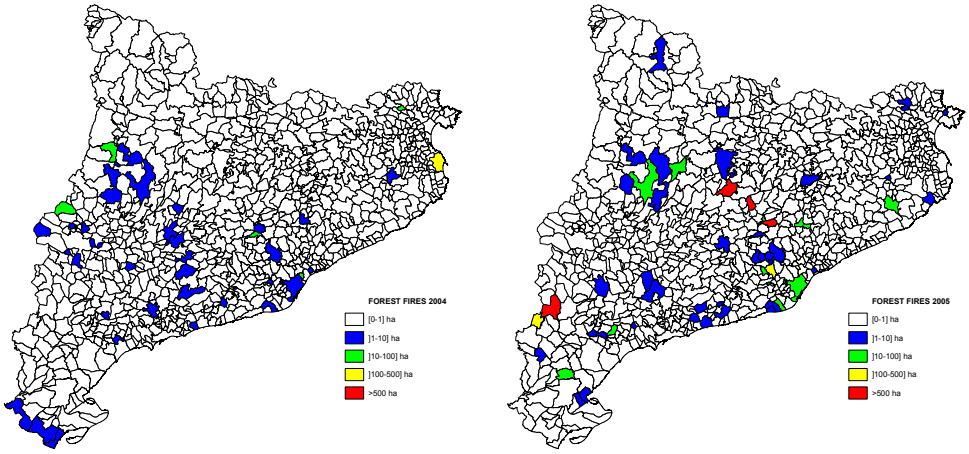

Figure 3.2 Area burned (hectares) in fires that broke out in the municipal districts of Catalonia. Period: 2000-2005 (months: June, July, August and September) (continued).

In 2000 a forest fire broke out in the municipal district of Garriguella, which devastated 6000 ha. This district is located at Serra de l'Albera, a region declared of natural interest. In 2001 a large forest fire (1600 ha of grassland and forest burned) broke out in the district of Cadaquès. Most of this district forms part of the Cap de Creus natural park. In 2002 there was only one large fire, which broke out in the municipal district of Montblanc and burned 520 ha of grassland and forest. Notable, in the same year a fire also broke out in the municipal district of Castellbisbal (130 ha of grassland and forest burned), which is a highly urbanized area. Also in 2002, fires affecting between 1 and 100 ha broke out in two municipal districts located close to the nuclear power stations in Ascó and Vandellós. In 2003, large forest fires broke out simultaneously in the municipal districts of Seròs (1500 ha burned), Gallifa (1240 ha burned), Sant Llorenç Savall (2950 ha burned) and Tordera (930 ha burned), all in the period 10-13 August. In 2004, only one forest fire of note was recorded, which broke out in the municipal district of Torroella de Montgrí and burned 500 ha of grassland and forest. Four large fires were reported in 2005, which broke out in the municipal districts of Talamanca (770 ha burned), Cardona (1230 ha burned), Castellnou de Bages (850 ha burned) and Riba-Roja d'Ebre (590 ha burned). During the same year, another two forest fires broke out simultaneously (reported on 5 July) in highly urbanized areas, one in the municipal district of Barcelona (11 ha burned) and the other in Castellbisbal (200 ha burned).

Figure 3.3 shows the total volume of water, foam and long-term retardant dropped from aircraft during summer campaigns over the period 2000-2005. The total volume of water dropped was largely constant during the period

2000-2003 and in 2005 (mean value: $1.9 \cdot 10^3$ m^3). However, in 2004 the amount of water dropped was 76% lower than this mean value. The same tendency is shown for foam. However, in 2005 the volume of foam dropped was 42% lower than the mean value for the period 2000-2003. The volume of long-term retardant dropped in 2003 is considerably higher than during the rest of the study period ($2.7 \cdot 10^3$ m^3). Lower-than-average volumes were dropped in 2002 and 2004; the two values are similar but their mean is 75% lower than the figure for 2003.

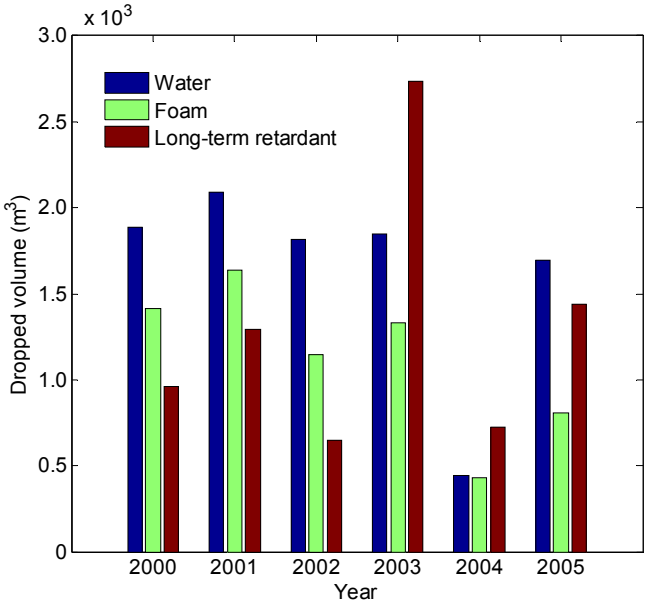

Figure 3.3 Volume of water, foam and long-term retardant dropped from aircraft. Period: 2000-2005 (months: June, July, August and September). Source: [3].

If we compare this figure with Figure 3.1 and consider the locations of fires shown in Figure 3.2, we can conclude that the maximum volume of retardant dropped in 2003 could be due to the simultaneous occurrence of large forest fires. Pronounced differences between the volumes of water and foam dropped in 2002 and 2004 – years that show similar figures for total hectares burned and number of fires – might be due to the type of vegetation in the affected areas (more wooded areas were burned in 2002 than in 2004) and the territorial location of fires reported in 2002, which broke out close to urban areas and nuclear infrastructures. The higher risk to human life posed by these fires may have been behind the decision to use firefighting aircraft to suppress the fires rapidly and effectively.

It should also be noted that in the early part of the study period (2000-2002), more foam was dropped than retardant, whereas a higher total volume of retardant was used in 2003-2005. This pattern could be due to the number of large fires (LF) recorded in each period; only one LF per year was recorded during 2000-2002, but four LFs were recorded in both 2003 and 2005. The preference for long-term retardant over foam in the latter period may have derived from the assumption that retardants are more effective than foams.

3.2 Analyzing the use of long-term retardants in Catalonia

During summer 2005 a series of interviews was carried out to obtain information on the use of long-term fire retardants in Catalonia and the views of staff responsible for coordinating fire suppression operations. Several fire chiefs and assistant chiefs from the Fire Department of the *Generalitat de Catalunya* took part in the study.

3.2.1 Methodology

Eleven individual interviews were conducted. Each participant was informed about the aim of the study and requested to answer sincerely. Participants were also asked to give their consent for the interview to be recorded, upon assurance that their responses would be kept anonymous, as it was considered that this would create a more relaxed atmosphere. The informal nature of the interviews meant that on some occasions the conversation focused on certain issues and others were not discussed.

The interviews covered several issues related to the use and evaluation of long-term retardants, which were broadly divided into six groups: personal information, suppression strategies applied with long-term retardants, supply issues, effectiveness evaluation, future perspectives and training of fire staff in the use of long-term retardants.

3.2.2 Results and discussion

The main characteristics of the staff interviewed in the study are shown in Figure 3.4. Forty-five per cent of the participants had more than 10 years of experience in the Firefighting Department, and only 27% had more than 3 years of experience as fire chiefs or assistant chiefs. As such, the study population can be considered comparatively young to be executing the specific functions of their positions.

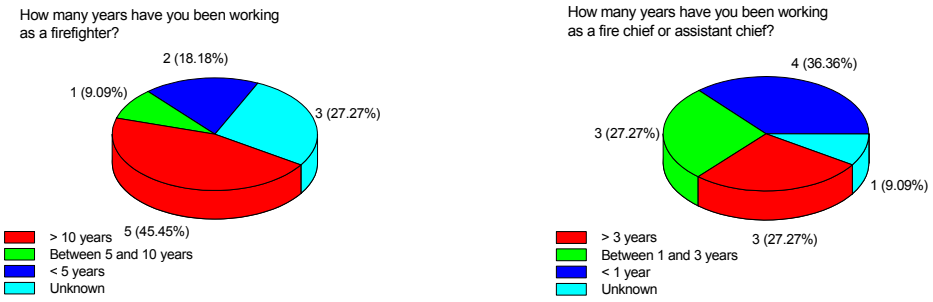

Figure 3.4 Personal characteristics of the study population. Results given as number of people and percentage of total respondents.

The application criteria and tactical actions for long-term retardants are closely related. The main application criteria indicated by the fire staff are shown in Figure 3.5. One of the four criteria clearly concerns the use of retardants in indirect attack operations (criterion (3)), whereas the others are general criteria for carrying out fire suppression activities using aircraft.

Criteria (1) and (2) from Figure 3.6 were the most frequently mentioned tactical actions for long-term retardants. This suggests that most of the interviewed staff oversee the use of long-term retardants in both direct and indirect attack operations. However, in the case of indirect attack operations, retardants are mainly discharged only a few meters away from the flame front.

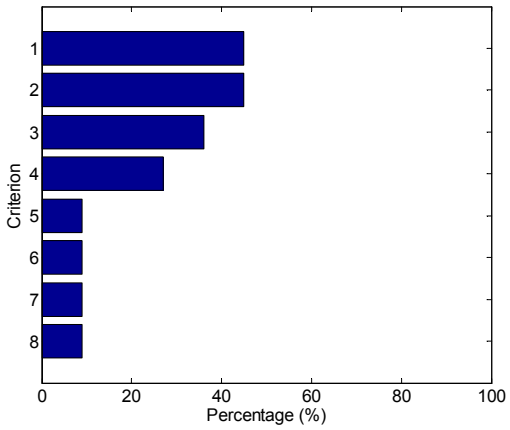

1. **Great difficulty for ground crews and fire engines to access the area of the fire.**
2. **High probability that the fire will affect priority areas (urban areas, nature reserves, transport routes).**
3. **Fire behavior allows suppression strategies to be planned away from active fire fronts.**
4. **It is considered necessary to discharge the retardant from a fixed-wing aircraft.**
5. **High probability of spotting fires.**
6. **High accumulation of dead fine fuel (diameter of fuel < 6 mm).**
7. **Fire intensity very high.**
8. **No criterion is given.**

Figure 3.5 Criteria considered when applying long-term retardants. Note: results do not total 100% because they are taken from a multiple response question.

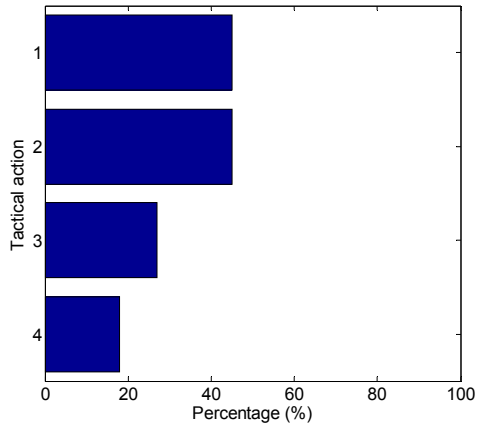

1. **Direct attack, discharging on the flank of the flame front.**
2. **Indirect attack, discharging a few meters away from the flame front with the support of ground crews.**
3. **Indirect attack, discharging on vegetation far away from the flame front.**
4. **Fireline to support backfiring operations.**

Figure 3.6 Tactical actions for long-term retardants. Note: results do not total 100% because they are taken from a multiple response question.

With regard to retardant supply issues, it should be noted that none of the staff interviewed had experienced constraints on the use of retardants due to lack of product. Moreover, the participants were aware of the retardant bases in their local region but did not know about the concentrations and coverage levels usually applied from fixed-wing aircraft. The only weak point stressed by staff was that the ground facilities needed to load the aircraft are unevenly distributed throughout the study area, Catalonia. Nevertheless, it was generally considered that the number of aircraft normally available during the summer campaign was sufficient.

Although water is a valuable cooling agent, the staff interviewed accepted that the effectiveness of extinction operations improves dramatically when water is mixed with long-term retardants. However, in general they were not able to specify a percentage increase in extinction efficiency in comparison with water, as shown in Figure 3.7.

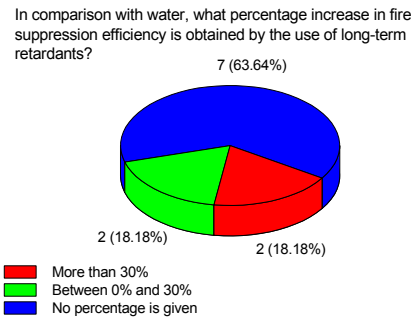

Figure 3.7 Percentage increase in the extinction efficiency of long-term retardants in comparison with water. Results given as number of people and percentage of total respondents.

Most respondents (64%) said that the use of long-term retardants does not make fire suppression much more expensive (see Figure 3.8). This opinion is understandable if we consider that the cost of the retardants is much lower than that of air-tankers. Figure 3.8 shows that 18% of respondents noted this issue.

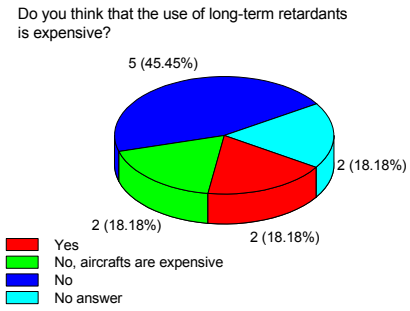

Figure 3.8 Evaluation of the cost of using long-term retardants. Results given as number of people and percentage of total respondents.

When asked about the harmful effects of long-term retardants on the environment, 64% of respondents stated that these products should not be harmful to the environment, given their composition and their approval for public use (Figure 3.9). Only 9% stressed the negative effects of retardants on water ecosystems.

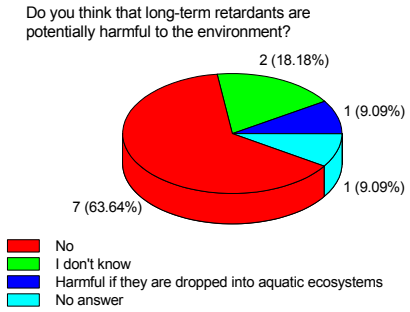

Figure 3.9 Evaluation of harmful effects of long-term retardants on the environment. Results given as number of people and percentage of total respondents.

Fifty-five per cent of the population believed that the prospects for the use of long-term retardants were positive (Figure 3.10), i.e. this percentage thought that the use of these substances would increase in the coming years. However, 27% were more pessimistic, and the remaining respondents did not give an opinion.

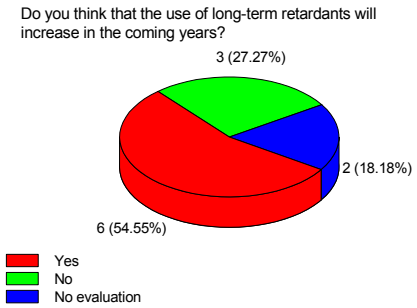

Figure 3.10 Evaluation of the use of long-term retardants in the coming years. Results given as number of people and percentage of total respondents.

On the subject of specific training in the use of retardants, it was pointed out that the basic aspects of long-term retardants are taught at Firefighters' School. Consequently, fire chiefs or assistants who have not worked specifically as firefighters may not have studied the basics. Despite this weak point, the staff interviewed considered that training in the use of retardants was not a prime objective. This view is understandable if we consider that firefighters are required to deal with many different types of incident.

3.2.3 Conclusions

The results obtained in this study show that the fire suppression staff interviewed have a positive view of the efficiency and supply issues (logistics and cost) of long-term retardants. With regard to application criteria and strategies, it has been shown that: (1) application criteria are not different to the general criteria of aerial operations; (2) discharges are usually applied in direct attack operations at the flame front or at a distance of only a few meters. On the basis of these results, it can be said that better use could be made of long-term retardants. Since these products are applied directly to the flame front, their retardant ability "in the long-term", which is actually their main added value with respect to foams and water, is not taken advantage of. Furthermore, according to [4], when retardants are used as fire suppressants in direct attack they provide comparatively little improvement over the use of plain water while increasing the cost. Another important result of this study is that most of the fire staff interviewed were unaware of the harmful effects of long-term retardants on water ecosystems. This may be due to the relatively low level of expertise of the participants. However, it also demonstrates that additional resources may have to be harnessed to integrate environmental issues into the acquisition process.

References

1. Department of Environment and Housing, Autonomous Government of Catalonia. Prevenció d'incendis. Estadístiques d'altres anys. Source: http://mediambient.gencat.net/cat/el_medi/incendis/estadistiques_any_curs.jsp. Last modified: 08/05/2009. Visiting date: 01/06/2009.

2. Department of Environment and Housing, Autonomous Government of Catalonia. Incendis. Source: http://www.mediambient.gencat.net/cat/el_medi/incendis/bdd_estadistiques.jsp. Last modified: -. Visiting date: 01/06/2009.

3. Logistic Support and Aerial Equipment Unit, Autonomous Government of Catalonia. Aerial discharges from 2000 to 2005. Data provided via email. Excel file format.

4. Xanthopoulos G. Chemicals against forest fires: infrastructure and application means, new technologies. Review paper of the ERAS Research Project.

CHAPTER 4

Different scales for studying the effectiveness of long-term forest fire retardants *

Chemical additives are widely used with water to fight forest fires in North America, Australia and the countries of the Mediterranean basin. The factors that influence the effectiveness of a fire-extinguishing operation using chemical additives are the type of product and application, the concentration of the product, the distribution ratio (i.e. coverage level or volume of retardant solution per unit surface area), the fuel type and arrangement, the weather conditions and the fire characteristics. Researchers have studied these factors for long-term retardants since the 1930s and two scenarios have been clearly distinguished. They have studied the application characteristics of the retardant solutions, i.e. the distribution ratios that reached the vegetation layer for different retardant formulations, aircraft models, and drop speeds and heights. This approach was reviewed in detail by Giménez et al. [1] and is a determining factor when evaluating the effectiveness of wildfire operations with retardants. Other research has considered pre-set distribution ratios or treatment levels and studied the behavior of treated fuel under thermal degradation in the

* The content of this Chapter was published as: Àgueda A, Pastor E, Planas E. Different scales for studying the effectiveness of long-term forest fire retardants. Prog Energ Combust 2008;34:782-96. See the first page of this article in the Appendix B.

absence of oxygen (pyrolysis) or in a combustion atmosphere, and the behavioral characteristics of flame fronts propagating on treated fuel. The second approach is reviewed in detail in this chapter.

The first studies of retardant effectiveness were carried out in the USA with water solutions containing different chemicals [2-5]. The most effective of these chemicals in reducing the rate of spread of a propagating front and the radiant heat flux were diammonium phosphate ($(NH_4)_2HPO_4$; henceforth referred to as DAP) and ammonium sulfate ($(NH_4)_2SO_4$; henceforth referred to as AS) [6]. Most subsequent studies analyzed only phosphate and sulfate based compounds to obtain more accurate quantifications of their combustion retarding effectiveness and to identify their basic fire-retarding mechanisms in light of the results of the first studies.

The effectiveness of retardants has been evaluated at three experimental scales. First, tests were done with analytical instrumentation, mainly in order to determine changes in the pyrolytic behavior of samples treated with retardant. Secondly, flame-spread tests in laboratory-scale set-ups were carried out. Finally, propagation experiments similar to laboratory flame-spread tests were performed in field plots with typical vegetation of the study area and under uncontrolled environmental conditions.

In this section we provide descriptions and critical evaluations of the tests carried out at these three levels of experimentation.

4.1 Analytical tests

The main aim of analytical experiments was to obtain data on the effect of retardants on pyrolysis and, to a lesser extent, on the combustion of cellulose and forest fuel particles. Analytical methodologies were developed for monitoring and identifying the products of pyrolysis and combustion of retardant-treated fuels. This research has given a better understanding of the mechanism of fire retardation. With this last concern, an introductory section describing the pyrolysis of cellulose is included here to offer a better understanding of the theories about the retardation mechanism proposed by some of the authors reviewed.

Various instruments have been used to evaluate the performance of the different products and the properties measured have depended on the instrumentation used. The main characteristics of the experimental

methodologies developed and the results obtained are detailed in the following sections.

4.1.1 Pyrolytic degradation of cellulose

The thermal degradation of cellulose has been widely studied during the last few years. Di Blasi [7] recently outlined the most up-to-date studies of the cellulose pyrolysis mechanism. We provide only a brief description of the mechanism proposed by Bradbury et al. [8] (Figure 4.1) because all subsequent advances are essentially modifications of this proposal and our study does not require detailed knowledge of recent developments.

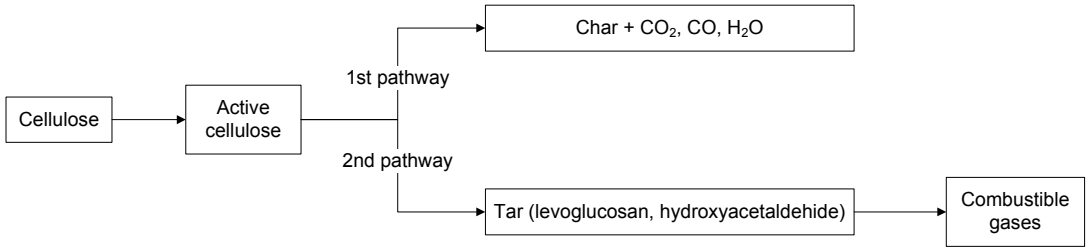

Figure 4.1 Schematic of the competing paths in the thermal degradation of cellulose.

The first step in the thermal degradation of cellulose is the formation of an intermediate molten phase (active cellulose). The active cellulose decomposes via two competitive pathways. The first occurs at low temperatures (below 300°C) and low heating rates. It consists of dehydration, formation of carboxyl and carbonyl groups, evolution of CO_2, CO and H_2O, and formation of char residue. Random bond scission of glucosan units reduces the degree of polymerization too. The second pathway is a generalized depolymerization process that takes place at high temperatures and heating rates and leads to the formation of tar, which decomposes further to produce mainly volatile products. The tarry products which can be obtained in the highest yield are levoglucosan (1,6-anhydro-β-D-glucopyranose) and hydroxyacetaldehyde. Other products include formic acid, acetic acid and glyoxal.

According to the literature, the presence of various inorganic acidic compounds enhances the performance of the first degradation pathway by catalyzing the dehydration reactions [9]. Some acidic compounds are formed during the decomposition of DAP (see Figure 4.2).

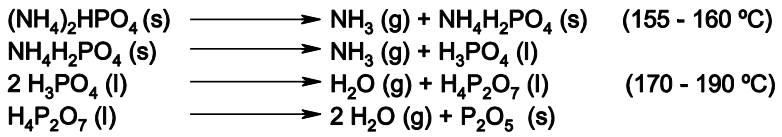

Figure 4.2 Decomposition reactions of diammonium phosphate [15].

However, levoglucosenone (1,6-anhydro-3,4-dideoxy-β-D-glycero-hex-3-enopyranos-2-ulose), which is the dehydration product of levoglucosan, was also obtained by pyrolysis of cellulose at high heating rates with large amounts of phosphoric acid [10]. Therefore, the retardant apparently acted after the levoglucosan had been formed.

Some of the studies reviewed here attempted to relate the results obtained (similar to those described above) to the effect of retardants on the degradation mechanism of cellulose and pine needles.

4.1.2 Experimental methodologies

Experimental methodologies in analytical chemistry depend strongly on the technique used to address the problem. Consequently, in this section we first describe the equipment used and then explain some other characteristics of the methodologies developed (the fuel type, the sample preparation, the thermal atmosphere, etc.).

The first studies at this scale generally used thermal analytical methods such as thermogravimetric analysis (TGA) [11-13], derivative thermogravimetry (DTG) [11], differential scanning calorimetry (DSC) [12,14] and differential thermal analysis (DTA) [11]. The authors of a recent study also used TGA, DTG and DTA to evaluate the performance of a new chemical (hydromagnesite) as a fire retardant [15].

TGA involves the exposure of a sample to a controlled increasing temperature and the monitoring of the weight of the sample at each temperature. A gas such as air, oxygen, nitrogen or helium is usually circulated around the sample. The careful selection of the gas helps to control the process under study. Pyrolysis is the process observed when the sample is heated in the presence of pure nitrogen; combustion refers to the process taking place in the presence of oxygen or air. DTG is used when it is also necessary to determine the rate of weight loss as a function of time or temperature. The most common variables obtained with these techniques are:

- Pyrolysis/combustion residue at a given temperature (net or total, depending on whether the retardant residue is subtracted or not)

- Maximum weight loss rate

- Temperature of the maximum weight loss rate (or peak temperature)

Whereas DTG measures the mass change of a sample, DTA and DSC techniques are used to measure energy changes [16]. DTA records the amount of heat liberated or absorbed as a sample moves from one physical state to another or undergoes a chemical reaction. This heat is determined by measuring the temperature differences between the sample and an inert control. The exposure temperature is increased at a linear rate and the resulting temperature difference is recorded against time. Air or another gas flows through the sample, as in TGA. DSC is similar to DTA, but the actual differential heat flow is measured when the sample and reference temperatures are equal [17]. The most common information considered with these techniques is:

- Profile pattern

- Temperatures of endothermic and exothermic peaks. The endothermic peak associated with the thermal decomposition of the fuel is called the pyrolysis temperature

Pyrolysis techniques (Py) have been combined with gas chromatography (GC) [18-19] and mass spectrometry (MS) [14] to separate and identify the pyrolysis products of forest fuels and cellulose before and after treatment with retardants. GC is a separation technique that provides data on the retention time and intensity of different chromatographic peaks. In some cases GC is unable to identify the compounds of a mixture with a high degree of accuracy, whereas MS identifies pure substances with almost total precision. One of the difficulties of both GC and MS was how to introduce the sample into the system, because the samples studied were solid. In [18-19] the samples were flash vaporized in a pyrolysis unit at different pre-set temperatures and the mixture of compounds was swept into the GC analytical column. Pappa et al. [14] used a direct insertion pyrolysis probe to introduce the samples into a mass spectrometer at different pre-set temperatures between 100^{o}C and 400^{o}C. However, the sample can also be introduced in the mass spectrometer by using a chromatograph, which is a more versatile method. Tzamtzis et al. [19] used a

combination of these three techniques (Py-GC-MS). The most common information considered with these types of instrument is:

- Identification of the compounds according to retention times (in GC) or mass-to-charge ratios (m/z) (in MS)

- Signal areas or intensities (for quantitative analysis, standard substances are previously analyzed to determine the necessary calibrations)

- Evolution of the intensity signals versus temperature for the different compounds

Other studies have used custom-made apparatuses to quantify and characterize the behavior of the volatile compounds produced during pyrolysis or combustion of cellulose and forest fuels before and after treatment with retardants. One study [20-21] constructed a furnace to investigate the effect of the retardants on the spontaneous ignitability of forest fuels. The basic parameter quantified in this study was the ignition delay time, i.e. the period between the initiation of heating and the formation of visible flames. Flammability experiments that are performed using a standard epiradiator also record this parameter [22]. Other specially designed equipment similar to a thermogravimetric unit was used to evaluate the fire extinguishing effectiveness of various chemicals on the smoldering combustion of forest fuels. However, this apparatus only recorded sample temperature versus time and not the mass evolution of the samples [23]. The temperature-time profiles were used to determine the maximum combustion temperature, the peak temperature area, the starting point of combustion and the combustion duration.

In [24-25] a thermobalance was used in combination with a mass spectrometer (TG-MS) to take advantage of the sensitivity, versatility and fast analysis time provided by MS. In these studies, an in-house developed TG-bridge system was used to introduce the samples into the mass spectrometer, which recorded signals in the range 10-200 m/z. Tzamtzis et al. [26] used the same TG-bridge system to combine a mass spectrometer with a furnace (TG-bridge/MS). They used single ion monitoring instead of full-scan mode to obtain data on the most representative masses of the combustion process (m/z: 44 (CO_2), 17 (NH_3), 78 (benzene), 91 (toluene), 94 (phenol)). These types of equipment generally measure the same kind of information as MS.

The mass and configuration of the samples were dependent on the technique used. Thermal analysis samples were in powdered form and their mass ranged from 7 to 50 mg. The samples used in chromatographs, mass spectrometers or other types of equipment combined with mass spectrometers were also in powdered form and had a mass of 0.5 - 10 mg. Liodakis et al. [20-21] conducted tests with 1 g cylindrical pellets of ground fuel and Tzamtzis et al. [26] constructed a pine-needle fuel bed measuring 23 cm x 12 cm x 7.5 cm (length x width x height).

The desired percent by weight of the chemicals was obtained, in most of the studies reviewed here, by adding a stock solution of known concentration of the chemical to a pre-weighed and ground sample of the fuel, which was then dried in an oven. The drying temperature and period varied between studies. In the first works, samples were dried at 32-35°C for a period of 48h. In the last ones, the oven temperature was 40°C or 60°C and the drying period was also 48h. In [20-21] the retardant was in powdered form and in [26] the treated fuel bed was prepared by spraying the untreated bed with a solution of retardant (20% v/v) to a given distribution ratio (1.6 l m^{-2}).

The most common retardant products in the literature were DAP and AS, both of which were used as reagents in powdered form. However, Liodakis et al. [13,15,23] worked with other chemicals (metals, metallic oxides and inorganic salts) and the authors of more recent works [15,23,25-26] analyzed the performance of the commercial retardant products Fire-Trol 931 (polyphosphate based), Fire-Trol GTS-R (AS and DAP based) and an unspecified Phos-Chek product.

Only a small number of fuel types were examined. *Pinus halepensis* needles and/or cellulose were used in almost all of the studies considered. This is mainly due to the fact that pine needles are fire prone and provide reasonable reproducibility, and also because *Pinus halepensis* is a typical species of the Mediterranean basin.

Most of the studies used retardant concentrations in treated samples of 10% w/w (mass of retardant per mass of fuel and retardant). Only the initial studies of George and Susott [11] and Pappa et al. [14] and, more recently, the study performed by Liodakis et al. [20], examined a wide range of concentrations (0 - 25% w/w). The 10% w/w retardant concentration was chosen because Pappa et al. [14] had observed that concentrations above this percentage did not yield larger net residues.

Table 4.1 provides a summary of these experimental characteristics. We also specify the thermal atmosphere, the heating rates and the flow rates.

4.1.3 Results

This section is ordered chronologically to illustrate the evolution of the instrumentation used and the results obtained.

George and Susott [11] conducted DTA and TGA/DTG experiments in nitrogen and air atmospheres for cellulose, DAP, AS and cellulose treated with DAP and AS. The DTA thermograms for the pyrolysis of cellulose (N_2 atmosphere) showed that the pyrolysis temperature was 364°C. This temperature fell to 293°C and 245°C respectively when a 3% w/w treatment concentration of DAP and AS was added. In TGA/DTG experiments, the peak temperatures for cellulose with and without retardants at the same concentration level and atmosphere were 367°C (cellulose), 298°C (cellulose and DAP) and 248°C (cellulose and AS). This level of coincidence between pyrolysis and peak temperatures in a nitrogen atmosphere should be expected despite the different thermal methods used.

TGA/DTG results also showed that when the retardant concentration was increased, the maximum weight loss rate only decreased for peak temperatures of up to 250°C in both atmospheres. Regarding to the net residue of cellulose obtained in TGA/DTG experiments, it increased when cellulose was treated with retardants. In addition, higher residues at 450°C were obtained in an air atmosphere when the cellulose was treated with DAP than when AS was used, whereas this effect was not observed in an N_2 atmosphere for treatment levels greater than 8% w/w. DTA results showed differences between the effects of DAP and AS on the combustion of cellulose. AS caused an exothermic peak larger than DAP's peak.

Table 4.1 Analytical studies with retardants and forest fuel.

Authors (year)	**Ref.**	**Technique** [a]	**Chemicals or retardant products**	**Fuel**	**Concentrations** [b]	**Sample configuration**	**Combustion or pyrolysis conditions**[c]
George and Susott (1971)	[11]	DTA, TG, DTG	DAP, AS	Cellulose reagent	0, 0.05, 0.1, 0.2, 0.3, 0.4, 0.5, 0.7, 1.0, 1.5, 2, 3, 4, 5, 6, 8, 10, 12, 15, 20, 25 % w/w	Powder (10 mg)	Pyrolysis ($25°C\ min^{-1}$, N_2) Combustion ($25°C\ min^{-1}$, air)
Pappa et al. (1995)	[14]	DSC, DI-MS	DAP, AS	Cellulose reagent *Pinus halepensis* needles	0, 0.2, 1, 4, 10, 15, 25 % w/w	DSC: Powder (50 mg) DI-MS: Powder (0.5 mg)	Pyrolysis ($10°C\ min^{-1}$, N_2)
Pappa et al. (1995)	[12]	DSC, TG	DAP, AS	Cellulose reagent *P. halepensis* needles Lignin and extractives obtained from pine needles	10 % w/w	DSC: Powder (50 mg) TG: Powder (7 mg)	Pyrolysis ($10°C\ min^{-1}$, N_2)
Liodakis et al. (1996)	[13]	DSC, TG	DAP, NaH_2PO_4, NaH_2PO_4, AS, $NaHCO_3$, $KHCO_3$, $(COONa)_2$, $Ca(OH)_2$, Na_2OCaO	Cellulose reagent *P. halepensis* needles	DSC: 4 % w/w TG: 4 %w/w cellulose and 10 % w/w pine needles	DSC: Powder (50 mg) TG: Powder (7 mg)	Pyrolysis ($10°C\ min^{-1}$, N_2)
Tzamtzis et al. (1997)	[18]	Py-GC	DAP, AS	Cellulose reagent	10 % w/w	Powder (7.5 mg)	Pyrolysis (flash pyrolysis, He)
Tzamtzis et al. (1999)	[19]	Py-GC, Py-GC-MS	DAP, AS	*P. halepensis* needles	10 % w/w	Powder (7.5 mg)	Pyrolysis (flash pyrolysis, He)

Table 4.1 Analytical studies with retardants and forest fuel (continued).

Authors (year)	**Ref.**	**Technique** [a]	**Chemicals or retardant products**	**Fuel**	**Concentrations** [b]	**Sample configuration**	**Combustion or pyrolysis conditions**[c]
Statheropoulos and Kyriakou (2000)	[24]	TG-MS, DTG	DAP, AS	Cellulose reagent	10 % w/w	Powder (2 mg)	Pyrolysis (50°C min^{-1}, He)
Liodakis et al. (2002)	[20]	Oven	DAP, AS	*P. halepensis* needles	0, 5, 10, 15, 25 % w/w	Pellets (1000 mg)	Combustion (500-600°C, 1.5 l min^{-1} air flow)
Liodakis et al. (2003)	[21]	TG, DTG, Oven	DAP, AS	Foliage of: *Arbutus andrachne* *Cistus incanus* *Pinus brutia* *Pinus halepensis* *Cupressus sempervirens* *Pistacia lentiscus* *Abies cephallonica*	20 % w/w	TG: Powder (10 mg) Oven: Pellets (1000 mg)	TG: Pyrolysis ($3.66 \cdot 10^{-2}$ K min^{-1}, N_2) Oven: Combustion (500-600°C, 1.5 l min^{-1} air flow)
Pappa et al. (2003)	[25]	TG-MS	DAP, AS, Fire-Trol 931	Cellulose of *P. halepensis* needles	10 % w/w	Powder (10 mg)	Pyrolysis (50°C min^{-1}, He)
Tzamtzis et al. (2006)	[26]	TG-bridge/MS	Fire-Trol 931	*P. halepensis* needles	12.8 % w/w	Fuel bed (0.18 g/cm^2)	Combustion (30°C min^{-1}, static air)

Table 4.1 Analytical studies with retardants and forest fuel (continued).

Authors (year)	**Ref.**	**Technique** [a]	**Chemicals or retardant products**	**Fuel**	**Concentrations** [b]	**Sample configuration**	**Combustion or pyrolysis conditions** [c]
Liodakis et al. (2006)	[23]	Oven	Cu, Fe, Al_2O_3, Fe_2O_3, $SiO_2 \cdot H_2O$, $NaHCO_3$, KI, KBr, KCl, NaCl, $CaCO_3$, $MnSO_4 \cdot 5H_2O$, $CuSO_4 \cdot 5H_2O$, $MgCl_2 \cdot 6H_2O$, $Na_2B_4O_7 \cdot 10H_2O$, Na_2HPO_4, Na_2CO_3, Na_2SiO_3, $ZnSO_4 \cdot 7H_2O$, $Zn_3(PO_4)_2 \cdot 2H_2O$, NH_4Br, NH_4Cl, NH_4HCO_3, $(NH_4)_2CO_3$, $NH_4H_2PO_4$ (MAP), DAP, AS, Fire-Trol GTS-R	*P. halepensis* needles	10 % w/w	Powder (2500 mg)	Combustion (0.5°C min^{-1}, static air)
Liodakis et al. (2006)	[15]	TG, DTG, DTA	$Mg_5(CO_3)_4(OH)_2 \cdot 4H_2O$, DAP, unspecified Phos-Chek product	Leaves of: *Erica manipuliflora* *Phillyrea latifolia*	10 % w/w	Powder (16 mg)	Combustion (10°C min^{-1}, O_2)

a. DTA: Differential Thermal Analysis, TG: Thermogravimetry, DTG: Differential Thermogravimetry, DI-MS: Direct Inlet Mass Spectrometry, Py-GC: Pyrolysis Gas Chromatography, Py-GC-MS: Pyrolysis Gas Chromatography Mass Spectrometry.

b. Percentage of weight of retardant per weight of fuel and retardant.

c. Heating rate and atmospheric gas in parentheses.

The authors in [11] suggested that the retardants had different effects on cellulose pyrolysis and combustion either because they used different mechanisms or because the availability of the compounds was different at high temperatures. AS was completely decomposed at 420°C whereas DAP was only completely decomposed at approximately 675°C. George and Susott also made some recommendations, which included comparing chemicals according to the effects they have on pyrolysis and combustion at more than one treatment level, and quantifying the volatile products as a function of the chemical concentration. However, most studies carried out since [11] have not considered this suggestion for further research.

Pappa et al. [14] observed that the pyrolysis temperature of cellulose decreased, whereas they could not clearly identify this temperature for pine needles. They also observed that the net pyrolysis residue of the two fuels increased under the effect of both retardants. They used MS to analyze the gaseous products of pyrolysis and considered the evolution rate of various masses evolved during pyrolysis (measured in arbitrary intensity units) as a function of temperature. They observed that volatiles (oxygen-containing products such as carbonyl compounds, furans and pyrans) developed at lower temperatures (from 320°C to 240°C) in pine needles in the presence of DAP. They also found that the peak attributed to levoglucosenone was more intense for treated cellulose than for untreated cellulose.

Pappa et al. [12] performed separate studies of the thermal degradation of cellulose, lignin and extractives and observed that DAP and AS seemed to have no significant effects on the pyrolysis of lignin and unclear effects on the extractives.

Liodakis et al. [13] also found that net residues increased and the pyrolysis temperature decreased in cellulose treated with DAP and AS. DSC curves of pure cellulose and treated cellulose (see Figure 3) exhibited sharp endothermic peaks. These authors obtained similar results for pyrolysis temperature and net residue by using NaH_2PO_4 instead of DAP. Consequently, they concluded that NH_3 had a minor effect on fire retardation. George and Susott [11] had previously carried out DTA thermograms in an air atmosphere with monoammonium phosphate ($NH_4H_2PO_4$) and reached a similar conclusion. The authors of [13] suggested that cellulose was not an ideal compound for studying the pyrolysis of pine needles under those experimental conditions because it has a different DSC profile to pine needles (see Figure 4.3). Complex reactions associated with the thermal conversion of pine needles complicate the

interpretation of DSC curves; broader peaks are exhibited and a well-defined pyrolysis temperature is not observable. Cellulose continued to be used in only a third of the later studies reviewed here.

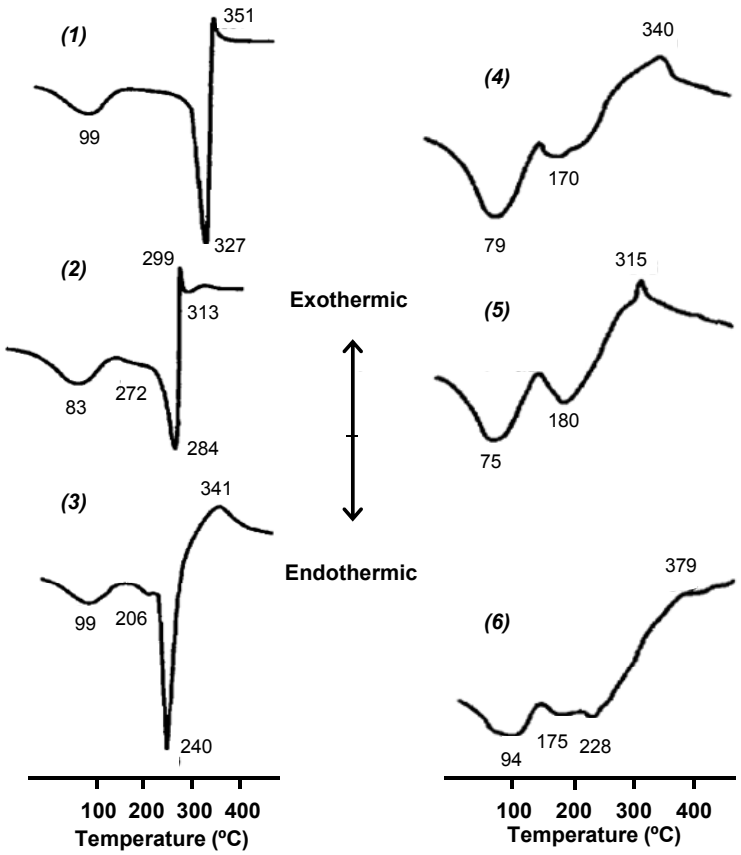

Figure 4.3 DSC curves in nitrogen of: (1) cellulose; (2) cellulose treated with 4% w/w DAP; (3) cellulose treated with 4% w/w AS; (4) untreated *Pinus halepensis* needles; (5) *Pinus halepensis* needles treated with 4% w/w DAP and (6) *Pinus halepensis* needles treated with 4% w/w AS. DSC curves were only used for comparing purposes and neither baseline assignments nor quantitative evaluations were done (source: [13]).

Tzamtzis et al. [18-19] and Statheropoulos and Kyriakou [24] analyzed the impact of DAP and AS on the pyrolytic degradation mechanism of cellulose and *Pinus halepensis* needles. Tzamtzis et al. [18] observed that the yield of low-volatility organic components (retention time > 14 min) increased in Py-GC tests carried out with cellulose treated with DAP and AS at different temperatures (250°C - 550°C). In [19] it was also studied the evolution rate of four volatile organic products of pine-needle pyrolysis in the presence of DAP and AS (levoglucosenone, aromatic nitrile, nitrophenyl and phenol) at temperatures from 100°C to 600°C. They recorded high yields of levoglucosenone in treated pine-needle samples but not in untreated samples

and therefore concluded that the chemical retardants studied did not favor the dehydration pathway which leads to the formation of char, CO_2, CO and H_2O. This statement was in fact untenable, mainly because the authors were unable to evaluate the evolution rate of these compounds under their experimental conditions as the detector used in GC, a flame ionization detector, was insensitive to non-flammable gases.

Statheropoulos and Kyriakou [24] carried out a study to quantify the percentage by weight of the H_2O and CO_2 that developed during cellulose pyrolysis before and after treatment with DAP and AS. The percentages of both compounds and net residues increased due to the presence of the retardants. The authors also found that the intensity of the MS peak corresponding to levoglucosenone increased. They claimed that the retardants used favored the first cellulose decomposition pathway. The DTG curves obtained for cellulose treated with AS revealed that the retardant had a two-step action. In the first step, the active component of the retardants (sulfuric acid for AS and pyrophosphoric acid for DAP) reacted with the hydroxyl groups to form aliphatic and aromatic groups, which caused the cellulose to dehydrate. A small quantity of levoglucosan was also formed, which readily dehydrated to produce levoglucosenone. In the second step, the aliphatic groups were decomposed, which led to the formation of char and the development of CO_2.

The studies [20-21] considered ignition delay time to analyze the ignitability of different fuel samples treated with DAP and AS. This parameter increased in the presence of the retardants and it showed higher values for samples treated with DAP than for those treated with AS. The tests were carried out in a furnace at different pre-set temperatures. The temperature range of study was 500-600°C with increments of 10°C. The largest increases for both retardants were recorded at low temperatures (500-540°C).

Pappa et al. [25] followed the work of Statheropoulos and Kyriakou [24] and carried out a chemometric evaluation of the mass spectra of cellulose and of cellulose treated with DAP, AS and Fire-Trol 931. In general terms, chemometric methods are particularly useful for analyzing MS spectra when there are a very large number of samples and it is too time-consuming to make a visual interpretation [27]. Pappa et al. found that the proportion of flammable products decreased and the proportion of lower flammability products such as CO_2, levoglucosenone, acetic acid and phenolic compounds increased. AS promoted the appearance of phenolic compounds whereas DAP and Fire-Trol 931 induced the appearance of acetic acid.

In [26] the authors monitored the evolution of CO_2, NH_3, benzene, toluene and phenol for samples treated with Fire-Trol 931 and combusted in a static air atmosphere furnace. These compounds appeared to evolve earlier than in the untreated samples and the maximum signal intensities for NH_3, benzene, toluene and phenol increased. The CO_2 evolution profiles were almost identical with and without retardant because the large amount of CO_2 in the experiments derived from the combustion process of the volatiles and it was therefore impossible to detect the retardant effect on CO_2.

The tests in [23] were also performed in a static air atmosphere. The authors evaluated the smoldering behavior of *Pinus halepensis* needles treated with various chemicals and a commercial product. The commercial product had the strongest overall smoldering combustion retardation effect. The total residues for samples treated with DAP and AS with respect to the residue of pure needles increased to 328% w/w and 20% w/w respectively at 500°C. In [11], the recorded residues for cellulose treated with the same retardants at the same treatment level and at 450°C were 345% w/w for DAP-treated cellulose and 287% w/w for AS-treated cellulose. The residue increased by the same order of magnitude for DAP-treated samples in both studies, whereas differences were observed for AS-treated samples. This difference remains to be further investigated.

Finally, Liodakis et al. [15] presented the results of calorimetric experiments in an oxygen atmosphere. They found that the temperatures of maximum weight loss rate (or peak temperatures) increased for the treated samples: the peak temperature of pure *Erica manipuliflora* was 306°C, which increased to 462°C for *Erica manipuliflora* treated with 10% w/w DAP. This result is not in agreement with the values obtained in [11]. The authors of this last study found that the peak temperature of cellulose treated with DAP at a treatment level of 10% w/w in an air atmosphere decreased with respect to the pure sample (from 349°C to 265°C). This discrepancy may be due to the differences in the fuel composition or in experimental conditions, although this needs to be clarified through further research.

4.2 Laboratory combustion tests

Research studies since 1965 have used laboratory combustion tables or tunnels to analyze the effectiveness of long-term retardants. These set-ups were designed specifically for evaluating the behavior of controlled flame fronts or flames under the effect of retardants. The fuel was exposed to a pre-set wind

speed in tunnel tests whereas tests on combustion tables were conducted in calm conditions.

Most of the studies examined the propagation of a linear flame front advancing across a forest fuel bed that was sprayed with a retardant solution. Generally the treated fuel was left to dry up until reaching the equilibrium with the environment (i.e. until the net exchange of moisture between the treated fuel particles and the environment was approximately zero) before the fuel bed was ignited. The fuel bed could have an untreated region before the treatment to give the fire a chance to approach a steady rate of spread before coming in contact with the treated fuel.

Researchers also studied the reactivation of flames, or combustion recovery, on forest fuel beds which were instantaneously and completely ignited and allowed to burn until the maximum energy release was reached, at which point the retardant solution was directly applied to the flames.

In the following sections the experimental conditions of the tests performed and the most relevant results are detailed.

4.2.1 Experimental methodologies

Table 4.2 shows the main characteristics of the laboratory-scale combustion studies reviewed in this work.

Most of the studies were carried out in the USA from 1965 to 1990. The most common retardants were DAP and AS but other, predominantly phosphate-based retardant formulations, were also evaluated. Some studies, particularly recent tests performed outside the USA, analyzed the effects of commercial retardant products (Fire-Trol 931, FR CROS 134P and Fire-Trol 934, all polyphosphate based).

Table 4.2 Experimental studies on long-term forest fire retardants' effectiveness in laboratory set-ups.

Authors (year)	**Ref.**	**Type of experiment**	**Environmental conditions** [a]	**Chemicals or retardant products**	**Fuel (load)**	**Dilution rates and distribution ratios** [b]	**Evaluation parameters**
Rothermel and Hardy (1965)	[37]	Propagation / retardant solution dried	I 32.2°C, 50%RH, 0.89 m s^{-1}. II 32.2°C, 20%RH, 0.89 m s^{-1}. III 32.2°C, 20%RH, 2.2 m s^{-1}	1 unspecified commercial long-term retardant	*Pinus ponderosa* needles (2.44 kg m^{-2})	25 % w/w 0.425 and 0.850 l m^{-2}	ROS, irradiation, rate of weight loss
George and Blakely (1970)	[38]	Propagation / retardant solution dried	32.2°C, 20%RH, 2.2 m s^{-1}	DAP, AS	*Pinus ponderosa* needles (2.44 kg m^{-2})	10 % w/w 0.850 l m^{-2}	ROS, rate of weight loss, residue
George and Blakely (1972)	[28]	Propagation / retardant solution dried	32.2°C, 20%RH, 2.2 m s^{-1}	DAP, AS	*P. ponderosa* needles (2.44 kg m^{-2}), shredded *Populus spp.* wood (1.6 kg m^{-2})	2.5, 5, 7.5, 10, 12.5, 15, 17.5 % w/w 0.850 l m^{-2}	ROS, rate of weight loss, residue
Rothermel and Philpot (1975)	[34]	Propagation / retardant solution dried	uncontrolled, 0, 0.9, 2.2 m s^{-1}	DAP, AS	*P. ponderosa* needles (1.6-3.2 kg m^{-2}), shredded *Populus spp.* wood (1-2 kg m^{-2}), square *P. ponderosa* sticks (2.2-6.2 kg m^{-2})	0.5 – 20 % w/w of retardant in fuel	ROS

Table 4.2 Experimental studies on long-term forest fire retardants' effectiveness in laboratory set-ups (continued).

Authors (year)	**Ref.**	**Type of experiment**	**Environmental conditions** [a]	**Chemicals or retardant products**	**Fuel (load)**	**Dilution rates and distribution ratios** [b]	**Evaluation parameters**
George et al. (1977)	[43]	Propagation / retardant solution dried	32.2°C, 20%RH, 2.2 m s^{-1}	Fire-Trol 931 L, Fire-Trol 931 N, Fire-Trol 931 P	*Pinus ponderosa* needles (2.44 kg m^{-2}), shredded *Populus spp.* wood (1.6 kg m^{-2})	20 % v/v 0.425 and 0.850 l m^{-2}	ROS, rate of weight loss, residue
Blakely (1983)	[44]	Propagation / retardant solution dried	32.2°C, 20%RH, 2.2 m s^{-1}	M-MAP, S-MAP, T-MAP, D-MAP, A-MAP	*P. ponderosa* needles (2.44 kg m^{-2}), shredded *Populus spp.* wood (1.6 kg m^{-2})	2.5, 5, 7.5, 10, 12.5, 15, 17.5 % w/w 0.850 l m^{-2}	ROS, rate of weight loss
Blakely (1985)	[35]	Reactivation	32.2°C, 20%RH, 2.2 m s^{-1}	MAP, water	*P. ponderosa* needles (2.44 kg m^{-2})	10, 15 % w/w MAP; 100 % w/w water 0.14-0.22 l m^{-2}	Rate of weight loss
Blakely (1988)	[45]	Propagation / retardant solution dried	32.2°C, 20%RH, 2.2 m s^{-1}	LC-A, GTS, D75, PSF, MAP, DAP, AS, AS/MAP [c]	*P. ponderosa* needles (2.44 kg m^{-2}), shredded *Populus spp.* wood (1.6 kg m^{-2})	Dependent on the product 0.425 and 0.850 l m^{-2}	ROS, rate of weight loss
Blakely (1990)	[36]	Reactivation	32.2°C, 20%RH, 2.2 m s^{-1}	MAP, water	*P. ponderosa* needles (2.44 kg m^{-2})	5.3, 7.7, 14.3 % w/w MAP; 100 % w/w water 0.14-0.22 l m^{-2}	Rate of weight loss
Xanthopoulos and Noussia (2000)	[29]	Propagation with a firebreak / retardant solution dried	uncontrolled, 0, 0.4, 0.9 m s^{-1}	Unspecified Fire-Trol product without gum thickening agents	*Pinus halepensis* needles (0.45, 0.9, 1.2 kg m^{-2})	20 % v/v 0.6 and 0.9 l m^{-2}	ROS, fuel temperature

Table 4.2 Experimental studies on long-term forest fire retardants' effectiveness in laboratory set-ups (continued).

Authors (year)	**Ref.**	**Type of experiment**	**Environmental conditions** [a]	**Chemicals or retardant products**	**Fuel (load)**	**Dilution rates and distribution ratios** [b]	**Evaluation parameters**
Pastor (2004) Pastor et al. (2006)	[31-32]	Propagation / retardant solution totally, partially or not dried	uncontrolled 0 m s^{-1}	Fire-Trol 931, FR CROS 134P, Fire-Trol 934	*Triticum aestivum* straw (0.25, 0.35, 0.5, 0.75 kg m^{-2}), *Pinus pinaster* needles (0.8 kg m^{-2})	3, 5, 10, 20 % v/v and 0.03 l m^{-2} (straw tests) 13 % v/v and 0.5 l m^{-2} (needles tests)	ROS, rate of weight loss, flame front radiant energy
Giménez et al. (2006)	[33]	Propagation / retardant solution dried	uncontrolled 0 m s^{-1}	Fire-Trol 931, FR CROS 134P	*Triticum aestivum* straw (0.4, 0.6, 0.8 kg m^{-2})	20 % v/v Fire-Trol 931; 5 % v/v FR CROS 134P 0.070 – 0.54 l m^{-2}	ROS
Ribeiro et al. (2006)	[30]	Propagation / retardant solution dried	uncontrolled 0 m s^{-1}	7 unspecified products	*Pinus pinaster* needles (1 kg m^{-2})	1 % v/v 0.2 l m^{-2}	ROS, rate of weight loss, flame length

a. Ambient temperature (°C), relative humidity (% RH) and wind velocity (m s^{-1}).

b. Dilution rates are expressed as a percentage of weight or volume of retardant per weight or volume of retardant and water (% w/w and % v/v, respectively). If a different notation is used it is specifically indicated. Distribution ratios are expressed as liters of solution per square meter.

c. Percentage of chemical in solution by weight (% w/w): LC-A: 7.57 % P_2O_5 (ammonium polyphosphate); GTS: 13.62 % AS, 1.21 % DAP; D75: 8.33 % AS, 2.77 % MAP; PSF: 9.84 % AS, 2.28 % DAP; MAP: 10.38 % MAP; DAP: 9.52 % DAP; AS: 14.02 % AS; AS/MAP: 9.45 % AS, 3.15 % MAP.

All the studies carried out in the USA used fuel beds consisting of *Pinus ponderosa* needles. George and Blakely [28] also performed flame front propagation studies with beds constructed from aspen excelsior (*Populus spp.*). Both species were used in most American subsequent studies. These two fuels have different chemical compositions, particularly in terms of the amount of extractives they contain. Excelsior contains less than 1% w/w of extractives whereas ponderosa pine needles contain approximately 10% w/w. Different species were used in the studies carried out by European researchers. Xanthopoulos and Noussia [29] constructed fuel beds from *Pinus halepensis* needles and Ribeiro et al. [30] and Pastor et al. [31-32] used *Pinus pinaster* needles. Pastor et al. [31-32] also worked with straw, as did Giménez et al. [33]. The dimensional characteristics of the fuel beds prepared in these works are shown in Table 4.3.

Table 4.3 Dimensional characteristics of fuel beds prepared for laboratory flame-spread tests (width and length).

Authors (year)	**Ref.**	**Width (cm)**	**Length (cm)**	
			Untreated area	**Treated area**
Rothermel and Hardy (1965)	[37]	45.72	91.44	243.84
George and Blakely (1970)	[38]			
George and Blakely (1972)	[28]			
Blakely (1983)	[44]			
Blakely (1988)	[45]			
Rothermel and Philpot (1975)	[34]	45.72	-	152.4
Rothermel and Philpot (1975)	[34]	45.72	-	243.84
George et al. (1977)	[43]			
Xanthopoulos and Noussia (2000)*	[29]	60	150	From 10 to 55
Pastor (2004) Pastor et al. (2006)	[31-32]	150	-	150
Pastor (2004) Pastor et al. (2006)	[31-32]	130	50	130
Giménez et al. (2006)	[33]	130	85	90
Ribeiro et al. (2006)	[30]	130	-	76.92

* There was a fuel gap of 5 to 50 cm in width between untreated and treated areas or after the treated area.

In relation to the application of the retardant solution, nearly all of the American studies used an overhead sprayer to apply the retardant solution to the fuel bed. An exception to this is the work of Rothermel and Philpot [34], who submerged the fuel beds in retardant solutions for pre-determined periods. In a European study [33] an automated sprayer system was also used to apply the retardant solutions. In contrast, manual commercial sprayers were used to apply the products to the fuel bed in [29-32]. The distribution ratios used in the different studies were between 0.03 and 0.9 l m^{-2} and the dilution rates ranged from 2.5 to 25% w/w. The retardant solution was totally dried prior to ignition in all of the propagation experiments except for the work of Pastor et al. [31-32], who used partially dried or undried retardant solutions and evaluated the contributions of the water and the retardant separately. Different methodologies were used to dry retardant solutions. They include halogen lamps, heaters, placing the fuel beds in combustion chambers under controlled conditions or letting the fuel dry under laboratory conditions.

Most of the American studies were carried out under controlled environmental conditions in tunnels with a constant wind speed of 2.2 m s^{-1} at the fuel bed level. However, more recent studies in European research facilities were performed under uncontrolled environmental conditions.

In the propagation studies various parameters for treated and untreated fuel beds were measured in identical or similar conditions to compare the performance of the retardants in reducing the intensity of the fire. The authors of all propagation studies reviewed in this work measured the rate of spread (ROS) of a flame front across a treated fuel bed and compared the value with the rate of spread of a flame front across a non-treated fuel bed or on an initial area of the same fuel bed that had not been treated (ROS_0). The rates of spread were measured by calculating the time that the flame front took to cover certain known distances. Most researchers also measured the rate of weight loss by using multiple strain gages or scales placed beneath the fuel bed. In some studies the authors also recorded the residual mass after the flame front had advanced. The flame length and the IR sequence of the flame front advance were registered only in [30] and [31-33], respectively. In reactivation tests [35-36] the rate of weight loss was recorded and related directly to the energy release rate through the fuel heat content value.

4.2.2 Results

Rothermel and Hardy [37] conducted burning experiments under three different environmental conditions. They concluded that a minimum ratio of

0.10 g of retardant liquid concentrate per gram of dead fuel was sufficient to suppress a fire. However, there is reason to believe that this ratio may not be generally effective in real situations. The ratio was established in terms of the amount of liquid concentrate but not in terms of the amount of retardant salt; it was also based on the results of burning dead fuel in laboratory set-ups, so its extrapolation to field situations with different fuel complexes and live fuel would be very approximate. In addition, only a limited number of experiments were carried out. Nevertheless, the equipment they employed to do the tests was used in all of the subsequent burning studies carried out in the USA and these subsequent tests were also conducted under one of the three environmental conditions tested (32.2°C ambient temperature, 20% relative humidity, 2.2 m s^{-1} wind speed).

George and Blakely [38] observed that DAP- and AS-treated beds produced similar ROS but they observed differences in the maximum rate of weight loss reduction (32% for DAP-treated beds and 44% for AS-treated beds), the residual mass increase (110% for DAP-treated beds and 30% for AS-treated beds) and the reduction in the energy released during the test (14% for DAP-treated beds and 5% for AS-treated beds). Therefore, they concluded that it was important to take into account both the ROS and the rate of weight loss (which was related to the energy released through the heat content of the fuel) when evaluating the effectiveness of fire retardants.

George and Blakely's next study [28] was more comprehensive: they used an additional fuel and different dilution rates. In this case they proved that DAP was more effective than AS in reducing the ROS, the weight loss rate and the mass loss. They also established that it was necessary to combine the pyrolysis and combustion analytical data on the effects of retardants with the data from laboratory combustion tests.

Rothermel and Philpot [34] carried out the further research suggested in [28]. They defined a non-dimensional parameter called the Retardant Damping Coefficient, that relates the propagating flux – previously defined by Rothermel [39] as the total heat that impinges on the fuel – measured from retardant-treated fuel to the propagating flux measured from untreated fuel (Eq. [4.1]).

$$\eta_r = \frac{R\ Q_{ig}}{R_0\ Q_{ig_0}} \qquad [4.1]$$

They used data obtained by George and Susott [11] to examine the effect of retardants on the heat of pre-ignition, assuming that the decrease in the ignition

temperature was proportional to the decrease in the temperature of maximum weight loss rate obtained by thermoanalysis in an air atmosphere. The study correlated the Retardant Damping Coefficient for no-wind propagation data with the ratio of retardant salt to fuel mass and with two of the fuel properties (the surface area-to-volume ratio and the extractive percentage). The authors verified the extinction condition by setting the parameter to zero for the latter correlation. They proposed an expression for determining the distribution ratio of retardant solutions in terms of fuel load and fuel dimensions (Eq. [4.2]). The expression used the standard dilution rates of two commercial retardants containing DAP or AS and an extractive percentage of 5% w/w.

$$Coverage = 1.764\ \mathrm{w}_0 \exp\left(-\frac{460}{\sigma}\right) \qquad [4.2]$$

As it is shown in Equation 2 the retardant requirement per unit surface area should increase for a given w_0 with σ. It can be explained by considering that the fraction of fuel involved in ignition increases with σ.

This study had a strong influence on the work of the United States Department of Agriculture (USDA) Forest Service, which used Equation 2 to determine the recommended retardant distribution ratios stated in air tanker performance guides. In addition, by determining the capacities of various vertical fuel models the USDA was able to introduce the retardant-film thickness concept and improve the accuracy of its recommended distribution ratios [40]. As it was mentioned in George [41], Rothermel used the increased number of fuel models in the USA [42] to update a definitive table of recommended distribution ratios.

USDA Forest Service studies carried out after [34] focused on evaluating different retardant formulations containing phosphates or sulfates. George et al. [43] examined the effectiveness of three formulations of Fire-Trol 931 in terms of a parameter called the Superiority Factor (SF). They calculated this parameter by combining the reduction terms of ROS, rate of weight loss and percentage of fuel consumed (or increase in residual mass) (Eq. [4.3]).

$$\begin{aligned} SF = {} & \frac{1}{4}\left[\left(\frac{R_0 - R}{R_0}\right)_{\text{needles}} + \left(\frac{R_0 - R}{R_0}\right)_{\text{excelsior}}\right] \\ & + \frac{1}{8}\left[\left(\frac{RW_0 - RW}{RW_0}\right)_{\text{needles}} + \left(\frac{RW_0 - RW}{RW_0}\right)_{\text{excelsior}}\right] \\ & + \frac{1}{8}\left[\left(\frac{Residue - Residue_0}{Residue_0}\right)_{\text{needles}} \right. \\ & \left. + \left(\frac{Residue - Residue_0}{Residue_0}\right)_{\text{excelsior}}\right] \end{aligned} \qquad [4.3]$$

The three tested formulations produced similar average SF values for all fuels and concentration levels (0.53, 0.53 and 0.51). These values were compared with the SF of DAP, which was 0.60 without taking into account the residue terms for a concentration rate of 10.6% w/w and assumed to be 0.50 when these terms were considered. The three formulations therefore had a slightly higher SF than DAP.

Blakely [44] used several formulations of monoammonium phosphate (MAP) with minor differences in composition and manufacturing process and observed no statistically significant differences between them. All of the formulations were as effective as DAP, so Blakely concluded that the presence of one or two ammonias did not affect the results. George and Susott [11] made previously the same observation at an analytical scale, as did Liodakis et al. [13] in a later study. Blakely [45] also analyzed different commercial products containing DAP, AS and/or MAP and quantified their ability to reduce the flammability of treated fuel beds. He used a similar formula to the one shown in Equation 3 but omitted the residue terms. This formula (Eq. [4.4]) is referred to as the Reduction Index (RI) and is currently used in standard burning tests in America to evaluate the performance of new commercial products [46]. The products examined in this study reduced similarly the flammability as indicated by the RI.

$$RI = \frac{1}{4}\left[\left(\frac{R_0 - R}{R_0}\right)_{\text{needles}} + \left(\frac{R_0 - R}{R_0}\right)_{\text{excelsior}}\right] + \frac{1}{8}\left[\left(\frac{RW_0 - RW}{RW_0}\right)_{\text{needles}} + \left(\frac{RW_0 - RW}{RW_0}\right)_{\text{excelsior}}\right] \quad [4.4]$$

Blakely observed synergy between DAP and AS, which was a very important finding. The RI for DAP-treated and AS-treated beds applied individually were lower than when the two retardants were used in combination. Although this result was unexpected, it was not investigated in subsequent studies. Nevertheless, five of the eight commercial products qualified by the USDA Forest Service contain combinations of MAP and AS [47].

Blakely [35-36] also studied the suppressant ability of retardants and water by applying them directly to the flames. He developed a method for quantifying the capability of water and MAP solutions to reduce fire intensity and recover combustion and performed a detailed analysis of weight loss versus time curves. He demonstrated that the retardants only slightly enhanced the capability of water to reduce flames to smoldering combustion but that retardant solutions considerably reduced the fire intensity and extended the period of smoldering combustion.

Blakely's paper [36] was the last formal research study on burn testing carried out by the USDA Forest Service. All these reviewed studies were useful for specifying the procedure for combustion effectiveness evaluation of commercial products [45]. Since 2000, most combustion test studies of fire retardants have been carried out in Europe.

Xanthopoulos and Noussia [29] conducted a study in the framework of the European ACRE Project and prepared fuel beds with firebreaks of 5 to 50 cm in width. They treated the fuel with a commercial retardant before or after the break and evaluated statistically whether the firebreak width could be reduced by placing treated fuel before or after the break. The results were inconclusive. They considered a large number of variables and observed that the results depended on the distribution ratio, the fuel load and the wind speed. Nevertheless, they also found that treated fuel withstood higher temperatures than untreated fuel. This was in agreement with the results obtained by Liodakis et al. [15], who observed that peak temperatures increased in an oxidizing atmosphere.

Pastor et al. [31-32] conducted laboratory combustion tests and applied three commercial products (Fire-Trol 931, FR CROS 134P and Fire-Trol 934). Retardant solutions were totally, partially or not dried. They defined three dimensionless parameters for studying the effect of retardants as a function of the ratio of water to dried fuel and the ratio of dried retardant to dried fuel. They calculated the ratios of ROS, rate of weight loss and radiant energy of the flame front for treated and untreated beds. The effect of the retardants on each variable was graphically analyzed, qualitatively assessed, and quantified in terms of ROS ratio and rate of weight loss ratio.

Giménez et al. [33] carried out propagation tests using Fire-Trol 931 and FR CROS 134P. They used the analytical methodology proposed by Pastor [31-32] to calculate ROS ratios for different burning conditions after the retardant solution had become completely dehydrated. They observed that the fuel bed configuration, the viscosity of the retardant solution and the characteristics of the retardant product were all determining factors of the ROS ratios.

Ribeiro et al. [30] used a parameter similar to the SF value applied in [44] to compare the effectiveness of seven unspecified retardant products but they also incorporated the reduction term for flame length (Eq. [4.5]):

$$SF' = \frac{1}{3}\left[\left(\frac{R_0 - R}{R_0}\right) + \left(\frac{RW_0 - RW}{RW_0}\right) + \left(\frac{FL_0 - FL}{FL_0}\right)\right] \qquad [4.5]$$

The calculated SF' values were 10 - 20%. We recalculated Ribeiro et al.'s SF' values without taking into account the flame length term and obtained lower values (average value 0.16) than Blakely [44]. Blakely used higher retardant treatment levels, which explains the different values obtained in the two studies.

4.3 Field tests

The researchers from the USDA Forest Service conducted extensive research into the performance of air tankers for aerial suppression and characterized the drop patterns [48]. However, field research into the effectiveness of retardants has been less comprehensive. Field tests carried out in 1984 and 1985 as part of the Australian Aquarius Project [49] were designed to gather data on the effect of chemical retardants and water on the intensity of fires in eucalyptus forests. The tests used the retardant DAP at a dilution rate of 10.7% w/w and in combination with additives. Table 4.4 shows more details on the experimental conditions. The authors of the study expressed the distribution ratios required to halt a fire (i.e. to stop it burning through a treated zone for at least one hour) according to the intensity of the fire. They found that single retardant drops were ineffective due to heavy spotting across the control line at fire intensities beyond a maximum value of approximately 2 MW m^{-1} for unsupported fires, i.e. in which there are no ground crews to attack the flames. Based on experimental observations at intensities below 2 MW m^{-1} an equation was derived for the distribution ratio required to halt a fire in a eucalyptus forest at different intensities (Eq. [4.6]).

$$Coverage = 0.24\, I_B^{0.87} \qquad [4.6]$$

Researchers in Portugal first carried out field tests to evaluate the effectiveness of retardants in 1985 [50]. They obtained inconclusive results due to a high degree of experimental inaccuracy in applying the concentration of the retardant product. Subsequently, two research campaigns were conducted in 1998 and 1999 to carry out propagation experiments in plots of Portuguese shrubland. Ten-meter-wide strips of land parallel to the ignition line of the plots were treated manually with hoses and left to dry for 24h [30, 51-52]. The researchers calculated the ROS of the flame front in both untreated and treated areas of the plot and the burned area percentage. Table 4.4 shows some other experimental characteristics of the tests. The data obtained from these tests were analyzed in [30] and a comparing parameter was calculated from a combination of factors including the reduction of ROS and burned area

percentage. The values obtained ranged from 40% to 60%, which are similar to the results obtained by Blakely [44] in laboratory tests using DAP (59%).

In addition, two field research campaigns into the effects of fire retardants were carried out in Portugal in 2003 and 2004 [31, 53]. The research consisted of testing a commercial product (Fire-Trol 934) and applying retardant solutions at high distribution ratios. Table 4.4 shows more details on the experimental conditions of the tests. The fire fronts under these experimental conditions stopped at the treated strips due to the high amount of retardant applied.

Pastor et al. [31-32] attempted to evaluate ROS reductions in the field on the basis of their laboratory results. They tested two commercial products (FR CROS 134P and Fire-Trol 934) on plots of Portuguese shrubland which had 4- and 7-meter-wide strips of treated-land parallel to the ignition line of the plots. These strips were treated manually with backpack sprayers and left to dry for 24h. The authors applied a similar experimental methodology to the one developed in [50] to compute ROS and an IR camera was used to calculate the temperature reduction at the propagating front (see Table 4.4). They analyzed the data by considering ROS and radiant heat flux as proportions of the same parameters measured in the untreated area of the plot. The burned area in the strip was graded according to the total strip area. The authors found that the qualitative behavior of the fire front at that scale and under the effect of retardants was the same as in the laboratory tests.

Vega et al. [54] conducted field experiments in a shrubland region of NW Spain. They compared the effects of water, foam and a commercial long-term retardant by considering the fuel load reduction after the fire, the residual diameters of shrub terminal branches and the ROS. Treatments were applied to a 10-meter-wide strip of a hexagonal plot immediately prior to igniting the fire and five replicates were performed for each treatment (see Table 4.4 for more details). The authors used statistical analysis to examine the results. They found no significant differences between treatments in terms of fuel load reduction after the fire, but the residual terminal diameters of the fuel branches treated with retardant were significantly smaller than those of the untreated branches. Vega et al. concluded that applying long-term retardant was the most effective treatment in reducing the severity of forest fires because intense fires generally leave only thick branches unburned. They also recorded the greatest reduction in ROS for the fuel treated with long-term retardant product.

Table 4.4 Experimental studies on long-term forest fire retardants' effectiveness in field tests.

Authors (year)	**Ref.**	**Type of experiment**	**Topographical and environmental conditions**	**Chemicals or retardant products**	**Fuel (mean load - type)**	**Dilution rates / Distribution ratios [a]**	**Evaluation parameters**
Loane and Gould (1986)	[49]	Propagation / retardant aerially dropped	unspecified slope and aspect; wind speed: 2-9 m s^{-1} [b]	DAP with gum thickener, corrosion inhibitor, anti-caking agent, coloring agent	Eucalyptus (2.79 kg m^{-2} - forest) [b]	10.7% w/w; unspecified distribution rate	ROS, burned area, fire intensity [b]
Pastor (2004) ERAS (2005)	[31, 53]	Propagation / retardant solution manually applied 24h before the ignition	15° and 7° slope; NE and NW aspect; wind speed: 0-5 m s^{-1}	Fire-Trol 934	*Erica umbellata*, *Erica australis*, *Chamaespartium tridentatum, Ulex parviflorus, Halimium spp.* (5.7 and 2.7 kg m^{-2} - shrubland)	15% and 20% v/v; 2 - 5 l m^{-2}	Fire stopping at the retardant strip
Pastor (2004) Pastor et al. (2006)	[31-32]	Propagation / retardant solution manually applied 24h before the ignition	7° slope; NW aspect; wind speed: 0-5 m s^{-1}	FR CROS 134P, Fire-Trol 934	*Erica umbellata*, *Erica australis*, *Chamaespartium tridentatum, Ulex parviflorus* (2.7 kg m^{-2} - shrubland)	FR CROS 134P: 5, 10, 15, 20 % v/v; 1 l m^{-2} Fire-Trol 934: 15, 20 % v/v; 2 and 3 l m^{-2}	ROS, burned area, temperature of the burning area

Table 4.4 Experimental studies on long-term forest fire retardants' effectiveness in field tests (continued).

Authors (year)	**Ref.**	**Type of experiment**	**Topographical and environmental conditions**	**Chemicals or retardant products**	**Fuel (mean load - type)**	**Dilution rates / Distribution ratios** [a]	**Evaluation parameters**
Viegas (1999, 2000) Ribeiro (2006)	[51-52, 30]	Propagation / retardant solution manually applied 24h before the ignition	20° slope; NW aspect; wind speed: unspecified	3 unspecified commercial products	*Erica umbellata*, *Erica australis*, *Chamaespartium tridentatum* (2.4 kg m^{-2} - shrubland)	Dilution rate specified by the manufacturers; 1 l m^{-2}	ROS, burned area
Vega et al. (2007)	[54]	Propagation / retardant solution manually applied before the ignition	unspecified slope and aspect; wind speed: 4 – 5.7 m s^{-1} at 6 m	FR CROS 134P	*Ulex gallii*, *Ulex europaeus* (2.8 kg m^{-2} - shrubland)	20% v/v; 1 l m^{-2}	ROS, fuel load, residual diameter of shrub terminal branches

a. Dilution rates are expressed as a percentage of weight or volume of retardant per weight or volume of retardant and water (% w/w and % v/v, respectively). If a different notation is used it is specifically indicated. Distribution ratios are expressed as liters of solution per square meter.

b. Data extracted from a publication of the Aquarius Project [57] where the general experimental procedures used in the project are described but tests with retardants are not specifically mentioned.

4.4 Discussion

Three different experimental scales have been used to study the performance of different forest fire retardants and all have been valuable for providing information on the effect of these products.

The studies have used commercial products and pure chemical reagents. Chemical reagents were used for most of the analytical scale experiments, whereas commercial products were used for most of the field tests. The laboratory tests have used both types, with most recent studies using commercial products.

Differences when using pure chemical reagents or commercial products may arise due to the existence of additives in commercial formulations. For instance, iron oxide is the most commonly used coloring agent and the authors of [43] stated that impurities including the iron concentration in the solution could tie up the phosphate to form compounds that are ineffective as fire retardants, which would reduce the actual effective phosphate percentage. However, this issue has not been studied. In propagation tests another difference between using pure chemical reagents and commercial products is the application patterns. Different thickening agents, which may be either gum- or clay-based, can produce patterns with a greater or lesser degree of compression and differences in the amount of retardant that adheres to the surface of the fuel bed and penetrates the fuel toward the bottom. This issue was highlighted by Giménez et al. [33], who worked with two commercial products that contained different thickening agents and the same retardant salt (ammonium polyphosphate).

The analytical scale is suitable for studying the flammability of treated forest fuels and the action mechanisms of retardants, but it cannot be used to analyze the global effect of retardants on forest fires. In addition, it is necessary to combine the results of the propagation tests with analytical data to produce a physical model of the phenomenon.

Analytical instrumentation can be used to determine intrinsic properties of forest fuels, i.e. thermal data (ignition temperature, pyrolysis temperature, specific heat, thermal conductivity, etc.), chemical data (activation energy, higher heating value, ultimate analysis, proximate analysis, etc.) and physical data (fuel density, porosity, surface area, etc.). It is possible to compare and characterize fuels on the basis of this type of parameters and this is the

approach used in the analytical studies reviewed to analyze the effectiveness of the different retardants.

However, it is important to remember that wildfires are dynamic processes. Rate of spread is a basic parameter in forest fire analysis that cannot be measured by the analytical equipment presented in this study. In addition, the fuel exposure conditions in wildfires differ considerably from the conditions used in analytical tests due to differences in, for example, bulk densities and surface area-to-volume ratios, among others. Figure 4.4 shows total residual masses obtained in analytical experiments and laboratory-scale propagation tests for different retardant treatment levels and highlights the differences that can be obtained.

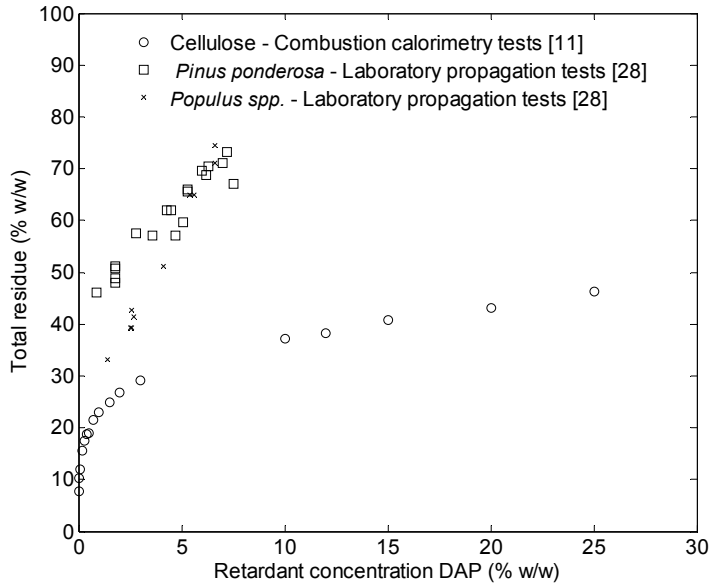

Figure 4.4 Percentage of total residue (fuel and retardant) vs. Retardant concentration (% mass of retardant per mass of fuel and retardant) for different experimental conditions and fuels.

The analytical researchers who carried out most of the studies reviewed here were aware of the limitations of the methodologies, which is why experts have designed enhanced equipment for more recent studies. For example, the authors of one recent study used fuel beds instead of powdered samples [26].

The principal aim of the laboratory propagation studies was to compare the relative effectiveness of different products and formulations rather than understanding the behavior of fire fronts under the effect of retardants. Most tests at this scale are now performed by management or research agencies in

order to evaluate commercial products for public use. However, the number of tests carried out in this field is currently decreasing because a wide range of products have already been evaluated and these types of organization generally prefer to limit the number of tests. For example, the retardant evaluation specification of the USDA Forest Service (5100-304c) states that burning tests are not required if the product contains a minimum percentage of active salt [55].

The number of experimental field studies was much lower than the number of laboratory tests. Even though this scale of evaluation does not completely reproduce operational fire fighting conditions, it provides a better approximation than laboratory experiments. Obviously, these types of experiments present more technical difficulties than laboratory experimentation, but they are vital for modeling fire behavior under the effect of retardants.

No study to date has successfully combined the results obtained at these three scales for either untreated forest fuels or for forest fuels treated with retardants. However, Rothermel and Philpot [34] used the concepts of ignition temperature and ROS to link analytical tests with laboratory propagation tests. Ribeiro et al. [30] and Pastor et al. [31-32] extrapolated laboratory methodologies to field studies and obtained encouraging results. However, Pastor et al. [32] also pointed out that it was important to consider how changing the experimental scale might affect the characteristic parameters that describe the fire behavior. Another effort to model the effect of retardants on fire propagation was done in the frame of the European project Extended Retardant Application System (ERAS) [53]. However, experimental data have not been published and only the approach followed and the results obtained has been described. Multiphase physical propagation models are designed to resolve the inherent reactive problems of forest fires (pyrolysis and combustion) [56] and generally use one-step Arrhenius kinetics to represent pyrolysis. A modification of the activation energy in the pyrolysis law was used to model the effect of the retardants. They used analytical data to obtain the pyrolysis law and laboratory data to validate the model.

An important operational application of the research studies reviewed in this study was implemented by the USDA Forest Service, as they were able to recommend different distribution ratios depending on fuel models.

Operationally important tests were conducted by [49] and [53]. Australian researchers made an important contribution in the framework of the Aquarius Project [49]. They studied the propagation of fires in a common vegetation type and determined the distribution ratio required to halt a fire for one hour and correlated this with fire intensity. They observed fires with different intensities in the same fuel complex. Fuel complex characteristics and other factors influencing the propagation of a forest fire (e.g. slope, wind speed, weather conditions) are implicitly considered if the fire intensity concept is employed. This kind of approach is more general than considering only fuel complex characteristics and it should be used to study fuel complexes independently.

The authors of [53] evaluated whether fire spread stopped at the retardant strip or not. This evaluation parameter is worthwhile for operational purposes but it has to be related to other parameters, such as fire intensity and distribution ratio. This step forward was not tackled in [53].

4.5 Conclusions

In this chapter we have summarized the experimental procedures and findings of several studies that were designed to evaluate the effectiveness of long-term forest fire retardants.

It is difficult to obtain data on the behavior of forest fires under the effect of retardants during wildfire operations. Thus, the three scales presented here represent useful scenarios for understanding and modeling the effects of these products on forest fires.

Most analytical experiments for evaluating the effect of fire retardants have been carried out since the beginning of the 1990s. The earliest tests used thermal analysis techniques, subsequent studies used gas chromatography and mass spectrometry, and current experiments use combined techniques. Most of these experiments were performed in a pyrolytic atmosphere. In trials with an oxidant atmosphere the temperatures of maximum weight loss were not consistent in between different studies. Therefore, it would be beneficial to perform additional analytical experiments in oxidant atmospheres over a wider range of treatment levels and with different forest species to resolve this issue.

Laboratory combustion tests were mainly focused on evaluating the relative effectiveness of different retardant products. Only a few studies have taken into account the effect of retardants in propagation models or attempted to quantify the usefulness of these products in reinforcing firebreaks.

Concerning field experimentation, although there is relatively little quantitative information on the effect of these products on fire behavior, evidence suggests that experiments carried out at this scale are useful and that the initial results are encouraging. It would be useful to design experimental scenarios at this scale to compensate for the small number of tests performed in the field to date.

The main conclusion that can be drawn from this review is that there is a lack of experimental studies focused on modeling the behavior of forest fires under the effect of long-term retardant products. Consequently, researchers should use the knowledge acquired at the analytical scale and from laboratory and field propagation tests to analyze this approach in more detail. Another important point is that it seems operationally worthwhile to relate the effectiveness of retardants to the intensity of the propagating fire front.

References

1. Giménez A, Pastor E, Zárate L, Planas E, Arnaldos J. Long-term forest fire retardants: a review of quality, effectiveness, application and environmental considerations. Int J Wildland Fire 2004;13(1):1-15.

2. Barrett LI. Possibilities of fire extinguisher chemicals in fighting forest fires. J Forest 1931;29(2):214-8.

3. Truax TR. The use of chemicals in forest fire control. USDA Forest Service, Forest Products Laboratory Report 1199; 1939.

4. Tyner HD. Fire extinguishing effectiveness of chemicals in water solution. Ind Eng Chem 1941;33(1):60-5.

5. Hardy C, Rothermel R, Davis J. An evaluation of forest fire retardants: a test of chemicals on laboratory fires. USDA Forest Service Research Paper 64; 1962.

6. George CW, Blakely AD, Johnson GM. Forest fire retardant research. A status report. USDA Forest Service General Technical Report INT-31; 1976.

7. Di Blasi C. Modeling chemical and physical processes of wood and biomass pyrolysis. Prog Energ Combust 2008;34(1):47-90.

8. Bradbury AGW, Sakai Y, Shafizadeh F. Kinetic model for pyrolysis of cellulose. J Appl Polym Sci 1979;23:3271-80.

9. Rowell RM, LeVan SL. Thermal Properties. In: Handbook of Wood Chemistry and Wood Composites (Ed. Rowell RM) CRC Press; 2005.

10. Shafizadeh F, Furneaux R, Stevenson T. Some reactions of levoglucosenone. Carbohyd Res 1979;71:169-91.

11. George C, Susott R. Effects of ammonium phosphate and sulfate on the pyrolysis and combustion of cellulose. USDA Forest Service Research Paper INT-18; 1971.

12. Pappa A, Tzamtzis N, Statheropoulos M, Parissakis G. Thermal analysis of *Pinus halepensis* pine-needles and their main components in the presence of $(NH_4)_2HPO_4$ and $(NH_4)_2SO_4$. Thermochim Acta 1995;261:165-73.

13. Liodakis S, Statheropoulos M, Tzamtzis N, Pappa A, Parissakis G. The effect of salt and oxide-hydroxide additives on the pyrolysis of cellulose and *Pinus halepensis* pine needles. Thermochim Acta 1996;278:99-108.

14. Pappa A, Tzamtzis N, Statheropoulos M, Liodakis S, Parissakis G. A comparative study of the effects of fire retardants on the pyrolysis of cellulose and *Pinus halepensis* pine-needles. J Anal Appl Pyrol 1995;31:85-100.

15. Liodakis S, Agiovlasitis I, Antonopoulos I, Stamatakis M. Fire retarding performance of hydromagnesite on forest species from a wildland/urban interface area in Athens. In: 'Proceedings of the 5th International Conference on Forest Fire Research' 27-30 November, Figueira da Foz, Portugal; 2006.

16. LeVan S. Chemistry of fire retardancy. In: The chemistry of solid wood (Ed. Rowell RM) Advances in Chemistry Series 207, Ch. 14, American Chemical Society; 1984.

17. Mermet JM, Otto M, Widmer HM (editors). Analytical Chemistry. Wiley-VCH; 1998.

18. Tzamtzis N, Liodakis S, Pappa A, Statheropoulos M, Parissakis G. The effect of $(NH_4)HPO_4$ and $(NH_4)_2SO_4$ on the composition of volatile organic pyrolysis products of cellulose: PY-GC studies. Polym Degrad Stabil 1997;56:287-90.

19. Tzamtzis N, Pappa A, Mourikis A. The effect of $(NH_4)HPO_4$ and $(NH_4)_2SO_4$ on the composition of the volatile organic pyrolysis products of *Pinus halepensis* pine-needles. Polym Degrad Stabil 1999;66:55-63.

20. Liodakis S, Bakirtzis D, Lois E, Gakis D. The effect of $(NH_4)_2HPO_4$ and $(NH_4)_2SO_4$ on the spontaneous ignition properties of *Pinus halepensis* pine needles. Fire Safety J 2002;37:481-94.

21. Liodakis S, Bakirtzis D, Dimitrakopoulos A. Autoignition and thermogravimetric analysis of forest species treated with fire retardants. Thermochim Acta 2003;399:31-42.

22. Núñez-Regueira L, Rodríguez-Añón JA, Proupín-Castiñeiras J. Using calorimetry for determining the risk indices to prevent and fight forest fires. Thermochim Acta 2004;422, 81-7.

23. Liodakis S, Vorisis D, Agiovlasitis I. Testing the retardancy effect of various inorganic chemicals on smoldering combustion of *Pinus halepensis* needles. Thermochim Acta 2006;444(2):157-65.

24. Statheropoulos M, Kyriakou S. Quantitative thermogravimetric-mass spectrometric analysis for monitoring the effects of fire retardants on cellulose pyrolysis. Anal Chim Acta 2000;409(1):203-14.

25. Pappa A, Mikedi K, Tzamtzis N, Statheropoulos M. Chemometric methods for studying the effects of chemicals on cellulose pyrolysis by thermogravimetry-mass spectrometry. J Anal Appl Pyrol 2003;67:221-35.

26. Tzamtzis N, Karma S, Pappa A, Statheropoulos M. On-line monitoring of pine needles combustion emissions in the presence of fire retardant using a 'thermogravimetry (TG)-bridge/mass spectrometry method'. Anal Chim Acta 2006;573-574:439-44.

27. Bart J. Polymer/additive analysis by flash pyrolysis techniques. J Anal Appl Pyrol 2001;58-59:3-28.

28. George C, Blakely A. Effects of ammonium sulphate and ammonium phosphate on flammability. USDA Forest Service Research Paper INT-121; 1972.

29. Xanthopoulos G, Noussia P. Small-scale evaluation of a retardant-reinforced firebreak required to stop a forest fire. ACRE Project Report. Mediterranean Agronomic Institute of Chania, Crete, Greece; 2000.

30. Ribeiro L, Viegas D, Batalha M. Assessment of fire retardant efficiency. In: 'Proceedings of the 5th International Conference on Forest Fire Research' 27-30 November, Figueira da Foz, Portugal; 2006.

31. Pastor E. Contribució a l'estudi dels efectes dels retardants en l'extinció d'incendis forestals. PhD Thesis, Universitat Politècnica de Catalunya, Spain; 2004.

32. Pastor E, Planas E, Ribeiro L, Viegas D. Modelling the effectiveness of long-term forest fire retardants. In: 'Proceedings of the 5th International Conference on Forest Fire Research' 27-30 November, Figueira da Foz, Portugal; 2006.

33. Giménez A, Arqués P, Arnaldos J. Experimental study for characterizing the effectiveness of long-term forest fire retardants and the influence of fuel characteristics on the reduction of the rate of fire spread. In: 'Proceedings of the

5th International Conference on Forest Fire Research' 27-30 November, Figueira da Foz, Portugal; 2006.

34. Rothermel R, Philpot C. Reducing fire spread in wildland fuels. In: 'Proceedings of the Meeting to Honor Clay Preston Butler' Stanford, CA: Stanford Research Institute; 1975.

35. Blakely A. Combustion recovery: a measurement of fire retardant extinguishment capability. USDA Forest Service Research Paper INT-352; 1985.

36. Blakely A. Combustion recovery of flaming pine needle fuel beds sprayed with water/MAP mixtures. USDA Forest Service Research Paper INT-421; 1990.

37. Rothermel R, Hardy C. Influence of moisture on effectiveness of fire retardants. USDA Forest Service Research Paper INT-18; 1965.

38. George C, Blakely A. Energy release rates in fire retardant evaluation. Fire Technol 1970;6(3):203-10.

39. Rothermel R. A mathematical model for predicting fire spread in wildland fuels. USDA Forest Service Research Paper INT-115; 1972.

40. Swanson DH, Luedecke AD, Helvig TN, Parduhn FJ. Development of user guidelines for selected retardant aircraft. Final Report. Honeywell Contract 26-3332 to Intermountain Forest and Range Experiment Station (Odgen, UT); 1975.

41. George CW. Determining air tanker delivery performance using a simple slide chart-retardant coverage computer. USDA Forest Service General Technical Report INT-41; 1981.

42. Deeming JE, Burgan RE, Cohen JD. The national fire-danger rating system. USDA Forest Service General Technical Report INT-39; 1977.

43. George C, Blakely A, Johnson G, Simmerman D. Evaluation of liquid ammonium polyphosphate fire retardants. USDA Forest Service General Technical Report INT-41; 1977.

44. Blakely A. Monoammonium phosphate: effect on flammability of excelsior and pine needles. USDA Forest Service Research Paper INT-313; 1983.

45. Blakely A. Flammability reduction comparisons of four forest fire retardants. USDA Forest Service Research Paper INT-381; 1988.

46. USDA Forest Service. Standard test procedures for the evaluation of wildland fire chemical products. Technology and Development Program, 5100-Fire Management; 2000.

47. USDA Forest Service. Long-term retardants qualified by USDA Forest Service in accordance with Forest Service Specification 5100-304b, as amended. Source: http://www.fs.fed.us/rm/fire/documents/qpl_r_r.pdf. Last modified: 02/05/2007. Visiting date: 12/09/2007.

48. George CW. Improving the performance of fire retardant delivery systems on fixed-wing aircraft. USDA Forest Service Research Note INT-400; 1992.

49. Loane IT, Gould JS. Aerial suppression of bushfires. Cost-benefit study for Victoria. CSIRO Publishing Report; 1986.

50. Serviço Nacional de Protecção Civil, Direcção Geral das Florestas, Serviço Nacional de Bombeiros. Testes com soluçoes retardantes. Internal document; 1985.

51. Viegas D. Gestosa 98: Shrubland experimental fires. Inflame Project, General Report; 1999.

52. Viegas D. Gestosa 99: Shrubland experimental fires. Inflame Project, General Report; 2000.

53. ERAS (Extended Retardant Application System). ERAS Project Contract Number: EVG1-CT-2001-00039. Reporting period: March 1, 2004 / February 28, 2005. Internal report; 2005.

54. Vega JA, Cuíñas P, Fonturbel T, Pérez JR, Vega DJ, Pérez-Gorostiaga P, Fernández C, Jiménez E. Comparing the effect of polyphosphate and foam addition to water on fire propagation in shrubland. In: 'Proceedings of the 4th International Wildland Fire Conference' 13-17 May, Seville, Spain; 2007.

55. USDA Forest Service. Specification for long-term retardants, wildland fire fighting 5100-304c. Technical Document; 2007.

56. Morvan D, Dupuy JL. Modelling of fire spread through a forest fuel bed using a multiphase formulation. Combust Flame 2001;127:1981-94.

57. Budd GM, Brotherhood JR, Hendrie AL, Jeffery SE, Beasley FA, Costin BP, Zhien W, Baker MM, Cheney NP, Dawson MP. Project Aquarius 4. Experimental

CHAPTER 5

Characterization of laboratory-scale fires propagating under the effect of a long-term retardant *

Most of the work done to date to predict the effects of long-term retardants has been in the development of procedures for comparing one product with another and classifying their effectiveness for commercial use. However, fewer attempts have been made to assess the amount of retardant that would be needed for different types of fuel or to quantify retardant effects for varying fire situations. A comprehensive review of all these studies is available in Chapter 4 and published in [1].

The most important modeling efforts include the works of Rothermel and Philpot [2], Pastor [3], and Giménez et al. [4]. In the laboratory study of Rothermel and Philpot, a mathematical approach was followed to estimate the maximum retardant coverage level that would be useful in preventing fire spread for a wide variety of fuel types. Pastor developed expressions for the ratios of rate of spread and rate of weight loss for retardant-treated and untreated fuel beds under no-slope/no-wind conditions. The proposed

* The content of this Chapter has been submitted for publication at the international journal Combust Sci Technol. It is currently under review.

expressions depended on the ratio between the amount of dry retardant to dry fuel and the amount of water to dry fuel. Other no-slope/no-wind laboratory experiments were performed by Giménez et al., who derived relationships between the ratio of rate of spread for retardant-treated and untreated fuel, and two variables: the ratio of the amount of dry retardant to dry fuel and a non-dimensional variable related to fuel-bed characteristics, i.e. the total surface area per unit horizontal area of fuel bed.

Though some progress has been made in understanding the fire behavior and in developing expressions that relate fire spread variables to retardant amounts, knowledge of fire behavior associated with slope- or wind-aided fires in retardant-treated fuels needs to be extended. Upslope and upwind fires are much more common in real scenarios than no-slope/no-wind fires but to date only little efforts have been made to characterize fire behavior under upslope or upwind conditions for retardant-treated fuel [5].

The present work aims to investigate the effect of slope and wind on the behavior of fires propagating through a retardant-treated strip in laboratory fuel beds and to describe fire behavior in retardant-treated areas by comparing results of fire behavior with retardant-treated fuel with those of fire behavior with untreated fuel. This approach is based on the idea that given a model able to correctly predict fire behavior under untreated conditions, it would be possible to predict fire behavior under retardant-treated conditions simply by considering reduction factors obtained using a retardant concentration on the fuel bed similar to that used in operational tasks. Reduction factors (in percentage units) can be expressed in a general notation applicable to any of the variables characterizing fire behavior, as is proposed in Eq. [5.1].

$$Reduction\ factor = 100\left(1 - \frac{Var^{t}}{Var^{ut}}\right) \qquad [5.1]$$

The variables commonly used to describe fire behavior are rate of spread, fire intensity, fuel consumption and flame-front dimensions. Characterization of the rate of spread and the fire intensity is important at both the planning and the suppression stages. In the planning stages, this information can be used to define the conditions under which a prescribed fire will be conducted. Predicted spread rate and intensity are used during a wildfire to determine suppression tactics [6]. Knowledge of fuel consumption is necessary to compute fire intensity, together with the heat of combustion of the fuel and the rate of spread. Flame characteristics are important to many applications of fire behavior and effects: flame length is related to fire intensity, flame height is

important in determining crowning potential, and flame angle and height are necessary to determine the amount of radiative heat transfer [7].

Reduction factors on rate of spread, fuel consumption ratio and fire intensity in retardant-treated straw fuel beds are reported in this study. The main results concerning fuel moisture content effect on rate of spread, as well as slope and wind effects on rate of spread, fire intensity, fuel consumption ratio and flame dimensions are also described for retardant-treated straw fuel beds.

5.1 Experimental method

5.1.1 Tests conditions

The experiments consisted of igniting the total width of a rectangular fuel bed in order to observe the flame front spread under no-slope/no-wind (C), upslope/no-wind (S) and no-slope/upwind (W) conditions. Flame fronts were propagating parallel to the slope or to the wind direction.

Experiments were conducted on a combustion table and on a wind tunnel, both placed in the ADAI's large experimental building near Lousã (Portugal). Both devices are essentially composed of a 4x4- and 2.6x8-m^2 platform, respectively. The wind tunnel has two lateral glass walls 2 m high, and two axial fans create a wind flow. The flow velocity can be varied with great precision using a frequency converter that controls the rotational speed of the fans.

Porous fuel beds with constant bulk density (7.5 kg m^{-3}) were tested. They were made up of straw (*Triticum turgidum*), spread as evenly as possible. The physical and chemical properties of the straw are given in Table 5.1. The tests performed on the combustion table had a fuel-bed length of 3.15 m, compared with 5.5 m in the wind tunnel when the fans were switched on and 3 m when they were switched off. The fuel beds were longer when there was an induced wind to allow the flame front to be stabilized. All fuel beds had a 0.50-m-long strip of retardant-treated fuel which was placed 0.50 m before the end of the fuel bed.

Table 5.1 Fuel properties (extracted from [3]).

Species	*Triticum turgidum* (straw)
Surface-area-to-volume ratio (m^{-1})	4734
Fuel particle density (kg m^{-3})	258
High heat of combustion (*HHC*) (kJ kg^{-1})	18,868

Fuel beds were 0.50, 1.00 or 1.25 m wide. Both fuel-bed loading and depth varied according to the fuel-bed width. The main characteristics of the fuel-beds configuration are indicated in Table 5.2 and the appearance of a 1.25-m-wide fuel bed prepared on the combustion table is shown in Figure 5.1. Since the aim of this work was to compare the fire behavior in the untreated and retardant-treated areas of the fuel bed, differences due to fuel-bed dimensions are not taken into consideration. The combustion table was inclined 10°, 20°, or 30°, and flow velocities induced in the wind tunnel ranged from 0.7 to 3.3 m s^{-1}. More details about the experimental program are available in [8]. A total of 36 C, 18 S and 18 W fires were conducted but some tests were excluded at the analysis stage either because certain data were lacking or because the propagation on the retardant strip was not uniform.

Table 5.2 Fuel-beds configuration.

Width (m)	**Fuel loading – dry basis (kg m^{-2})**	**Depth (m)**
0.50	0.30	0.04
1.00	0.60	0.08
1.25	0.75	0.10

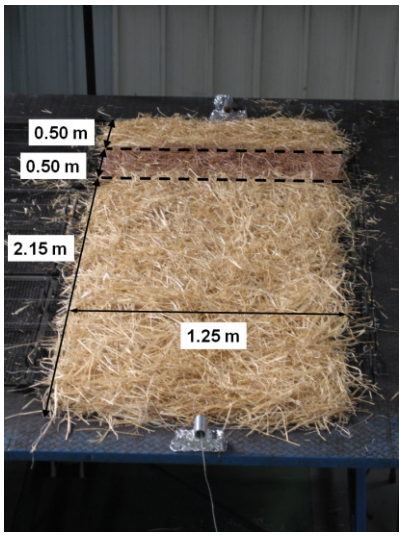

Figure 5.1 1.25-m-wide fuel bed prepared on the combustion table. The retardant-treated strip (0.50-m-long) is placed within the two dashed lines. The length of the untreated areas is also displayed.

Immediately prior to ignition, two samples of straw were extracted for moisture analysis from the untreated and the retardant-treated areas of the fuel bed. Moisture content of untreated samples was determined with a moisture

analyzer (infrared drying; AND A&D Weighing, MX-50) and retardant-treated samples were analyzed by oven drying at a temperature of 373K for 24 h. These two different methods were employed to reduce time before ignition after the preparation of the fuel bed.

Ambient air properties were quite stable during the experimental period. The mean temperature and the mean relative humidity were respectively 302.2K and 41%. Their standard deviation was respectively 3.9K and 10%.

5.1.2 Retardant treatment

A long-term retardant product (Fire-Trol 931) commercialized as liquid concentrate was used in the experiments. It was diluted with water at a mix ratio of 20% v/v and three coverage levels were applied according to the fuel-bed loading (0.4, 0.8 and 1.0 l m^{-2}, respectively). These coverage levels maintained constant a ratio of 0.2 kg of dry retardant product per kg of fuel, since the liquid concentrate has a density of 1220 kg m^{-3} and a proportion of dry retardant product of 59% w/w [3]. This amount of dry retardant product per kg of fuel is usually applied during extinction operations. A manual sprayer was used to apply the retardant dilution to the fuel-bed strip.

Retardant-treated fuel-bed strips were prepared at least 24 h before the fuel-bed ignition in order to allow the fuel to dry up naturally until it reached the equilibrium with the environment (i.e. until the net exchange of moisture between the treated fuel particles and the environment was approximately zero). To optimize the number of tests carried out during the experimental period, retardant-treated fuel-bed strips were prepared in an area separate from the combustion table and the wind tunnel. Before each experiment the corresponding strip was taken to the corresponding device and carefully joined to the rest of the fuel bed.

5.1.3 Rate of spread

The rate of spread (R) was computed by following the methodology described in the Appendix A and published in [9], based on thermal image processing. An infrared camera (AGEMA Thermovision 570-Pro) positioned so that the entire fuel bed was visible was used to record the advancing flame front. The fire front developed a curvature in many S and W tests. The most advanced points of the flame front was used to compute R.

5.1.4 Fuel consumption

The amount of fuel consumed per unit area (w_a) was calculated by subtracting the residual loading from the initial fuel loading. To obtain the residual loading two (fires in the combustion table) or three (fires in the wind tunnel) aluminum plates (177 cm^2) were randomly distributed under the untreated area of the fuel bed. After the test, the mass contained within each plate was measured with a balance (Mettler PM600) and the residual loading was then deduced by averaging the two or three measurements and by considering the area of the plates. The same procedure was applied to the retardant-treated fuel-bed strip, but only one aluminum plate was placed under it. Due to the methodology used in this study to obtain w_a, the values presented here may include a slight mass loss occurring after the flame front but this contribution is not significant.

Fuel consumption ratios (FCR) were also computed and deduced by dividing the amount of fuel consumed per unit area by the initial fuel loading.

5.1.5 Fire intensity

The heat released per unit time per unit length of fire front, termed fire intensity, was computed according to the definition of Byram [10] and the considerations of Alexander [11] on the heat yield. More specifically, Eq. [5.2] was used.

$$I_B = (HHC - 1263 - 24\,X_w)\,w_a\,R \qquad [5.2]$$

Figures 1263 and 24 stand for the latent heat absorbed when the water of reaction is vaporized and the heat required to vaporize one moisture content percentage point at 100°C, respectively. HHC is the high heat of combustion of the fuel (kJ kg^{-1}), X_w is the fuel moisture content in a dry basis (%), w_a is the fuel consumption (kg m^{-2}) and R is the rate of spread (m s^{-1}).

5.1.6 Effective wind velocity for S fires

S and W fires were analyzed together on the assumption that there is an analogy between slope effect and wind effect on fire behavior. An effective wind velocity was computed for S fires following the approach presented in [12], in which the upslope component of the fire's buoyant velocity was used to produce effective values of wind.

5.1.7 Flame dimensions

Flame characteristics for each fire were documented with video cameras. After completion of the experimental fires, flame images were analyzed with Matlab. For each test, fifty images corresponding to the period in which the flame front was propagating through the untreated area of the fuel bed and fifty more corresponding to the period in which the flame front was propagating through the retardant-treated fuel-bed strip were used to obtain mean values of flame characteristics. Two variables were determined: flame length (L) and angle (α). They were determined by using as a reference the leading edge of the flame (see Figure 5.2).

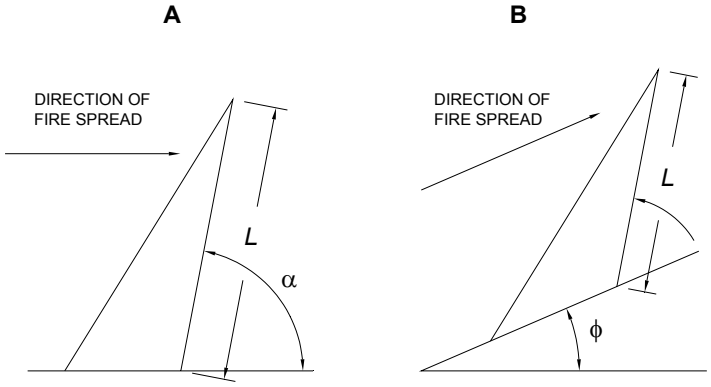

Figure 5.2 Flame measurements. A) No-slope fires; B) Upslope fires. L: flame length; α: flame angle; ϕ: slope angle of the combustion table.

Figure 5.3 gives an example of the points that were manually marked on each image to obtain flame characteristics. Point 1 corresponds to the base of the flame with respect to the fuel bed and point 2 corresponds to the tip of the main flame.

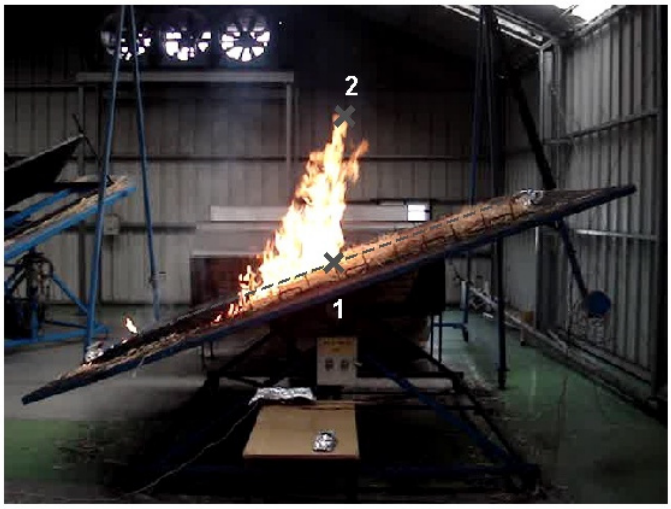

Figure 5.3 Image illustrating points used to measure flame dimensions (upslope fire). The dashed line indicates the central line of the fuel bed and was used as a reference.

5.2 Results and discussion

5.2.1 Rate of spread

The rate of spread (R) was calculated for each test in the untreated and the retardant-treated areas. As is shown in Table 5.3, rate of spread values for C fires ranged from 0.005 to 0.021 m s^{-1} and from 0.003 to 0.008 m s^{-1} for untreated and retardant-treated areas, respectively. An evident increase in mean R values with the initial fuel loading was observed for untreated fuel. This increase was not as evident in C fires for retardant-treated fuel.

Table 5.3 Statistical values for the rate of spread (R) (m s^{-1}) of no-slope/no-wind (C) fires in untreated and retardant-treated areas for different fuel loadings (kg m^{-2}). RSD: relative standard deviation (%); n: number of tests.

Fuel loading	n	*R* (untreated; C fires)				*R* (retardant-treated; C fires)			
		Min	Max	Mean	RSD	Min	Max	Mean	RSD
0.30	10	0.005	0.013	0.009	29	0.003	0.006	0.004	23
0.60	10	0.008	0.017	0.013	26	0.003	0.008	0.005	28
0.75	12	0.010	0.021	0.015	26	0.003	0.006	0.005	23

Given that fuel moisture content greatly influences the rate of spread, Figure 5.4 shows the changes in R with fuel moisture content for C fires, making a distinction between untreated and retardant-treated areas and fuel loadings. Mean fuel moisture contents were 0.086 (RSD 17%) and 0.080 (RSD 29%) for untreated and retardant-treated fuel data, respectively. Both mean values fell in a range of fuel moisture contents (0-0.090) in which R decreases almost

linearly, as was previously underlined in [3] based on the results shown by Rothermel [13] and Anderson [14]. However, as is shown in Figure 5.4, fuel moisture content only had a large influence on untreated fuel, but not on retardant-treated fuel because the retardant action masked the moisture effect.

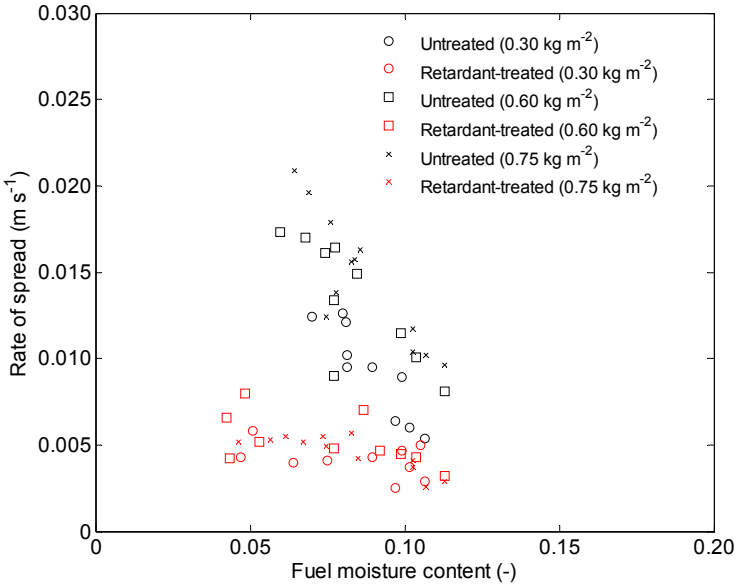

Figure 5.4 Rate of spread versus fuel moisture content of no-slope/no-wind fires in untreated and retardant-treated areas. Initial fuel loading has been differentiated.

For S/W fires, rate of spread values ranged from 0.009 to 0.146 m s^{-1} and from 0.003 to 0.050 m s^{-1} for untreated and retardant-treated areas, respectively. In Figure 5.5, the rate of spread calculated in untreated and retardant-treated areas for S/W fires is shown as a function of the wind velocity, with a distinction between slope- and wind-aided fires. The power dependence of R on the wind velocity, already pointed out by other authors (see [15]), is clearly observable in this figure for untreated fuel data. It is also visible that S fires follow the same tendency as W fires, which validates the assumption that there is an analogy between slope and wind effects.

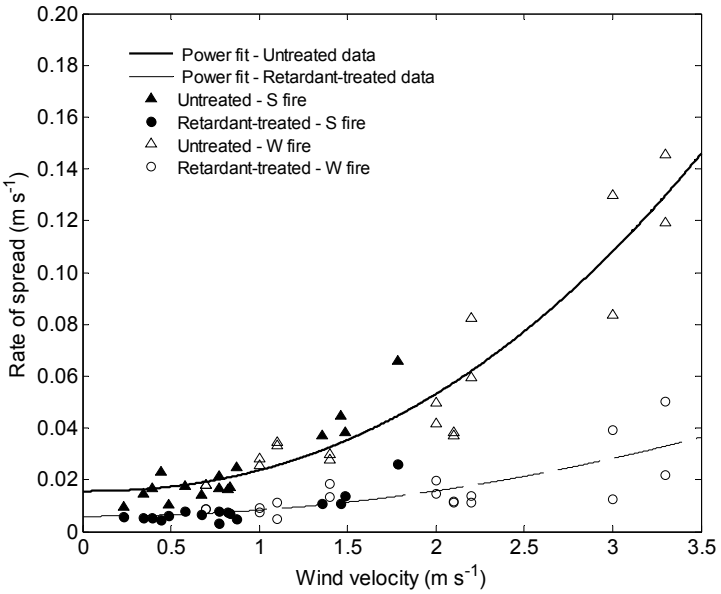

Figure 5.5 Rate of spread versus wind velocity of upslope/no-wind (S) and no-slope/upwind (W) fires in untreated and retardant-treated areas.

Fitting results for data displayed in Figure 5.5 are shown in Eqs. [5.3] and [5.4]. A greater proportion of variance was accounted for by the power model associated with untreated data and the intercepts of the two models roughly agreed with mean R values computed for C fires (0.013 and 0.005 for untreated and retardant-treated data, respectively).

Untreated data: $R = 0.008\, U^{2.2} + 0.016$ (R^2 0.90) [5.3]

Retardant-treated data: $R = 0.002\, U^{2.0} + 0.006$ (R^2 0.62) [5.4]

The rate of spread in the retardant-treated area is plotted against the rate of spread in the untreated area for C and S/W fires in Figure 5.6. All data points fall beneath the black line, indicating that the rate of spread was reduced by the presence of retardant.

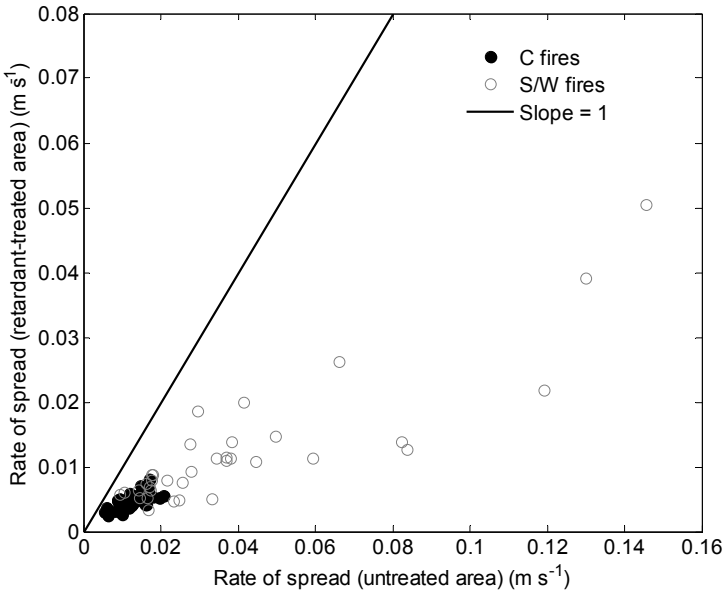

Figure 5.6 Rate of spread in the retardant-treated area versus rate of spread in the untreated area. No-slope/no-wind (C) fires and upslope/no-wind and no-slope/upwind (S/W) fires have been differentiated. Black line indicates a non-reducing behavior.

According to the general definition indicated in Eq. [5.1] for the reduction factor, mean reduction factors on rate of spread for C and S/W fires are shown in Table 5.4. The mean reduction factor on rate of spread for C fires was lower than that for S/W fires. An analysis of variance (ANOVA) was performed with both sets of data to infer whether this difference was statistically significant. Since the ANOVA p-value was greater than 0.05 (fixed significance level), it was possible to state that the difference was not significant and to calculate a mean reduction factor on rate of spread of 63.3% for both types of fire.

Table 5.4 Statistical values for the reduction factor on rate of spread.

Type of fire	C fires	S/W fires
Mean value (%)	61.1	65.4
RSD value (%)	15.7	19.7
ANOVA p-value	0.123	
Mean value considering both types of fires (%)	63.3	

5.2.2 Fuel consumption

Results on the fuel consumption ratio, both for C and S/W fires, are shown in Table 5.5. Data indicate that the FCR was greater for untreated fuel. The action mechanism of the retardants can be evoked to explain the different levels in FCR between untreated and retardant-treated fuel. For untreated fuel, the FCR

is near to unity because non-mineral material was totally consumed. FCRs are lower for retardant-treated fuel because ammonium-phosphate-based retardants enhance the production of char and act against smoldering combustion [16].

Table 5.5 Statistical results obtained for the fuel consumption ratio (FCR) (-) of no-slope/no-wind (C) fires and upslope/no-wind and no-slope/upwind (S/W) fires in untreated and retardant-treated areas for different fuel loadings (kg m^{-2}). RSD: relative standard deviation (%); n: number of tests.

Fuel loading	**n**	***FCR* (untreated; C fires)**				***FCR* (retardant-treated; C fires)**			
		Min	**Max**	**Mean**	**RSD**	**Min**	**Max**	**Mean**	**RSD**
0.30	10	0.93	0.95	0.94	1	0.49	0.80	0.69	14
0.60	10	0.89	0.96	0.94	2	0.50	0.63	0.57	8
0.75	12	0.90	0.98	0.94	2	0.49	0.71	0.60	13
Fuel loading	**n**	***FCR* (untreated; S/W fires)**				***FCR* (retardant-treated; S/W fires)**			
		Min	**Max**	**Mean**	**RSD**	**Min**	**Max**	**Mean**	**RSD**
0.30	11	0.91	0.96	0.94	2	0.47	0.66	0.58	12
0.60	12	0.91	0.96	0.93	2	0.46	0.70	0.59	11
0.75	12	0.89	0.97	0.94	2	0.42	0.72	0.56	18

A higher variability for FCR was obtained for retardant-treated data. This is probably due to the fact that only one aluminum plate was placed under the retardant-treated fuel-bed strip; it may also be due to random variability produced by uncontrolled factors during retardant treatment (e.g. homogeneity of the retardant dilution manually applied). ANOVA was also used in this case to compare mean reduction factors on FCR within the type of fire and it showed that there were no significant differences within the type of fire (see Table 5.6), so a mean reduction factor on FCR of 36.4% was calculated.

Table 5.6 Statistical values for the reduction factor on the fuel consumption ratio.

Type of fire	C fires	S/W fires
Mean value (%)	34.4	38.2
RSD value (%)	27.9	21.9
ANOVA p-value	0.085	
Mean value considering both types of fires (%)	36.4	

5.2.3 Fire intensity

In Figure 5.7, fire intensity data points in the retardant-treated area are plotted against fire intensity data points in the untreated area, with a distinction between C and S/W fires. In Table 5.7, ranges of fire intensity calculated for C and S/W fires are shown. As it was expected, fire intensities at the retardant-treated area (I_B^t) are lower than fire intensities at the untreated area (I_B^{ut}) (all data points fall beneath the black line in Figure 5.7).

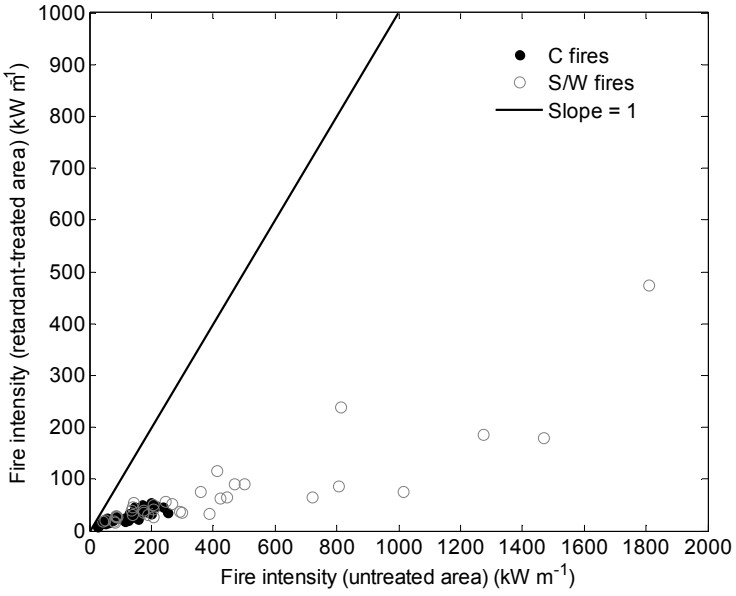

Figure 5.7 Fire intensity in the retardant-treated area versus fire intensity in the untreated area. No-slope/no-wind (C) fires and upslope/no-wind and no-slope/upwind (S/W) fires are differentiated. Black line indicates a non-reducing behavior.

With regard to fire intensity values, it is worth noting that the flame front was able to propagate through the retardant-treated fuel even at a I_B^t of 7 kW m^{-1} (the corresponding I_B^{ut} is 26 kW m^{-1}). Moreover, a test which did not propagate in the retardant-treated area (not included in Table 5.7) had a fire intensity in the untreated area of 22 kW m^{-1} and a fuel moisture content of 0.115, the lowest and the highest values computed for all tests, respectively. Although the extinction point of spreading fires is difficult to define, based on these two observations it can be said that, for the type of fuel beds used in this study, minimum fire intensities supporting spread ranged between 22 kW m^{-1} and 26 kW m^{-1}. In Figure 5.7 it can be seen that most fire intensity values in the untreated area were lower than 600 kW m^{-1} and fire intensities higher than this value were only computed for seven tests. Six of these seven tests correspond to tests conducted under a wind velocity equal to or greater than 2.2 m s^{-1}; the

other test was conducted on the combustion table with a slope of 30° and the fuel, in both the untreated and retardant-treated areas, had a low moisture content (about 0.075) in comparison with its replicate, which had a lower fire intensity value because the fuel moisture content was about 0.107.

Table 5.7 Ranges of fire intensity (kW m^{-1}) of no-slope/no-wind (C) fires and upslope/no-wind and no-slope/upwind (S/W) fires in untreated and retardant-treated areas for different fuel loadings (kg m^{-2}). n: number of tests; I_B^{ut}: fire intensity in the untreated-area (kW m^{-1}); I_B^t: fire intensity in the retardant-treated area (kW m^{-1}).

Fuel loading	**n**	I_B^{ut} **(C fires)**		I_B^t **(C fires)**	
		Minimum	**Maximum**	**Minimum**	**Maximum**
0.30	10	26	63	7	24
0.60	10	77	172	20	50
0.75	12	116	254	19	53
Fuel loading	**n**	I_B^{ut} **(S/W fires)**		I_B^t **(S/W fires)**	
		Minimum	**Maximum**	**Minimum**	**Maximum**
0.30	11	45	189	17	54
0.60	12	136	1274	31	186
0.75	12	206	1811	27	474

Mean reduction factors on fire intensity for C and S/W fires are shown in Table 5.8. The mean reduction factor on fire intensity for C fires was lower than that for S/W fires. However, ANOVA results indicated that mean reduction factors for the two types of fire showed no statistically significant differences. A mean reduction factor on fire intensity for both types of fire of 76.4% was calculated.

Table 5.8 Statistical values for the fire intensity reduction factor.

Type of fire	C fires	S/W fires
Mean value (%)	74.2	78.4
RSD value (%)	11.0	11.5
ANOVA p-value	0.052	
Mean value considering both types of fires (%)	76.4	

The reduction factor can also be obtained by combining reduction factors obtained for rate of spread and FCR (see Eq. [5.5]). Note that the corresponding fire intensity reduction factor (76.7%) is almost equal to the one obtained by using intensity values.

$$I_B^t = \frac{(100 - 63.3)}{100}\frac{(100 - 36.4)}{100} I_B^{ut} = 0.233\, I_B^{ut} \qquad [5.5]$$

5.2.4 Flame length

Flame length values in the retardant-treated area are shown in Figure 5.8 against flame length values in the untreated area. From the examination of the data points shown in this figure, it is seen that flame length was also reduced due to the presence of retardant.

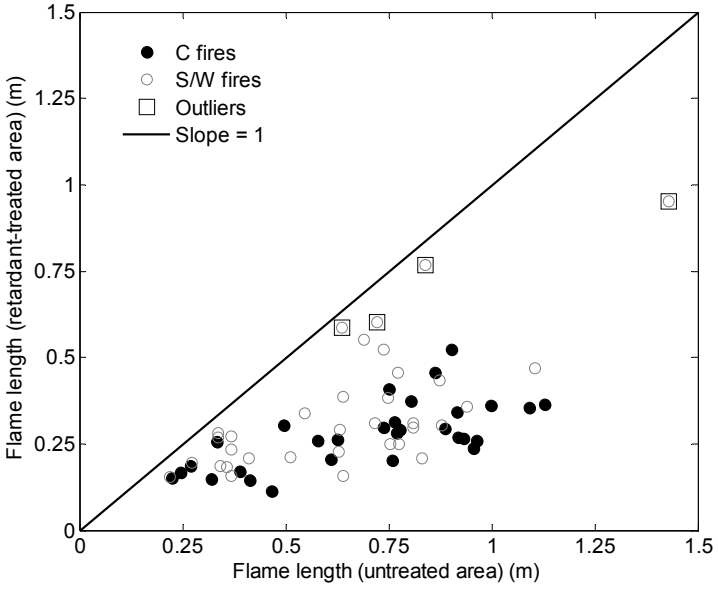

Figure 5.8 Flame length in the retardant-treated area versus flame length in the untreated area. No-slope/no-wind (C) fires and upslope/no-wind and no-slope/upwind (S/W) fires have been differentiated. Black line indicates a non-reducing behavior.

Large data point dispersion is observable in this figure, so in order to guarantee reliable estimations for the reduction factor on flame length, flame length in the retardant-treated area and flame length in the untreated area were linearly correlated and standardized residuals were examined to identify potential outliers. In the check, four outliers were found (standardized residuals > ±2; see Figure 5.8) and they were not taken into consideration in the calculation of the reduction factors. Determined outliers corresponded to fires carried out at high wind velocities (≥ 3 m s^{-1}) and to fires carried out with high slopes and low fuel moisture contents. This outlying behavior might be explained based on visual observations. As is seen in Figure 5.9, flame fronts obtained under these conditions (Figure 5.9A and B) were totally different from fronts with low wind velocities or slopes (Figure 5.9C and D); fronts experienced a high degree of

curvature at high wind velocities and high slopes due to the limiting width of the fuel bed. When the most advanced point of the flame front propagated into the retardant-treated strip, it was affected by wind, retardant presence, and heat transfer due to untreated fuel burning behind the retardant-treated fuel-bed strip. Flame length at the leading edge of the flame front was then not reduced at the same ratio as for fires propagating under low wind velocities and slopes, which had a low degree of curvature and the flame front entering into the retardant-treated strip was only affected by wind and the presence of retardant.

Figure 5.9 Images illustrating different fire situations on a fuel bed of 0.75 kg m^{-2}. A) Untreated area; wind velocity: 3.3 m s^{-1}; B) Retardant-treated area; wind velocity: 3.3 m s^{-1}; C) Untreated area; wind velocity: 1.1 m s^{-1}; D) Retardant-treated area; wind velocity: 1.1 m s^{-1}.

On the subject of calculating reduction factors, it is seen in Table 5.9 that both types of fire can be used together to compute a mean reduction factor on flame length (p-value > 0.05). As is shown in Table 5.9, flame length was approximately reduced by a factor of 53.8%.

Table 5.9 Statistical values for the flame length reduction factor.

Type of fire	C fires	S/W fires
Mean value (%)	57.2	50.2
RSD value (%)	25.2	32.2
ANOVA p-value	0.085	
Mean value considering both types of fires (%)	53.8	

The relationship between flame length and fire intensity has been previously described to be a power function ($L = aI_B{}^b$). Regression coefficients obtained for both types of fire are specified in Table 5.10, with a distinction between untreated and retardant-treated data. Coefficients obtained here for both

untreated and retardant-treated fuel in the case of no-slope/no-wind fires were in great agreement with the values presented in the model of Thomas [17] ($a = 0.0266$ and $b = 2/3$), a widely used model for this type of fire based on dimensional analysis. Powers reported here for fires propagating under the effect of wind, in both the untreated and the retardant-treated area, were close to the empirical predictions of Byram [10] for wind-aided fires ($b = 0.46$). The power corresponding to untreated fuel was only 22% lower than the one reported by Byram and the power corresponding to retardant-treated fuel was 11% higher. Differences on the coefficient a were 16% higher and 48% lower for untreated and retardant-treated fuel, respectively, than the value reported by Byram ($a = 0.0775$). All these results indicate that equations governing flame length for untreated fuel are equally valid for retardant-treated fuel.

Table 5.10 Power regression coefficients ($L = aI_B{}^b$) and R-square value for no-slope/no-wind (C) fires and upslope/no-wind and no-slope/upwind (S/W) fires in untreated and retardant-treated areas. L: flame length (m); I_B: fire intensity (kW m^{-1}).

Type of fire	Area	a	b	R^2
C	Untreated	0.03	0.64	0.94
C	Retardant-treated	0.03	0.66	0.75
S/W	Untreated	0.09	0.36	0.59
S/W	Retardant-treated	0.04	0.51	0.48

5.2.5 Flame angle

Figure 5.10 presents flame angle data in the retardant-treated area versus flame angle data in the untreated area. In the absence of wind and in a horizontal fuel-bed, convective forces are induced by buoyancy generated in the reaction zone, so in principle the flame front should be vertical [18]. However, values greater than 90° obtained in this work for C fires indicate that the flame front was inclined towards the burned zone. This is due to convection of hot residues that remained behind the fire front. For S/W fires, flame angles were lower than 90°, indicating that the horizontal flow induced by wind was able to bring the flame front to the vicinity of the unburned fuel.

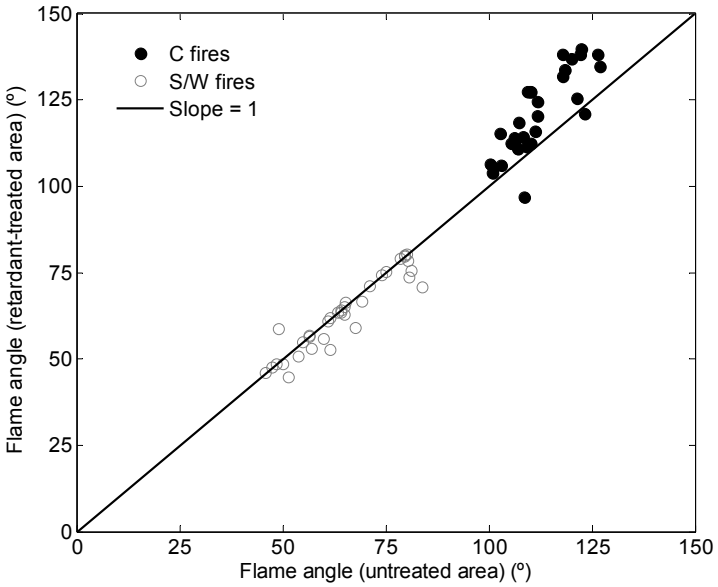

Figure 5.10 Flame angle in the retardant-treated area versus flame length in the untreated area. No-slope/no-wind (C) fires and upslope/no-wind and no-slope/upwind (S/W) fires have been differentiated. Black line indicates no effect on flame angle.

Differences in flame angle due to the presence of retardant are not significant for S/W fires; in general S/W fire data points fell on the line indicating no effect on flame angle (black line in Figure 5.10). This is probably because the wind effect dominated the retardant effect on this variable. However, slight differences on flame angle due to the presence of retardant are visible in Figure 5.10 for C fires; in general C fire data points fell above the no-effect line. This probably results from flame dimensions on the retardant-treated strip: flames were smaller here than in the untreated area, so they were proportionally more affected by convection behind the backing edge of the flame front than flames in the untreated area and consequently they were bent to a higher degree.

5.3 Conclusions

Propagation experiments were conducted in straw fuel beds with constant bulk density (7.5 kg m^{-3}) in order to study the extent to which the rate of spread, the fuel consumption ratio and the fire intensity decrease as a flame front initially propagating on an untreated area enters into an area previously treated with a long-term retardant. Moreover, flame length and angle were determined for the same flame fronts and the effect of retardant on these geometrical variables was also analyzed.

Experimental results indicate that, for the retardant concentration used in this study, the reduction factor on rate of spread, fuel consumption ratio and fire intensity depends neither on the characteristics of the propagating front before the retardant-treatment nor on the type of fire (wind- or slope-aided fires, or no-slope/no-wind fires). This result is applicable for a range of fire intensities of a flame front propagating in an untreated area from around 25 to 1800 kW m^{-1}. Approximate rate of spread, fuel consumption ratio and fire intensity reduction factors of 63%, 36% and 77%, respectively, were computed. It was also observed that the flame length at the retardant-treated area decreases by approximately 54% and that the effect of retardants of flame angle is not significant. Similar reduction factors should be expected for low-to-moderate surface fires propagating under the effect of a polyphosphate-based retardant.

Nomenclature

a, b	constants
FCR	fuel consumption ratio (w_a/w_0) (-)
HHC	high heat of combustion of the fuel (kJ kg^{-1})
I_B	fire intensity (kW m^{-1})
L	flame length (m)
X_w	fuel moisture content (-)
R	rate of spread (m s^{-1})
U	wind velocity (m s^{-1})
Var	any variable characterizing fire behavior
w_0	initial fuel loading (kg m^{-2})
w_a	fuel consumption (kg m^{-2})

Superscripts

t	at the retardant-treated area of the fuel bed
ut	at the untreated area of the fuel bed

Greek symbols

α	flame tilt angle defined as the angle between the leading edge of the fire front and the ground surface (see Figure 5.2) (degrees)
ϕ	slope angle (radians or degrees)

References

1. Àgueda A, Pastor E, Planas E. Different scales for studying the effectiveness of long-term forest fire retardants. Prog Energ Combust 2008;34:782-96.

2. Rothermel R, Philpot C. Reducing fire spread in wildland fuels. In: 'Proceedings of the Meeting to Honor Clay Preston Butler' Stanford, CA: Standford Research Institute; 1975.

3. Pastor E. Contribució a l'estudi dels efectes dels retardants en l'extinció d'incendis forestals. PhD Thesis, Universitat Politècnica de Catalunya, Spain; 2004.

4. Giménez A, Arqués P, Arnaldos J. Experimental study for characterizing the effectiveness of long-term forest fire retardants and the influence of fuel characteristics on the reduction of the rate of spread. In: 'Proceedings of the 5th International Conference on Forest Fire Research' 27-30 November, Figueira da Foz, Portugal; 2006.

5. Giménez A. contribució a l'estudi de l'efectivitat dels retardants a llarg termini aplicats als tallafocs químics en la lluita contra incendis forestals. PhD Thesis, Universitat Politècnica de Catalunya, Spain; 2006.

6. Pyne SJ, Andrews PL, Laven RD. Introduction to wildland fire. John Wiley and Sons, New York, 1996; 769 pages.

7. Anderson W, Pastor E, Butler B, Catchpole E, Dupuy JL, Fernandes P, Guijarro M, Mendes-Lopes JM, Ventura J. Evaluating models to estimate flame characteristics for free-burning fires using laboratory and field data. In: 'Proceedings of the 5th International Conference on Forest Fire Research' 27–30 November, Figueira da Foz, Portugal; 2006.

8. Pérez Y, Àgueda A, Pastor E, Planas E. Effect of wind and slope when scaling the forest fires rates of spread of laboratory experiments. In: 'Proceedings of the 6th Mediterranean Combustion Symposium' 8-12 June, Ajaccio, France; 2009.

9. Pastor E, Àgueda A, Andrade-Cetto J, Muñoz M, Pérez Y, Planas E. Computing the rate of spread of linear flame fronts by thermal image processing. Fire Safety J 2006;41:569-79.

10. Byram G. Combustion in forest fuels. In: Forest Fire Control and Use (Ed. Davis KP) McGraw-Hill, New York, 1959; 61-89.

11. Alexander M. Calculating and interpreting forest fire intensities. Can J Bot 1982;60:349-57.

12. Nelson R. An effective wind speed for models of fire spread. Int J Wildland Fire 2002;11:153-161.

13. Rothermel R. A mathematical model for predicting fire spread in wildland fuels. USDA Forest Service Research Paper INT-115; 1972.

14. Anderson H. Heat transfer and fire spread. USDA Forest Service Research Paper INT-69; 1969.

15. Fendell FE, Wolff MF. Wind-aided fire spread. In: Forest Fires: Behaviour and Ecological Effects (Eds. Johnson E, Miyanishi K) Academic Press, London; 2001.

16. Liodakis S, Vorisis D, Agiovlasitis IP. Testing the retardancy effect of various inorganic chemicals on smoldering combustion of *Pinus halepensis* needles. Thermochim Acta 2006;444:157-65.

17. Thomas H. The size of flames from natural fires. In: 'Proceedings of the 9th Symposium (International) on Combustion' (Ed. The Combustion Institute) Academic Press, New York, 1963; 844.

18. Viegas DX. Convective processes in forest fires. In: Buoyant Convection in Geophysical Flows (Eds. Plate EJ, Fedorovich EE, Viegas DX and Wyngaard JC), Kluwer Academic Publishers, AA Dordrecht, The Netherlands, 1998; 401-20.

bushfires, suppression procedures, and measurements. Int J Wildland Fire 1997;7(2):99-104.

58. Coops N. Eucalypt forest structure and synthetic aperture radar backscatter: a theoretical analysis. Trees-Struct Funct 2002;16:28-46.

CHAPTER 6

Characterization of the thermal degradation and heat of combustion of *Pinus halepensis* needles treated with ammonium-polyphosphate-based retardants *

As previously mentioned in Chapter 1 retardants, after being mixed with water in a prescribed ratio, can be applied from aerial or ground application equipment to slow the spread and reduce the intensity of a fire. They continue to be effective after the water they contain has evaporated [1] and the main active compounds of commercial long-term retardants are ammonium phosphate and sulfate salts. These compounds alter the thermal decomposition (pyrolysis) of forest species. Acids generated during the thermal degradation of the salts catalyze pyrolysis dehydration reactions of forest fuels and promote the appearance of char at the expense of volatiles or flammable tars [2]. Long-term forest fire retardants have been studied for more than 20 years. Analytical trials and tests of flame-front propagation have been carried out to quantify the effectiveness of different products and to gain knowledge about their chemical action mechanisms. Most analytical research has been performed with

* The content of this Chapter has been accepted for publication as: Àgueda A, Liodakis S, Pastor E, Planas E. Characterization of the thermal degradation and heat of combustion of *Pinus halepensis* needles treated with ammonium-polyphosphate-based retadants. J Therm Anal Calorim; DOI: 10.1007/s10973-009-0134-0. See the first page of the proofs of the article in the Appendix B.

diammonium phosphate salts and less attention has been paid to commercial products based on ammonium polyphosphates.

The general goal of this study is to obtain data that can be used to predict the behavior of forest fires that propagate in fuel treated with long-term retardants. This study is guided by the hypothesis that in real extinction operations retardants alter the burning behavior of the species rather than the extrinsic characteristics of the structure of the forest fuel (surface-area-to-volume ratio, bulk density, packing ratio, etc.). Based on this idea, the heat of combustion of a forest species (*P. halepensis* needles) treated with two commercial long-term retardants containing ammonium polyphosphate (APP) (Fire-Trol 931 (FT1) and Fire-Trol 934 (FT4)) was examined. Heat of combustion is generally used to calculate the calorific power of propagating forest fires.

A prior thermogravimetric analysis was carried out to characterize the pyrolytic behavior of *P. halepensis* needles treated with the two retardants. Thermogravimetric analyses are used to evaluate the performance of fire retardants [3-5] and to analyze differences in the thermal decomposition characteristics. The retardants used in this study are both APP-based. FT1 only differs from FT4 in that it contains a small amount of coloring agent (iron oxide) and attapulgite clay to suspend the color. According to George et al. [6], small percentages of iron can tie up phosphates to form insoluble compounds that may be ineffective fire retardants. Based on this statement, both products were used and thermogravimetric analyses were performed to determine whether this is the case.

6.1 Heat of combustion background in forest fires

The heat of combustion is the energy released when a species undergoes complete combustion with oxygen, and as such it gives an estimate of the amount of energy available per mass of fuel involved in a forest fire. When this term is used, it is important to specify whether it refers to the: high heat of combustion (HHC), low heat of combustion (LHC), heat yield (HY), heat of combustion of the volatiles (HC_{vol}) or effective heat of combustion (EHC).

The HHC value of a dried sample can be obtained with an oxygen bomb calorimeter. It is a maximum value because the sample burns under complete combustion conditions (high pressure and pure oxygen inside the bomb) and it contains the heat given up when the water vapor of the combustion reaction condenses and cools to the temperature of the bomb. In forest fires, this water vapor escapes as steam, so it is more accurate to subtract this energy

contribution and instead consider the LHC. The LHC value can be obtained by subtracting from the HHC the latent heat of vaporization of water multiplied by the amount of water generated during the combustion reaction per amount of fuel. This proportion can be obtained by considering the hydrogen percentage of the dried sample. Thus, if a given amount of forest fuel is completely combusted, the LHC can be obtained according to Eq. [6.1].

$$LHC = HHC - \Delta h_{v\,H_2O}\, 9\, X_H \qquad [6.1]$$

The HY value was defined by Byram [7] as being numerically equal to the HHC value minus the heat losses associated with the vaporization of the water formed during combustion, the presence of moisture in the fuel, the incomplete combustion and the radiation losses (see Eq. [6.2]). The heat loss associated with the vaporization of the water of reaction was equal to the reduction term used to compute the LHC value. The heat loss associated with the presence of moisture in the fuel included both the heat of vaporization and the heat of desorption. The term of incomplete combustion remained a matter of subjective judgment, since only a rough guideline was given for its estimation based on visual inspections of smoke and fire intensity [7]. In a later report [8] it was pointed out that the last term, associated with radiation losses, should not be considered because radiation contributes greatly to fire behavior.

$$HY = HHC - \Delta h_{v\,H_2O}\, 9\, X_H - \left(\Delta h_{v\,H_2O} + \Delta h_{dsp\,H_2O}\right) X_w - Q_{inc} - Q_{rad} \qquad [6.2]$$

Susott [9] determined HC_{vol} as shown in Eq. [6.3]. He did not specify whether the heat of combustion of the fuel (HC_f) and char (HC_c) had been computed as HHC or LHC. However, the use of LHC is more suitable because it is closer to real fire conditions.

$$HC_{vol} = HC_f - X_c\, HC_c \qquad [6.3]$$

The HC_{vol} term was basically introduced to consider rapidly spreading forest fires, which propagate primarily by flaming combustion of volatiles, with residual smoldering combustion of char contributing little to propagation [10].

The effective heat of combustion (EHC) is normally computed from data obtained by oxygen consumption calorimeters. The primary data taken from this type of equipment are a heat-release rate curve and a mass-loss rate curve [11]. The heat-release rate is obtained by considering the heat of combustion

per mass of oxygen consumed nearly constant and equal to 13.1 MJ kg^{-1} [12], and by measuring the consumption of oxygen due to combustion (see Eq. [6.4]).

$$\dot{q} = (\Delta h_c / r_0)\left(\dot{m}_{O_2,\infty} - \dot{m}_{O_2}\right) \quad [6.4]$$

On the basis of the terminology introduced in the previous paragraphs, two test methods are clearly distinguished for use in determining heats of combustion: oxygen bomb calorimetry and oxygen consumption calorimetry.

Ground samples of the test material are used in oxygen bomb calorimetry, so considerations of vegetation structure are avoided. Wood LHC values obtained by bomb calorimetry tests have been reported in the range of 16 to 18 MJ kg^{-1} [11].

Oxygen consumption calorimeters basically differ from one another in two ways: apparatus design (ignition/heating system, weighing system and dimensions) and gas analysis instruments. For instance, in [13] and [9], the authors designed an oxygen consumption calorimeter by adapting a gas chromatograph detector for thermal analysis. Another type of oxygen consumption calorimeter was used in [14]. These authors used an intermediate-scale calorimeter consisting basically of equipment for measuring O_2, CO_2 and CO concentrations, two platforms of load cells, a propane line burner and a three-sided ceramic board enclosure. However, the most widely used oxygen consumption calorimeter is the cone calorimeter [15], which is a bench-scale heat-release-rate apparatus that is commonly used to evaluate the combustion characteristics of building materials. It can also be used to test foliage and twig samples and rank vegetation flammability. In [11], the authors reported cone calorimetry EHC values of 12 to 13 MJ kg^{-1} for wood.

Weise et al. [14] indicated that the main distinction between the effective heat of combustion found by cone calorimeters and the heat of combustion found by oxygen bomb calorimeters is the residual charred material. For instance, 20-30% of a wood sample is not consumed in a cone calorimeter [14]. As a result, cone calorimeter values are normally lower than oxygen bomb calorimeter values.

Dibble et al. [11] pointed out certain methodological matters that need further refinement before the cone calorimeter can be widely used to measure forest fire behavior characteristics. In [14], the authors showed that further work should be done to clarify the effect of the physical characteristics of the test

sample (e.g. mass and thickness), heat flux level and sample holding system on the flammability properties measured. Because of all these open questions related to cone calorimetry, and because it is actually a more standardized methodology, a bomb calorimeter was used in this study.

Ammonium-phosphate-based retardants reduce the amount of fuel available in the gas phase and act against smoldering combustion [2,16-17]. Thus, the energy contribution of char combustion is not available when fuel treated with the above retardants is burning. In particular, the heat of combustion of the volatiles (HC_{vol}) is therefore the most suitable term for studying flame-front propagation after fuel treatment with ammonium-phosphate-based retardants.

The HC_{vol} term has been used in several studies to describe the flame properties of either spreading [18] or static [19] fires. In [18], the authors used this value to compute the fireline intensity of a flame front spreading through an untreated and homogeneous fuel bed. They then used the fireline intensity value to model flame characteristics (angle and height) and the radiation heat transfer mechanism. In [19], the authors studied the properties of flames stemming from the combustion of a simulated isolated small shrub. They calculated the maximum rate of heat release from the maximum rate of mass loss and the value of heat of combustion of the volatiles.

In this study, the HC_{vol} term was computed for samples with different retardant concentrations. This value was determined by subtracting the heat of combustion of the charred residue left after pyrolysis from the total heat of combustion of the fuel. The char was prepared in a pyrolytic furnace, and the samples and the corresponding char were burned in an oxygen bomb calorimeter.

6.2 Methods

6.2.1 Samples

The forest species used was *P. halepensis*. Mature needles were collected on October 4, 2006 in an area of Thrakomakedones, a wildland-urban interface area in the foothills of Mount Parnitha, north of Athens (Greece). The needles were immediately brought to the laboratory and dried in a vacuum oven for 24h under 1333 Pa of pressure at a temperature of 60°C. Afterwards, they were ground and a size fraction ranging from 0.1 to 0.2 mm was separated and used for the tests.

Two commercial long-term forest fire retardants were used: Fire-Trol 931 (FT1) and Fire-Trol 934 (FT4). To ensure a homogeneous treatment of the ground pine needles, the retardant liquid concentrate was converted into powder by evaporation of the water solvent. It was dried in a vacuum oven for 72h under 1333 Pa of pressure at a temperature of 60°C. The resulting solid was ground and a size fraction of less than 0.02 mm was used for the experimental tests.

The retardant treated samples were prepared by thoroughly mixing the pine needle powder with the retardant powder at three treatment levels: 10, 15 and 20% w/w. Pure pine needle powder was also tested.

6.2.2 Thermogravimetric analysis (TGA)

TG/DTG experiments were performed using a Seteram thermobalance (1200 model). Measurements were carried out using nitrogen gas, with a flow rate of 200 ml min^{-1}. Powder samples of 7 mg were placed in an open platinum crucible and heated from 23°C to 600°C with a low heating rate of 10°C min^{-1}. Low heating rates make it possible to distinguish DTG peaks, whereas high heating rates may cause peaks to overlap. Four replicates were performed with each sample.

6.2.3 Char preparation

To prepare char, the samples were heated under a 400 ml min^{-1} flow of nitrogen. In forest fires, fuel is heated in the presence of air, so pyrolysis and combustion reactions are in fact simultaneous processes. In our experiments, however, it was necessary to prepare char under pyrolytic conditions because the two processes were simulated separately.

A horizontal, electrically heated cylindrical furnace (30 cm long) containing a Pyrex tube (3.8 cm diameter) was used to produce the char. The inlet of the furnace was connected to a compressed nitrogen cylinder via a rubber tube. Volatile pyrolysis products were released to the environment, whereas the tarry pyrolyzate fraction was condensed into a funnel located at the outlet of the horizontal furnace.

A 24 cm^3 (2 x 2 x 6 cm^3; height x width x length) open sample holder made from stainless wire mesh was used to accommodate 3 g of powder sample into the tube furnace. A thermocouple was also placed in the furnace to monitor the oven temperature. The following heating steps were programmed by a controller device to control the furnace temperature:

- First step: Ramp rate of 10°C min^{-1}, from ambient temperature to 350°C

- Second step: Constant temperature (350°C) for 5 min

- Third step: Heating is stopped and the cooling period begins

During the cooling period to room temperature, nitrogen was flowed into the furnace to avoid the oxidation of the char prepared.

Some preliminary tests were performed to adjust the minimum flow of nitrogen. Five different values were tested. The products obtained using 60, 250, 300 and 350 ml min^{-1} contained little amount of ash (grey residue). However, with a flow of 400 ml min^{-1}, a deep black residue was observed.

The initial mass of pure or treated pine and the residual mass of char in the sample holder were recorded to compute the char yield value (X_c). Residual masses of char were later burned in a bomb calorimeter.

6.2.4 Bomb calorimetry

Bomb calorimetry tests were conducted using a plain jacket bomb calorimeter (Parr Instrument, model 1341) and powder samples (1 g) of pure and treated *P. halepensis* needles, and of the corresponding char. Before performing tests on the samples, the bomb calorimeter was standardized with benzoic acid pellets and its energy equivalent factor was determined (mean value 10.15 kJ $^{o}C^{-1}$; relative standard deviation 0.64%). The experimental procedure followed to determine the high heat of combustion of the samples (HHC_f and HHC_c according to Eq. 6 and 7) was specified in the operating instructions provided by the manufacturer and a fuse wire correction was applied.

6.2.5 Heat of combustion of the volatiles

To estimate the heat of combustion of the volatiles (HC_{vol}) of samples treated with retardants, Eq. [6.3] was modified to express this value on an initial mass of pine basis (MJ kg^{-1} of *P. halepensis*) (see Eq. [6.5]). It is better to use these units, instead of MJ kg^{-1} of pine and retardant, because the results are easier to interpret. The terms HC_f, HC_c and X_c of Eq. [6.5] are expressed on an initial mass of the sample basis.

$$HC_{vol} = \left(HC_f - X_c\, HC_c\right)[100/(100 - X_r)] \quad [6.5]$$

The terms HC_f and HC_c were computed as shown in Eqs. [6.6] and [6.7]. These equations are based on the definition of low heat of combustion. The differences are due to the presence of moisture and retardants in the samples used in this study.

$$HC_f = HHC_f - \Delta h_{v\,H_2O}\left(9\, X_H^f + X_w^f + 9\ 1/3\ X_H^f\, X_r\right) \quad [6.6]$$

$$HC_c = HHC_c - \Delta h_{v\,H_2O}(9\, X_H^c + X_w^c) \quad [6.7]$$

The term associated with the vaporization of the water generated during the combustion reaction was quantified based on the hydrogen content of the fuel and char samples (X_H^f and X_H^c, respectively). Carbon, hydrogen and nitrogen analyses were performed with elemental analyzers (Flash Thermo Finnigan 1112 and Carlo Erba 1108) and Table 6.1 shows the corresponding percentages.

Table 6.1 Elemental composition (C, H and N) of dried samples of pine (PH), retardants (FT1 and FT4) and char of untreated and treated pine. The data obtained are the mean values of two measurements, with relative standard deviation values lower than 5%.

Sample	**C (% w/w)**	**H (% w/w)**	**N (% w/w)**
PH	51.82	6.68	0.84
FT1	0.81	4.62	11.30
FT4	0.53	5.19	12.27
PH char	64.94	3.73	1.50
PH + 10 % FT1 char	56.18	3.10	2.62
PH + 15 % FT1 char	52.24	2.79	2.93
PH + 20 % FT1 char	47.73	2.84	3.34
PH + 10 % FT4 char	56.19	3.11	2.91
PH + 15 % FT4 char	51.51	2.92	3.25
PH + 20 % FT4 char	48.56	2.82	3.66

A term associated with the vaporization of the water present in the samples as moisture was also included. The mean X_w value of the samples was 2.8%. It is worthwhile to notice that the energy associated with the moisture of the samples was much lower than that of the water of the combustion reaction. For instance, for the untreated *P. halepensis* sample, 0.061 MJ kg^{-1} were associated

with the water present as moisture, whereas 1.3 MJ kg^{-1} were associated with the water of reaction.

Since water is generated during the decomposition of the retardants, another term was included to compute HC_f. The amount of water generated due to the degradation of the retardants was estimated based on the hydrogen percentage present in the retardants (X_H^r) (see Table 6.1) and the stoichiometry of the diammonium phosphate decomposition reaction [20]: 4 $(NH_4)_2HPO_4$ *(s)* → 8 NH_3 *(g)* + 6 H_2O *(g)* + 2 P_2O_5 *(s)*

This water contribution was not considered in Eq. [6.7] because it was assumed that the retardant residue present in the char samples was basically P_2O_5 and, thus, water from the retardants was not generated during char combustion. This assumption is based on the fact that diammonium phosphate decomposition reactions take place at approximately 200°C, which is lower than the char preparation temperature (350°C).

6.3 Results and discussion

6.3.1 Thermogravimetric analyses

Table 6.2 shows thermal analysis data taken from pyrolysis TG/DTG experiments carried out with *P. halepensis* needles before and after treatment with retardants. Percent mass loss was recorded after a temperature of 150°C to assure that the water in the sample had been driven off. According to the literature [21], APP begins to decompose at temperatures higher than 150°C. Thus, the assumption of recording the percent mass loss after a temperature of 150°C is appropriate when working with APP-treated samples.

Table 6.2 DTG parameters of *P. halepensis* needles before and after treatment with FT1 and FT4 in N_2 atmosphere (200 ml min^{-1}) at a heating rate of 10°C min^{-1}. The data obtained are the mean values of four measurements, with relative standard deviation values lower than 3%.

Sample	PT_1 (°C)	DR_1 ($10^3 \cdot s^{-1}$)	PT_2 (°C)	DR_2 ($10^3 \cdot s^{-1}$)	PT_3 (°C)	DR_3 ($10^3 \cdot s^{-1}$)	R_{550} (%)
PH	344	1.00	-	-	406	0.29	26
PH + 10 % FT1	302	0.69	349	0.58	406	0.31	34
PH + 15 % FT1	300	0.70	347	0.52	-	-	38
PH + 20 % FT1	301	0.71	348	0.53	-	-	40
PH + 10 % FT4	299	0.72	348	0.52	385	0.30	35
PH + 15 % FT4	296	0.72	349	0.52	-	-	37
PH + 20 % FT4	299	0.73	349	0.57	-	-	40

Biomass pyrolysis can be represented as a simple superposition of the behavior of its three components (hemicellulose, cellulose and lignin). In biomass decomposition curves, the main DTG peak is dominated by the decomposition of cellulose, while the shoulder at a lower temperature can mainly be attributed to hemicellulose decomposition. Lignin decomposes at a lower rate in a wide temperature range (200-600°C) [22]. This characteristic profile is clearly shown in the sample PH in Figure 6.1. Retardant decomposition reactions were also visible in Figure 6.1 as shoulders on the DTG curves of the treated samples at approximately 200°C.

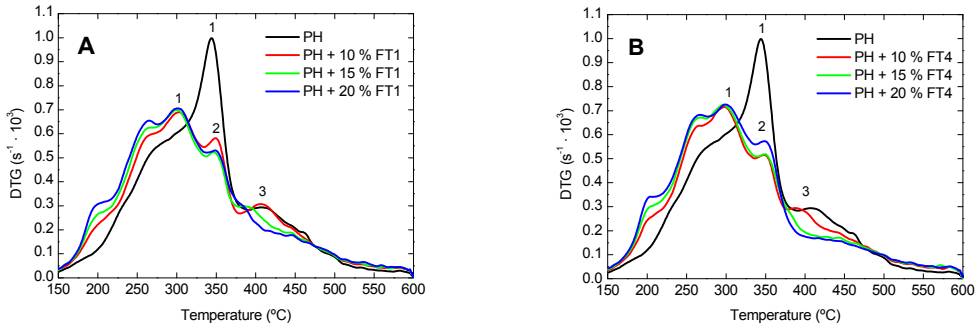

Figure 6.1 DTG curves of *P. halepensis* needles (PH) before and after treatment with FT1 (A) and FT4 (B) at three concentration levels (10, 15 and 20% w/w) in N_2 atmosphere (200 ml min^{-1}) at a heating rate of 10ºC min^{-1}.

Based on the results shown in Table 6.2 and visual inspection of Figure 6.1, the decomposition profiles were found to be different for untreated pine and pine treated with retardants. Much of the difference between the pure and treated pine needle profiles had to do with the peak at high temperatures associated with lignin decomposition (peak 3), which is not visible at high retardant concentrations. Moreover, for both retardants, in the temperature range of 225°C to 375°C, multiple separate peaks were obtained (Figure 6.1). In pure PH samples, only a peak associated with cellulose decomposition and a shoulder associated with hemicellulose decomposition were recorded. This means that the decomposition mechanism is getting more complex when retardants are applied on fuel.

In comparison with untreated samples, it was also found that treated samples started decomposing earlier, the primary DTG peak occurred at a lower temperature (reduced on average by about 13% with both retardants), the maximum rate of decomposition was considerably smaller (reduced on average by about 30% with FT1 and 28% with FT4), and the residual mass at 550°C was

increased by the presence of retardants (on average by about 44% with both retardants).

Comparing both retardant products, it was observed that the profiles, peak temperatures and residual masses were similar, and the only distinction between them was a slight difference in the primary rate of decomposition (0.70 10^{-3} s^{-1} and 0.72 10^{-3} s^{-1} for FT1 and FT4, respectively). Thus, our results seem to be contrary to the statement pointed out by George et al. [6], who supported that small percentage of iron can tie up phosphates to form insoluble compounds that may be ineffective fire retardants.

Based on our results, both retardants were used as a unique group representing APP-based commercial products and in the following sections data from the two products are not differentiated.

6.3.2 Char yield

The char yield (X_c) of the samples was obtained from char preparation experiments. The computed values of char yield are plotted in Figure 6.2. As expected, the char yield was higher for samples containing retardants than for untreated samples. The experimental data initially showed a fairly steep increase, but they leveled off to a more gradual increase. They were fitted using a rational model and the R-square fit result was 0.95 according to the equation shown in Figure 6.2.

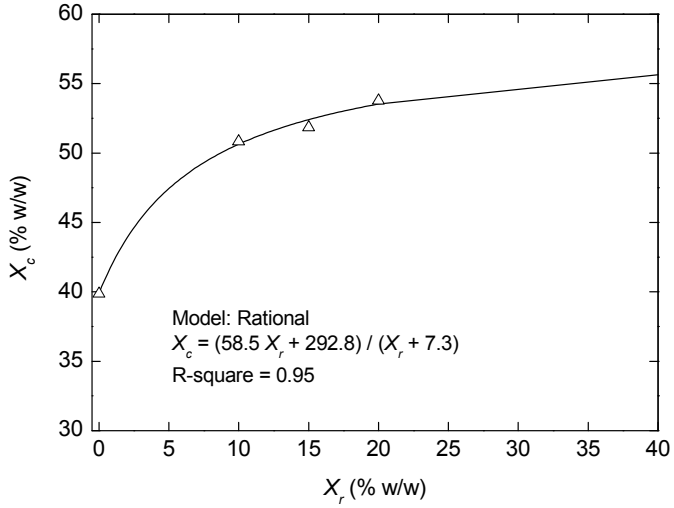

Figure 6.2 Char yield evolution of *P. halepensis* needles before and after treatment with retardants (FT1 and FT4) at three concentration levels (10, 15 and 20% w/w). The data obtained are the mean values of four measurements, with relative standard deviation values lower than 3%.

The char obtained from treated samples was more compact than the char from untreated pine. Phosphorus oxide, the solid decomposition product of APP, has been shown to form a viscous fluid coating [20], which may have contributed to the char's compactness at room temperature.

6.3.3 Bomb calorimetry results

Experimental heat of combustion values obtained in bomb calorimetry tests were corrected according to Eqs. [6.6] and [6.7]. The mean values, expressed on a dry initial mass of the sample basis, decreased as the retardant concentration in the samples increased (Table 6.3). This reduction simply reflects the smaller proportion of organic matter in the sample, since the tests were performed using a constant total mass and, thus, the amount of retardant increased as the amount of pine decreased.

The total heat of combustion of the samples expressed on a mass of dry fuel basis (according to Eq. [6.5], the term $HC_f[100/(100 - X_r)]$) was found to be approximately equal for untreated pine samples (20.7 MJ kg^{-1}) and samples treated with retardants (mean value 20.9 MJ kg^{-1}; mean relative standard deviation 0.7%). This is a result that might be expected since the main energetic processes in the complete combustion of all the samples are the oxidation of

carbon-carbon and carbon-hydrogen bonds and the energetic of these processes is independent of the presence of retardants.

Table 6.3 Mean heat of combustion values of pure and treated *P. halepensis* needles (pure and treated samples contained 4 and 8 observations, respectively) and of the corresponding char (2 and 4 observations were used for pure and treated samples, respectively). *HC* values are expressed on an initial mass of the sample basis.

X_r (% w/w)	HC_f (MJ kg^{-1}) [a]	HC_c (MJ kg^{-1}) [a]
0	20.7 (0.6)	25.1 (0.3)
10	18.9 (1.3)	21.3 (1.0)
15	17.6 (0.4)	19.5 (2.1)
20	16.7 (0.5)	18.1 (1.7)

a. Dry basis. The moisture content was obtained after drying two pellets per retardant concentration in a vacuum oven under 1333 Pa of pressure and at a temperature of 60°C until constant mass. The relative standard deviation values are shown in parenthesis in percent units.

The mean heat of combustion obtained for untreated pine samples was very comparable with the values reported in the literature. For instance, Liodakis et al. [23] obtained a high heat of combustion of 21.7 MJ kg^{-1} for *P. halepensis* needles using the same apparatus employed in this study. Based on the hydrogen content of the *P. halepensis* needles in this study, which in turn is in agreement with the value presented in [24] (6.68% in this study and 6.72% in [24]), this high heat of combustion corresponds to a heat of combustion value of 20.3 MJ kg^{-1}.

The heat of combustion of the untreated char sample (25.1 MJ kg^{-1} char) was lower than the values found in the literature for char from *P. ponderosa* needles. No references on *P. halepensis* char were found. In [25], a low heat of combustion value of 26.3 MJ kg^{-1} was obtained after heating 1 g dried fuel samples at 15°C min^{-1} to 400°C. This higher value may be due to the different composition of the species or to the different heating treatment temperature. In [26], it was reported that the carbon percentage of the residual char of cellulose samples was 59.9% w/w when they were pyrolyzed in a preheated furnace at a treatment temperature of 350°C for 5 min, whereas 76.5% w/w was computed at a treatment temperature of 400°C. Thus, since the heat content of the char depends on the available carbon in the char sample, it also depends on the

treatment temperature. If these considerations are taken into account, the experimental value presented in this study appears to be consistent with those reported previously.

6.3.4 Heat content of the volatiles

The heat content of the volatiles (HC_{vol}) was calculated using Eq. [6.5]. Mean HC_{vol} values were against retardant concentration in Figure 6.3. They were found to decrease according to an exponential decay model; Figure 6.3 shows the expression obtained. R-square fit results were very good (0.99).

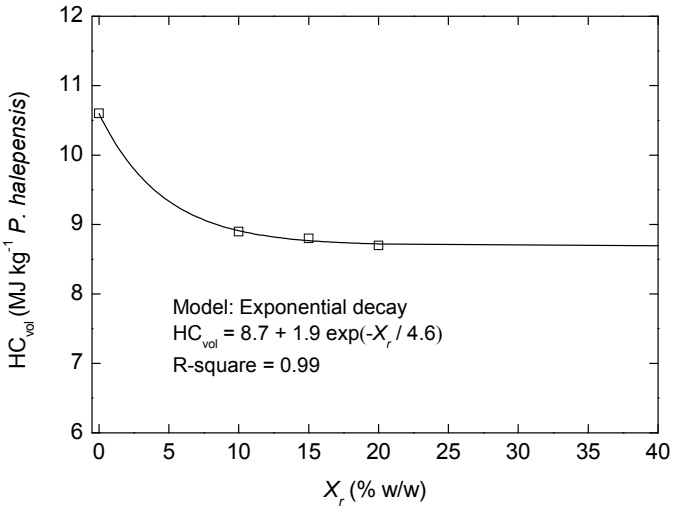

Figure 6.3 Heat of combustion of the volatiles vs. retardant concentration (mean values).

In [19], for *P. pinaster* needles, the authors reported a mean value of the heat of combustion of the volatiles of 15.9 MJ per kg of volatiles. This value corresponded to a heat of combustion of the volatiles per unit mass of pine of 11.5 MJ kg^{-1}, taking into consideration that the mean char yield was 27.5% w/w. Thus, the heat of combustion of the volatiles obtained in our study for untreated *P. halepensis* needles (10.6 MJ kg^{-1}) is similar in order of magnitude to the value reported in [19].

Figure 6.3 shows that the heat of combustion of the volatiles was kept practically constant for retardant concentrations above 10% w/w. This is a consequence of the char yield profile that was obtained and is consistent with the results of [27]. These authors stated that diammonium phosphate concentrations above 10% w/w appeared to be sufficient to exercise nearly the maximum action on the yield of the main classes of fir wood pyrolysis products.

6.4 Conclusions

The pyrolytic degradation profiles (DTG graphs) of *P. halepensis* needles treated with FT1 and FT4 were different from the profiles of pure *P. halepensis* needles. The primary rates of decomposition were lowered and shifted to lower temperatures, and the mass residue was increased. Also the DTG peak associated with lignin decomposition found in pure samples was not obtained when high retardant concentrations were applied. The thermal degradation profiles of FT1-treated samples were similar to those of FT4-treated samples. Thus, both products were studied in this work as a single group, representing APP-based commercial retardants.

The heat of combustion of the volatiles in retardant-treated samples was computed by subtracting the heat contribution of the char fraction from the total heat of combustion of the sample. The heat of combustion of the volatiles did not vary significantly for retardant concentrations in the range of 10 to 20% w/w. The mean reduction percentage with respect to the untreated sample was 18% in this range of retardant concentrations. An exponential decay model fitted data on heat of combustion of the volatiles as a function of the retardant concentration, and a rational model fitted char yield data.

A mean value of heat of combustion of the volatiles of 8.8 MJ kg^{-1} (on a dry fuel basis) was determined for *P. halepensis* needles treated with polyphosphate-based retardants in the treatment range of 10 to 20% w/w. This value could be used to predict the calorific power of a spreading flame front that propagates through fuel treated with polyphosphate-based retardants. Corrections for incomplete combustion should not be applied to this value because they are already taken into account since only the calorific contribution of the volatiles is considered.

Further work should be done with other species to explore the tendency of the heat of combustion of the volatiles as a function of retardant concentration.

Nomenclature

APP	ammonium polyphosphate
DTG	differential thermogravimetry
DR	DTG peak decomposition rate ($10^3 \cdot s^{-1}$)
EHC	effective heat of combustion (MJ kg^{-1} fuel consumed)
FT1	Fire-Trol 931
FT4	Fire-Trol 934
HC	heat of combustion (MJ kg^{-1})
HHC	high heat of combustion (MJ kg^{-1})
HY	heat yield (MJ kg^{-1})
$(\Delta h_c/r_0)$	heat of combustion released per kg of oxygen consumed (13.1 MJ kg^{-1})
$\Delta h_{dsp\ H_2O}$	heat of desorption of bound water in the fuel (MJ kg^{-1})
$\Delta h_{v\ H_2O}$	latent heat of vaporization of water at 100°C (MJ kg^{-1})
LHC	low heat of combustion (MJ kg^{-1})
$\dot{m}_{O_2,\infty}$	oxygen mass flow at ambient conditions (kg s^{-1})
$\dot{m}_{O_2}$	instantaneous oxygen mass flow (kg s^{-1})
PH	*Pinus halepensis*
$\dot{q}$	heat rate (kW)
Q_{inc}	heat loss due to incomplete combustion (MJ kg^{-1})
Q_{rad}	heat loss due to radiation losses (MJ kg^{-1})
R_{550}	percentage of residual mass at 550°C to initial mass at 150°C (% w/w)

PT	DTG peak temperature (^{o}C)
X_c	char yield (% w/w)
X_H	percentage of hydrogen (% w/w)
X_r	retardant concentration (% w/w)
X_w	moisture content on a dry basis (% w/w)

Subscripts / superscripts

c	charred residue
f	fuel
r	retardant
vol	volatiles
1, 2, 3	peak number in DTG graphs

References

1. USDA Forest Service. Specification for long-term retardants, wildland fire fighting 5100-304c. Technical document; 2007.

2. Sekiguchi Y, Shafizadeh F. The effect of inorganic additives on the formation, composition, and combustion of cellulosic char. J Appl Polym Sci 1984;29:1267-86.

3. Àgueda A, Pastor E, Planas E. Different scales for studying the effectiveness of long-term forest fire retardants. Prog Energ Combust Sci 2008;34:782-96.

4. Liodakis S, Antonopoulos I, Agiovlasitis I, Kakardakis T. Testing the fire retardancy of Greek minerals hydromagnesite and huntite on WUI forest species *Phillyrea latifolia* L. Thermochim Acta 2008;469:43-51.

5. Mostashari SM, Mostashari SZ. Combustion pathway of cotton fabrics treated by ammonium sulfate as a flame-retardant studied by TG. J Therm Anal Calorim 2008;91:437-41.

6. George C, Blakely A, Johnson G, Simmerman D. Evaluation of liquid ammonium polyphosphate fire retardants. USDA Forest Service General Technical Report INT-41; 1977.

7. Byram G. Combustion in forest fuels. In: Forest Fire Control and Use (Ed. Davis KP) McGraw-Hill, New York, 1959; 61-89.

8. Alexander M. Calculating and interpreting forest fire intensities. Can J Bot 1982;60:349-57.

9. Susott R. Characterization of the thermal properties of forest fuels by combustible gas analysis. Forest Sci 1982;28:404-20.

10. Wilson R. Observations of extinction and marginal burning states in free burning porous fuel beds. Combust Sci Technol 1985;44(3-4):179-93.

11. Dibble A, White R, Lebow P. Combustion characteristics of north-eastern USA vegetation tested in the cone calorimeter: invasive versus non-invasive plants. Int J Wildland Fire 2007;16:426-43.

12. Huggett C. Estimation of rate of heat release by means of oxygen consumption measurements. Fire Mater 1980;4:61-5.

13. Susott R, Shafizadeh F, Aanerud T. A quantitative thermal analysis technique for combustible gas detection. J Fire Flammability 1979;10:94-104.

14. Weise D, White R, Beall F, Etlinger M. Use of the cone calorimeter to detect seasonal differences in selected combustion characteristics of ornamental vegetation. Int J Wildland Fire 2005;14:321-38.

15. Babrauskas V. Development of the cone calorimeter –A bench-scale heat release rate apparatus based on oxygen consumption. Fire Mater 1984;8:81-95.

16. LeVan S. The chemistry of fire retardancy. In: The chemistry of solid wood (Ed. Rowell RM) Advances in Chemistry Series 207, Ch. 14, American Central Society; 1984.

17. Liodakis S, Vorisis D, Agiovlasitis I. Testing the retardancy effect of various inorganic chemicals on smoldering combustion of *Pinus halepensis* needles. Thermochim Acta 2006;444:157-65.

18. Catchpole WR, Catchpole EA, Tate AG, Butler B, Rothermel RC. A model for the steady spread of fire through a homogeneous fuel bed. In: 'Proceedings of the 4th International Conference on Forest Fire Research' 18-23 November, Luso, Portugal; 2002.

19. Dupuy JL, Maréchal J, Morvan D. Fires from cylindrical forest fuel burner: combustion dynamics and flame properties. Combust Flame 2003;135:65-76.

20. Di Blasi C, Branca C, Galgano A. Effects of diammonium phosphate on the yields and compostion products from wood pyrolysis. Ind Eng Chem Res 2007;46:430-8.

21. Levchik GF, Levchik SV, Sachok PD, Selevich AF, Lyakhov AS, Lesnikovich. Thermal behaviour of ammonium polyphosphate-inorganic compound mixtures. Part 2. Manganese dioxide. Thermochim Acta 1995;257:117-25.

22. Mészáros E, Jakab E, Várhegyi G, Szepesváry P, Marosvölgyi B. Comparative study of the thermal behavior of wood and bark of young shoots obtained from an energy plantation. J Anal Appl Pyrol 2004;72:317-28.

23. Liodakis S, Vorisis D, Agiovlasitis IP. A method for measuring the relative particle fire hazard properties of forest species. Thermochim Acta 2005;437;150-7.

24. Liodakis S, Kakardakis T. Measuring the relative particle foliar combustibility of WUI forest species located near Athens. J Therm Anal Calorim 2008;93:627-35.

25. Susott R, DeGroot W, Shafizadeh F. Heat content of natural fuels. J Fire Flammability 1975;6:311-25.

26. Shafizadeh F, Sekiguchi Y. Development of aromaticity in cellulosic chars. Carbon 1983;21:511-6.

27. Di Blasi C, Branca C, Galgano A. Thermal and catalytic decomposition of wood impregnated with sulfur- and phosphorus-containing ammonium salts. Polym Degrad Stabil 2008;93:335-46.

CHAPTER 7

Experimental study of the emissivity of flames resulting from the combustion of forest fuels *

As previously introduced in Chapter 1, thermal radiation is one of the three types of heat transfer responsible for forest fire propagation, together with convection and conduction. Heat transfer by radiation has been taken into account to predict propagation in most forest fire models [1-2]. It is known to be the dominant mechanism in cases where a flame front propagates in a homogeneous horizontal fuel bed in the absence of wind [3]. However, the role of the various heat transfer mechanisms in forest fire propagation is being further investigated for other forest fuel bed configurations, i.e. considering slope, or ambient conditions, such as the presence of wind [4-6].

In physical models for forest fires propagation, extinction coefficient and radiative intensity associated to the flame are necessary parameters to solve the radiative transfer equation [2]. However, flame emissivity is a required parameter in quasi-physical models [1]. In this last type of models, heat transfer by radiation in forest fires is normally formulated according to the Stefan-

* The content of this Chapter has been submitted for publication at the Int J Therm Sci. It is currently under review.

Boltzmann law in terms of flame temperature and emissivity, and by considering the view factor between the flame and the fuel ahead of the flame front. Flame temperature and emissivity can not easily be evaluated experimentally because flames generated during forest fires are heterogeneous and turbulent, and most authors assume an isothermal flame surface with a certain emissivity [7] or use emissive power data to handle with radiation [8-9].

A few experimental studies have used various methods to measure the emissivity of forest fuel flames. Most of the authors of these studies have based their work on the assumption that emissivity values can be given for a kind of equivalent medium. Most of these studies have found emissivity values to be related to flame thickness, but there is disagreement on the results of the coefficient relating these two variables, i.e. the extinction coefficient. Furthermore, recent years have seen an increase in the use of infrared (IR) cameras in applications related to forest fires. IR systems behave like a heat flux transducer formed by a two-dimensional array of sensors and can transform signals from the sensors into temperatures by specifying the ambient temperature, relative humidity, distance and emissivity of the viewed object. Thus, quantitative thermal measurements made with IR cameras require a good estimate of the emissivity of the object under study (that is, the flame or the burning fuel bed, in forest fire applications). Moreover, most comprehensive studies were done before the 1980s, at a time when IR imaging systems were not commonly used in applications related to forest fires. This study takes advantage of the spatial resolution of the IR cameras to compute the emissivity of forest fuel flames.

The first specific aim of this study was to review experimental methods used up to the present time to compute flame emissivity, and to analyze their differences and results. Based on this review, a second specific aim was defined: to apply two different IR-based methods to compute flame emissivity, to compare the results with those presented in the literature, and to examine the types of results obtained by the two methods. The first method (Method 1) is based on the measurement of flame transmissivity. The second one (Method 2) is based on the use of heat flux data obtained by a transducer. The third specific aim was to improve knowledge of the relationship between the emissivity and thickness of a flame by studying a range of thicknesses (greater than 2 m) that were wider than those covered in other studies. The last specific aim was to determine whether the presence of an ammonium-polyphosphate-based retardant product could have some effect on flame emissivity.

The hypothesis guiding this last specific aim was that differences might be observed in flame emissivity values, since concentrations had increased for some gaseous products (H_2O, NH_3, etc.) generated during the combustion of forest fuels that had previously been treated with long-term retardants [10-11]. As noted by King [12], high concentrations of water can have a great influence on flame emissivity. Moreover, because ammonia has absorption bands within the IR range [13], the presence of this compound could modify the spectral distribution of the radiant energy from the flames.

The medium which is of interest here, forest fuel flames, is heterogeneous (temporarily and locally). However, results presented in this study have been obtained for a kind of equivalent medium with average radiative properties. Since the main objective of this study was to compute emissivity values by using two different methods, this simplification had to be undertaken to be able to compare them.

7.1 Background on forest fuel flames

Flames generated during the combustion of forest fuels are turbulent, diffusive and very luminous. They emit energy in the visible and IR regions of the electromagnetic spectrum. The emitted radiation comes from both hot gases (basically CO_2 and H_2O vapor, and also CO) and solid particles of incandescent soot. Gases present in the flame have discrete absorption bands in the IR spectrum. The maximums for CO_2 are at 2.7, 4.4 and 15 μm; for H_2O they are at 1.4, 1.9, 2.7, 6 and 17 μm. Soot particles emit radiation in a continuous spectrum over a wider region from the visible to the IR. The more the wavelength increases, the greater the drop in radiation emissivity [14]. Nevertheless, this reduction in emissivity is disregarded by most authors [15] and soot particles are considered to behave as grey bodies (i.e. absorptivity is independent of wavelength and temperature). Hägglund and Persson [16] estimated the relative contribution of soot radiation and band radiation (associated to hot gases) at different flame thicknesses. They obtained that for thin flames (< 0.20 m) band radiation dominated, whereas the contribution of soot radiation to flame radiation dominated with increasing flame thickness.

Radiation originates throughout the flame and travels through the atmosphere before being captured by an object (e.g. fuel, a firefighter, a sensor, etc.). Since the atmosphere contains CO_2 and H_2O vapor, in some regions of the electromagnetic spectrum the atmosphere absorbs to some degree the IR radiation of these gases. These regions contrast with others, known as atmospheric windows, where the atmosphere is almost transparent and high

atmospheric transmissivity is assured. The most important windows are the visible/near IR region (from 0.4 to 2.5 μm), the middle IR region (from 3 to 5 μm) and the thermal IR region (from 8 to 12 μm). In the most recent studies, the sensors used to compute flame emissivity operate in the thermal IR region. In this spectral range, the CO_2 and the H_2O vapor make a small contribution to the radiation and the emission of radiant energy is dominated by soot [17].

The radiation properties of soot are usually described by the Mie theory, which applies to the polydispersion of spherical particles. According to this theory, if the diameter of the particles is small with respect to the wavelength (Rayleigh limit), then the radiation scattering coefficient is negligible. Since the diameter of soot particles generated during the combustion of forest fuels normally ranges from 0.02 to 0.7 μm [17], in the thermal IR range, it can be assumed that the Rayleigh limit is valid and the reflectivity of the flame is zero. The emissivity of the flame is given by Eq. [7.1] if it is assumed that Kirchoff's law holds for soot particles in the spectral range of the camera. According to this law, at thermal equilibrium, the emissivity of a flame is equal to its absorptivity.

$$\varepsilon_f = \alpha_f = 1 - \tau_f \qquad [7.1]$$

According to Eq. [7.1], forest fuel flames constitute a medium that absorbs and transmits radiation. Bouguer's law (see Eq. [7.2]) states that radiation intensity along a path is attenuated exponentially while it passes through an absorbing medium. If the medium is uniform, the exponent is equal to the product of the path length traversed (δ) and a coefficient known as the extinction coefficient (κ).

$$I_\delta = I_0 \, exp(-\kappa \, \delta) \qquad [7.2]$$

Using Eq. [7.1], this equation can be rewritten to obtain an expression (Eq. [7.3]) for the emissivity of the flame that depends on the extinction coefficient and the length of the absorbing path (in this case, flame thickness).

$$\varepsilon_f = 1 - exp\left(-\kappa_f \, \delta_f\right) \qquad [7.3]$$

7.2 Review of experimental methods

Since 1971, several authors have performed experimental studies to determine the emissivity of flames generated during the combustion of forest fuels. The

earliest studies used heat flux transducers (HFT), spectrophotometers (SPH) and thermocouples (TC), whereas the most recent studies used IR systems.

In the earliest studies, the authors burned either *Picea excelsa* cribs or heather and gorse fuel beds in stationary and propagating fires, respectively. The maximum measured flame temperature was 1353K and the maximum estimated flame emissivity was 0.94 for flame thicknesses of 2 m. Table 7.1 shows other relevant experimental characteristics and results.

Table 7.1 Main experimental characteristics and results of the methods developed to measure the emissivity of the flames generated during the combustion of forest fuels with heat flux transducers (HFT), spectrophotometers (SPH) and thermocouples (TC) (n.s.: unspecified parameter; δ_f: flame thickness; T_f: flame temperature; ε_f: flame emissivity; κ_f: flame extinction coefficient).

Reference		[18]	[19][a]	[16]
Number of tests		5	7	16
Fuel		*Picea excelsa* cribs	Heather and gorse fuel beds	*Picea excelsa* cribs
Fuel bed dimensions (m)	**Height**	0.76	0.35-1.50	n.s.
	Width	1.14-1.52	n.s.	1.20
	Depth	0.38-1.91	n.s.	n.s.
Equipment	**Flame radiant intensity**	HFT	HFT	SPH (1-5.5 μm)
	Flame thickness	Lateral visual observations	Photographs	Lateral visual observations
	Flame temperature	TC	TC	TC
Results	$\boldsymbol{\delta_f}$ **(m)**	0.27-1.88	0.80-3.00 (base of the flame)	0.15-2.00
	$\boldsymbol{T_f}$ **(K)**	644-1289	1253-1353	873-1303
	$\boldsymbol{\varepsilon_f}$ **(-)**	0.11-0.66	0.06-0.47	0.12-0.94
	$\boldsymbol{\kappa_f}$ **(m^{-1})**	0.51	0.10	1.03

a. Tilted flame front

Each study used a different method to compute flame emissivity. Beyreis et al. [18] determined flame emissivity with an HFT and a thermocouple. HFT outputs (in voltage units) were directly used to compute flame emissivity because they used the same geometric arrangement of the radiating source and the HFT in the calibration of the HFT with a blackbody and in the experiments. The

quotient between the HFT output for flame radiation and for the blackbody source at flame temperature gave an emissivity value (see Eq. [7.4]).

$$\varepsilon_f = \frac{V_f}{(V_{bb})_{T=T_f}} \qquad [7.4]$$

Thomas [19] determined the emissivity of tilted flames of propagating fire fronts. He measured flame temperatures with thermocouples and flame irradiance with an HFT. He used the Stefan-Boltzmann law to quantify the emissive power of the flames, assumed an atmospheric transmissivity equal to 1 and calculated the view factor between the flame and the HFT to obtain an emissivity value (see Eq. [7.5]).

$$\varepsilon_f = \frac{q''_{rt}}{\sigma\, T_f^4\, F_f} \qquad [7.5]$$

Thomas obtained low emissivity values. This can be explained by the more efficient combustion in the flame resulting from the increased air entrainment due to wind. In this study, a slightly modified version of this author's approach was used to compute flame emissivity according to Method 2.

Some years later, Hägglund and Persson [16] computed flame emissivity from radiant spectral intensity data obtained with a spectrophotometer in the 1-5.5 μm range. They integrated spectral intensity curves to obtain the radiation intensity of the flame (I_f) and assumed a somewhat arbitrary flame temperature of 1300K to solve Eq. [7.6].

$$\varepsilon_f = \frac{I_f}{\sigma\, T_f^4} \qquad [7.6]$$

In a recent study [20], irradiation measures obtained with two HFTs were used to compute a mean extinction coefficient of a simulated flame front. This approach was clearly aimed at simulating flame fronts typical of forest fires, but the authors used propane as fuel to obtain experimental data. They represented the flame as a triangular prism with a constant temperature.

In recent studies, IR systems have been used to calculate flame emissivity. The relationship shown in Eq. [7.1] has been used in all studies to deduce an emissivity value from flame transmissivity.

The emissivity of a flame can be estimated by measuring the fraction of energy transmitted by the flame that comes from a body of known emissivity at a given temperature. More precisely, Eq. [7.7] can be written if a flame of unknown

transmissivity is placed between a body of known emissivity (in this case, equal to 1) and an IR camera. The energy emitted by the flame (I_f) and the energy transmitted from the blackbody placed behind it ($\tau_f\, I_{bb1}$) are partial contributions of radiation with respect to the total radiation captured by the IR camera (I_{f+bb1}). An analogous equation can be written for a blackbody at another temperature (Eq. [7.8]) assuming an identical flame transmissivity. This effect is assumed to be less important when blackbody temperatures are close. By combining the two equations, in accordance with Eq. [7.1] an expression for flame emissivity can be obtained (see Eq. [7.9]).

$$I_{f+bb1} = I_f + \tau_f\, I_{bb1} \quad [7.7]$$

$$I_{f+bb2} = I_f + \tau_f\, I_{bb2} \quad [7.8]$$

$$\varepsilon_f = 1 - \frac{I_{f+bb2} - I_{f+bb1}}{I_{bb2} - I_{bb1}} \quad [7.9]$$

The total radiation emitted by a flame cannot be accurately measured with an IR camera because this device is only sensitive in a specific region of the electromagnetic spectrum. However, if it is assumed that forest fuel flames behave like grey bodies, it is not necessary to know the total radiation emitted by the flame in order to apply Eq. [7.9] because radiation measurements determined within a specific range are compared with each other.

In this study, this methodology is referred to as the 'flame transmission method'. It was applied to compute flame emissivity in Method 1. More details about the theoretical deduction of Eq. [7.9] are given in [17].

Only three experimental studies carried out with forest fuels have computed flame emissivity using the flame transmission method. Table 7.2 shows their main experimental characteristics, as well as the emissivity ranges obtained. The main difference between these studies lies in the number, arrangement and temperature of the blackbodies that were used. The studies of Den Breejen et al. [21] and Pastor et al. [22] used just one blackbody ($bb1$). In fact, measurements relative to the $bb2$ blackbody in Eq. (9) were taken with the background behind the flame. In the study of Den Breejen et al. [21], a chopper placed in front of the $bb1$ blackbody was quickly opened and closed. When the chopper was closed, only background radiation remained. The $bb1$ blackbody had a temperature of 900K. Pastor et al. [22] assumed a symmetric flame and placed the $bb1$ blackbody (at ambient temperature) on one side of the two halves that vertically divided the flame. Dupuy et al. [17] used three blackbodies. Two of

them were radiating at the same temperature (ambient temperature) and their mean radiation intensity was used as data for the blackbody *bb*1. The other blackbody (*bb*2) had a temperature of 523K. Figure 7.1 shows the position of the blackbodies that were used in these studies.

Table 7.2 Main experimental characteristics and results of the methods developed to measure the emissivity of the flames generated during the combustion of forest fuels with IR systems (n.s.: unspecified parameter; H: height; W: width; *bb*1: blackbody 1; *bb*2: blackbody 2; δ_f: flame thickness; ε_f: flame emissivity; κ_f: flame extinction coefficient).

Reference		[21]	[22]	[17]
Number of tests		n.s.	4	45
Spectral range (μm)		5, 10	7.5-13	7.5-13
Fuel		n.s.	*Pinus halepensis* needles and fine branches *Rosmarinus officinalis* branches	*Pinus pinaster* needles
Characteristic length of the fuel bed (m)		0.08 (diameter)	0.25, 0.50, 1.00 (side of a square)	0.20, 0.28, 0.40 (diameter)
Blackbody dimensions (H x W; m)		*bb*1: n.s.	*bb*1: 0.8 x 0.4	*bb*1: n.s.[a] *bb*2: 0.1 x 0.1
Temperature of *bb*1 (K)		900	Ambient temperature	Ambient temperature
Temperature of *bb*2 (K)		-	-	523
Results	δ_f **(m)**	n.s.	0.25, 0.50, 1.00[b]	0.11-0.23
	ε_f **(-)**	0.23-0.40	0.55-0.83	0.02-0.28 (0.10-0.55[c])
	κ_f **(m^{-1})**	n.s.	3.11, 2.24	n.s. (0.70-6.20[c])

a. Two *bb*1 blackbodies

b. Side of the fuel bed

c. For soot at the complete spectral range

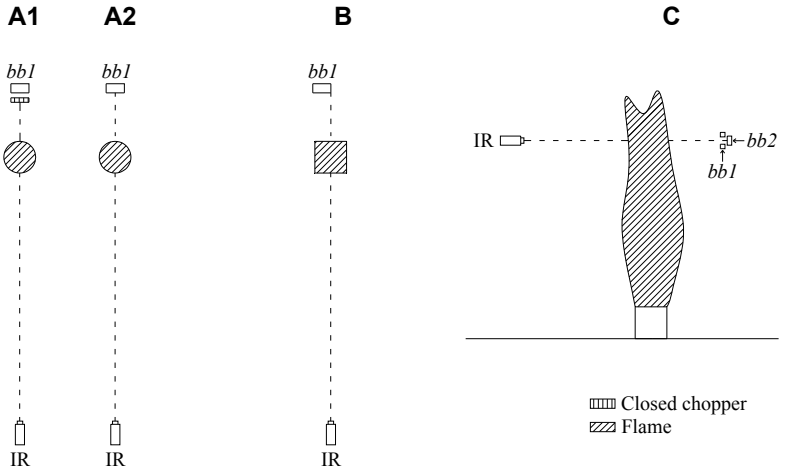

Figure 7.1 Outline of the transmission devices used in: A) Den Breejen et al. (1998) [21] (A1 sketches a time instant in which the chopper was closed and A2 sketches a time instant in which the chopper was opened) (top view); B) Pastor et al. (2002) [22] (top view); and C) Dupuy et al. (2007) [17] (lateral view) (*bb*1: blackbody 1; *bb*2: blackbody 2; IR: infrared camera).

A common characteristic of these three works was that experimental data were obtained in a specific wavelength or spectral range. If it is assumed that flames are dominated by soot and that soot emissivity is not dependent on wavelength, this is not a problem but, according to the results of [16], this is only true if flame thickness is greater than 0.20 m. According to Table 7.2, this condition was only probably fulfilled by flames in [22]. For this reason, the authors of the study [17] may have computed total properties for soot. They calculated gas emissivities to correct the values of measured transmittance for soot contribution only, and then computed the contribution of soot to the total extinction coefficient (see [17] for more details). This approach was not followed in this study on the assumption that flames were soot dominated. In the results and discussion section this assumption is commented.

7.3 Experimental methodology

In this study, experiments with static fires were carried out under laboratory and field conditions. Four tests were performed in the laboratory and five tests in the field. Two of the laboratory tests used Method 1, while the other two used Method 2. In the field experiments, both methods were applied in all of the tests. Laboratory tests were replicated one time. Most field tests were carried out only once due to performance difficulties associated with this type of fires and the variability of the test conditions, in terms of wind, temperature and relative humidity. Only field tests performed with retardant-treated fuel could be replicated.

7.3.1 Tests conditions

Four common Mediterranean species were used as fuel to be burned. Distinctions between species were not considered when analyzing the experimental results. *Pinus halepensis* needles were used in the laboratory tests. The field tests used branches and dead leaves of three species: *Erica arborea*, *Quercus ilex* and *Quercus humilis*. Only fuel with a diameter of less than 15 mm was used in the field tests. Different fuels had to be used due to availability constraints. However, distinctions between species were not considered when analyzing the experimental results on the assumption that flames composition of burning fine forest fuels was similar regardless of the small differences in chemical constitution and surface area to volume ratios.

Circular fuel beds were arranged and burned. The ones prepared in the laboratory had a mean diameter of 0.35 m, while those prepared in the field had a diameter of 2.5 m. The mean bulk density of the fuel beds was 22 and 10 kg m^{-3} for laboratory and field tests, respectively. Table 7.3 shows the specific values corresponding to each test.

Table 7.3 Main characteristics of the experimental tests: bulk density and dimensions of fuel bed, and flame thickness (D: diameter; H: height; δ_{f_m}: mean flame thickness; $\delta_{f_{rp}}$: thickness of the flame in the region vertically covered by the radiating panels; SD: standard deviation).

Test type	**Test name**	**Forest species**	**Fuel bed bulk density (kg m^{-3})**	**Fuel bed dimensions (D x H; m)**	**δ_{f_m} (SD) (m)**	**$\delta_{f_{rp}}$ (SD) (m)**
Laboratory	PH1	*Pinus halepensis*	19.9	0.30 x 0.20	-	0.24 (0.06)
	PH2		21.5	0.30 x 0.20	-	0.28 (0.06)
	PH3[a]		22.9	0.40 x 0.20	0.27 (0.09)	-
	PH4[a]		22.8	0.40 x 0.20	0.25 (0.17)	-
Field	EA	*Erica arborea*	10.6	2.50 x 0.70	2.28 (0.54)	2.28 (0.12)
	EA ret1[b]		10.2	2.50 x 0.70	1.10 (0.44)	1.35 (0.25)
	EA ret2[b]		9.7	2.50 x 0.73	1.77 (0.34)	1.97 (0.10)
	QI	*Quercus ilex*	10.3	2.50 x 0.70	1.00 (0.51)	1.40 (0.20)
	QH	*Quercus humilis*	8.8	2.50 x 0.60	1.52 (0.78)	1.32 (0.06)

a. Test without radiating panels

b. Fuel treated with a commercial long-term retardant product

The mean ambient conditions for the laboratory tests were an ambient temperature of 290K and a relative humidity of 45%. Before the experiments, the pine needles were dried in an oven at 353K for 24h. The mean ambient conditions for the field experiments were an ambient temperature of 283K and a relative humidity of 63%. In these tests, the mean fuel moisture was 12.5% (SD 3.7%). Differences in fuel moisture content were not considered in the analysis of the experimental results because, according to the results of King [12], this variable can only change emissivity values significantly at values greater than 20%.

The fuel used in the field tests EA ret1 and EA ret2 (see Table 3) was previously treated with a commercial long-term retardant product called Fire-Trol 931, which is ammonium-polyphosphate based. For each kg of fuel, a 0.75 l dilution of the product with water (15% v/v) was applied. Before the burnings, the water of the dilution was evaporated. According to Vélez [23], a coverage level of 1 l m^{-2} is commonly applied on fuel models 4, 5 and 6 [24], which are typical of the Mediterranean basin. The ratio used in this study is equivalent to the mean value that would be obtained if the same product dilution were applied to the aforementioned fuel models.

Different methods were used to ignite the fuel beds in each type of test. In the laboratory, ignition was carried out by placing under the fuel bed a circular receptacle containing alcohol which was removed after complete ignition of the fuel bed. It was possible to perform this kind of ignition because the fuel bed was placed on a wire netting 0.2 m above the ground. With this type of ignition, the fuel bed was completely ignited almost instantaneously. In the field, the fuel bed was placed on the ground and ignition was done on the top surface. Two people carried out a homogeneous ignition with drip torches. Due to the dimensions of the fuel bed, combustion propagated downwards through it during the test.

7.3.2 Experimental set-ups

Method 1

The devices needed to compute flame emissivity according to Method 1 were an IR camera and two hot blackbodies. Qian and Saito [25], who worked with hydrocarbons, also used two hot blackbodies to compute emissivity values for hexane flames. The blackbodies used in this study were placed on either side of the vertical axis of symmetry of the bed, one next to the other. Figure 7.2A and C show the arrangement of the blackbodies with respect to the IR camera for

laboratory and field experiments, respectively. There was a distance of 0.4 and 0.6 m between the base of the radiating panels and the base of the fuel beds in the laboratory and field tests, respectively.

Two black-colored radiating panels (0.5 m tall, 0.3 m wide) were used to simulate the blackbodies. They were heated to temperatures of around 573K and 673K. The temperatures were regulated by a PID controller that considered the value measured by a thermocouple (type J; 0.3 cm in diameter) placed in the middle of the panel. The set temperatures allowed us to work in the medium and high brightness temperature ranges of the IR camera (see Table 7.4) because the IR camera can, in fact, measure brightness temperatures outside of the ranges indicated by the manufacturer. For example, in the high range, the camera can measure brightness temperatures starting at around 500K.

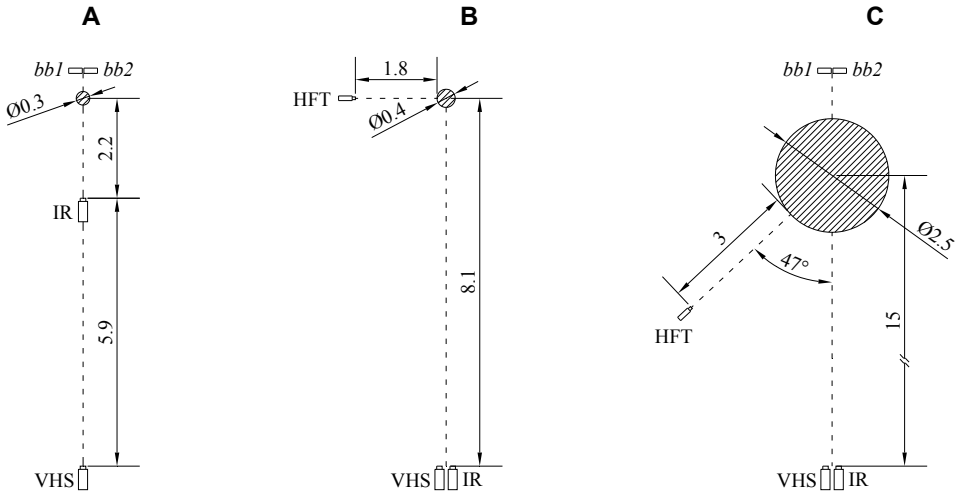

Figure 7.2 Outline of the experimental set-ups used in this study (top view): A) Laboratory tests, Method 1; B) Laboratory tests, Method 2; C) Field tests, Method 1 and Method 2. Patterns of inclined lines are associated with flame. Units are in m.

Table 7.4 Technical specifications of the AGEMA 570 camera.

Field of view	24º x 18º
Thermal sensitivity	<0.15K
Image frequency	4 Hz
Detector type	Focal plane array (FPA), uncooled microbolometer, 320 x 240 pixels
Spectral range	7.5-13 μm
Brightness temperature measurement ranges	Low: 253-393K / Medium: 353-773K / High: 623-1773K
Measurement accuracy	±2º

The IR camera that was used (AGEMA Thermovision 570-Pro) operates at the thermal IR window. Table 4 specifies its main technical characteristics. IR image sequences were recorded in the medium and high brightness temperature range in laboratory and field tests, respectively. A conventional digital VHS camera (Sony Handycam Vision CCD-TR840E), which records visible light, was also used to film the experiments. In the field tests, the IR and VHS cameras were placed side by side (see Figure 7.2C). The distance between the fire and the cameras (15 m) was such that the entire flame was visible. In the laboratory tests, however, the distance between the fire and the IR camera (2.2 m) was such that only the area between the two radiating panels was visible. The flame was only viewed in its entirety by the VHS camera, which was placed 8.1 m from the center of the fuel bed (see Figure 7.2A).

Method 2

The devices needed to compute flame emissivity according to Method 2 were a heat flux transducer (HFT) and an IR camera. A VHS camera was also used to record the evolution of the flame. The HFT used in this work (Medtherm, Schmidt-Boelter thermopile, 64-2-16) has a recording frequency of 2 Hz and its working range is from 0 to 23 kW m^{-2}. The cameras were the same ones mentioned in the previous subsection.

The position of the HFT varied depending on the type of test. In the laboratory, it was placed 2 m from the center of the fuel bed, forming a right angle with the line defined by the IR camera and the center of the fuel bed (x-axis), and 0.38 m above the base of the fuel bed. In field tests, the HFT was placed 4.25 m from the center of the fuel bed, forming an angle of 47º with the x-axis, at a height of 1.34 m. Figure 7.2B and C show the position of this device. The HFT was placed at an

angle to the x-axis in order to prevent its shape from blocking part of the flame in the recorded images. In the field tests, this position made it possible to disregard the contribution of the radiating panels to irradiance, because their view factor was negligible with respect to that of the flame.

The tests were recorded with both the IR camera and the VHS camera. The distance between the cameras, placed side by side, and the fire was such that the entire flame was visible. They were placed 8.1 m and 15 m from the center of the fuel bed in the laboratory and field tests, respectively (see Figure 7.2B and C). IR image sequences were recorded in the camera's high brightness temperature range.

7.4 Calculation methods

7.4.1 Flame emissivity

Method 1

This method applies the flame transmission method using the set-up described above. The application of this method is limited to flames that present geometric and thermodynamic symmetry with respect to the radiating panels. From a practical point of view, 'geometric symmetry' means that the tilt angle of the flame is zero. The thermodynamic characteristics of a flame (e.g. composition, temperature, etc.) have to be similar with respect to both radiating panels in order for a flame to be completely symmetric. In order to meet the condition of geometric symmetry, each test was studied only in a time domain in which the tilt angle of the flame was practically zero ($\pm 5^{o}$ and $\pm 15^{o}$ for laboratory and field experiments, respectively). An algorithm developed with MATLAB [26] was used to determine the tilt angle of the flame as a function of time. Images recorded with the VHS camera were used to obtain this angle. The condition of thermodynamic symmetry was assumed to be met.

IR image sequences recorded in the presence of the radiating panels were used to apply Method 1. Calculations were performed using an output unit of the IR camera that is proportional to the amount of radiation sensed by the camera detector, the Object Signal (OS) unit.

For each image of the time domain selected for each test, the OS values of the pixels inside the areas limited by the radiating panels were extracted. Two 10-by-10 matrices were created (see Figure 7.3) and each of their elements contained the mean OS value of the corresponding pixels ($OS_{f+bb673_{(n,m)k}}$ and

$OS_{f+bb573_{(n,m)k}}$). In the laboratory tests, around 130 pixels were considered in order to compute the mean OS value of each element of the matrices. In the field tests, since the distance between the radiating panels and the fuel bed was greater, only around two pixels were considered. The area of each element of the matrices represented 15 cm^2. The area occupied by the radiating panels was divided into 100 subareas in order to restrict the study to those subareas covered by the flame and also to observe whether there were any spatial trends within the flame.

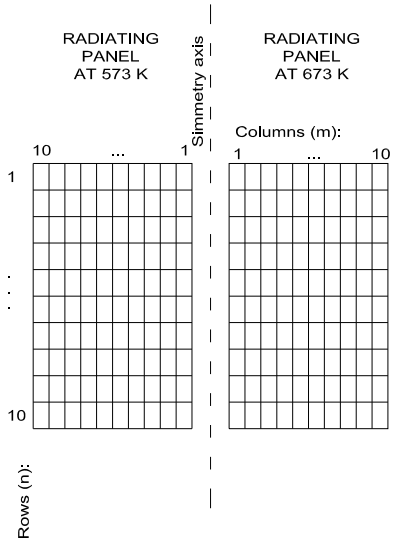

Figure 7.3 Splitting of the study area into two 10-by-10 matrices for flame emissivity calculation according to Method 1.

The same procedure was followed for an IR image of the beginning of the sequence in which only the radiating panels were present, without flame in front of them. The OS values of the elements of the radiating panels were determined ($OS_{f+bb673_{(n,m)}}$ and $OS_{f+bb573_{(n,m)}}$) and considered to be constant for each test. Eq. [7.10], which is analogous to Eq. [7.9], was applied to each pair of elements (n, m) of the matrices in order to obtain an emissivity value for each pair of elements at each time instant k.

$$\varepsilon_{(n,m)k} = 1 - \frac{OS_{f+bb673_{(n,m)k}} - OS_{f+bb573_{(n,m)k}}}{OS_{f+bb673_{(n,m)}} - OS_{f+bb573_{(n,m)}}} \quad [7.10]$$

The emissivity value for each test, which is associated with the flame in the chosen time domain and in the area limited by the radiating panels, was computed as the median of all physically valid emissivity values (between 0 and 1) of the elements of the matrices in which there was flame. The median

estimate was used because this measure is resistant to outliers, which were mainly observed in laboratory tests.

Method 2

In Method 2, heat flux data recorded with the HFT and image sequences recorded with the IR camera were used to obtain a mean emissivity value of the flame.

The time domain used in Method 2 was the same as the one used in Method 1 for field tests. In laboratory tests, it was fixed according to the same criterion used in Method 1.

The heat flux captured by the HFT was considered to be coming from the thermal radiation of the fire, which had two different sources: the flame and the fuel bed burning with glowing combustion. Since the distance between the IR camera and the fire was high, the fire was considered to be an imaginary wall that showed the apparent temperature distribution obtained by the IR camera and was placed perpendicular to the HFT. The temperature of each element of the wall, i.e. each pixel in the IR image, was transformed into emissive power using the general case of the Stefan-Boltzmann law (i.e. for a grey body characterized by a given emissivity). Afterwards, emissive power values were transformed into irradiance by considering the atmospheric transmissivity and the view factor between each element of the imaginary wall and the HFT. Eq. [7.11] expresses the corresponding energy balance.

$$q''_{rt} = \varepsilon_f \, \sigma \sum_{i=1}^{P} \sum_{j=1}^{320} \left[\left(T_{(i,j)k}(\varepsilon_f) \right)^4 \tau_a \, F_{(i,j)k} \right] + \varepsilon_b \, \sigma \sum_{i=P+1}^{240} \sum_{j=1}^{320} \left[\left(T_{(i,j)k}(\varepsilon_b) \right)^4 \tau_a \, F_{(i,j)k} \right] \quad [7.11]$$

In this equation temperature terms $T_{(i,j)k}(\varepsilon_f)$ and $T_{(i,j)k}(\varepsilon_b)$ account for emissivity dependent temperatures.

The pixels row of IR images at the interface between the flame and the fuel bed (P) was visually estimated and fixed for each test. To distinguish the fire from its surroundings, the pixels of the IR images were marked as 'fire' pixels if their temperature was greater than a threshold value of 500K, and as 'background' pixels otherwise. The chosen threshold corresponded to a value slightly higher than the minimum temperature sensed by the IR camera. View factors were computed only for fire pixels; background pixels were assumed to have a view

factor value of zero. A differential receptor was considered to compute the view factors. It was located perpendicular to the imaginary wall at distances of 1.8 m and 3 m from the wall for the laboratory and field tests, respectively. The atmospheric transmissivity, determined using the specific model integrated in the IR camera, was around 0.98 in all of the tests. The explicit function form of the model was reserved by the camera manufacturer [27].

As indicated in Eq. [7.11], temperature values ($T_{(i,j)k}$) were implicitly dependent on the emissivity value introduced as an input parameter in the ThermaCAM™ Researcher 2001 software. For fire pixels belonging to the burning fuel bed, emissivity (ε_b) was assumed to be equal to 1 [28]. The emissivity of the fire pixels belonging to the flame (ε_f) was the unknown variable.

To solve Eq. [7.11], which was implicitly defined, a least-squares method was used. The first term on the right-hand side of Eq. [7.11] was obtained by considering different ε_f values. The summed square of the difference between the left- and the right-hand sides of Eq. 11 at each time instant k of the time domain was then minimized.

7.4.2 Flame thickness

Since an axisymmetric medium was assumed for emissivity estimations, the thickness of the flame along the line of sight of the cameras (x-axis) was expected to be the same as the thickness along the y-axis (perpendicular to the x-axis).

The thickness of the flame was obtained from VHS images. The contour of the flame was extracted by converting grayscale images into binary images based on a luminosity threshold value. The distance between each pair of pixels of the contour of the flame along the horizontal axis of the image (y-axis in real coordinates) was computed in pixel units and converted to meters.

The mean thickness of the flame was computed by considering, at each time instant of the time domain, the complete contour of the flame. This variable was named δ_{f_m}. The thickness of the flame in the region covered by the radiating panels was computed in the same way as δ_{f_m} but only for this region and was named $\delta_{f_{rp}}$. As an example, Figure 7.4 shows an image of the QI field test, together with the contour extracted for the flame. The two horizontal lines in the figure indicate the part of the flame contour used to compute $\delta_{f_{rp}}$.

Figure 7.4 VHS image of an arbitrary time instant of the QI field test that shows the flame contour extracted to compute flame thickness. The red lines indicate the part of the flame vertically covered by the radiating panels.

7.5 Results and discussion

Figure 7.5A and B show examples of the type of flames obtained in the laboratory and field tests, respectively. Figure 7.5A shows that the laboratory fires had a non-luminous region just above the burning fuel bed (at the flame base). This was a fluctuating region in which the flow was laminar. It can be attributed to gaseous compounds that remained unburned and to the smoke that was formed. The transition to turbulence occurred just above this region. Since gases, rather than soot, were predominant in this region, the radiating panels were placed just above it. Such a region was not present in the field fires because the flame was thoroughly turbulent. Corlett [29] already mentioned the presence (or lack thereof) of this region in pool fires.

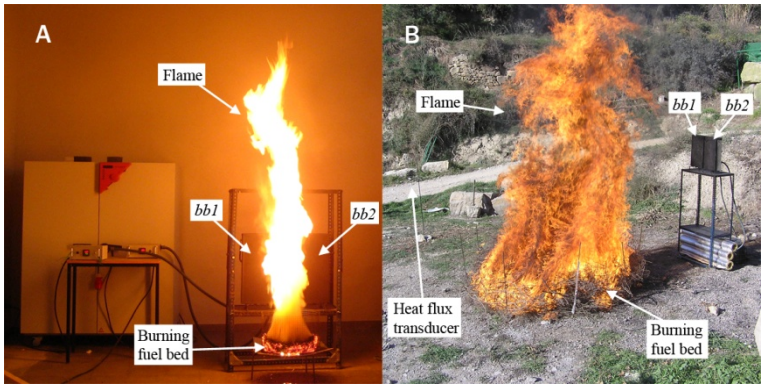

Figure 7.5 Typical flames generated in experimental tests: A) Laboratory fire; B) Field fire. The devices, the flame and the burning fuel bed are indicated ($bb1$: blackbody 1; $bb2$: blackbody 2; HFT: heat flux transducer).

Tests performed in the laboratory had a mean duration of 60 s. Three different phases of flame behavior could be distinguished: an ignition phase of 5-10 s, an almost steady-state combustion phase (pseudo-stationary phase) lasting around 35 s (the time domains selected for emissivity calculations were all within this phase), and a third phase, lasting about 15 s, of transient combustion, characterized by unstable flame behavior, flame extinguishment and significant release of smoke. Finally, there was an extinguishing phase characterized by the glowing combustion of the remaining fuel residue. The field fires lasted around 150 s and 225 s for untreated and retardant-treated fuel tests, respectively. It was possible to distinguish three phases of flame behavior in these tests, as well. For tests performed with untreated fuel, the following phases were observed: an ignition phase lasting 15 to 40 s, a pseudo-stationary combustion phase lasting around 55 s (the time domains selected for emissivity calculations were all within this phase), and a third phase, lasting about 70 s, of transient combustion, characterized by unstable flame behavior and flame extinguishment. The glowing combustion of the remaining fuel residue was also observed after flame extinguishment. The three phases could be seen in the HFT curves. For tests performed with treated fuel, the corresponding phases lasted 40 - 100 s, 60 s and 95 s. Figure 7.6 shows HFT data from a laboratory test and a field test, as well as the corresponding phases.

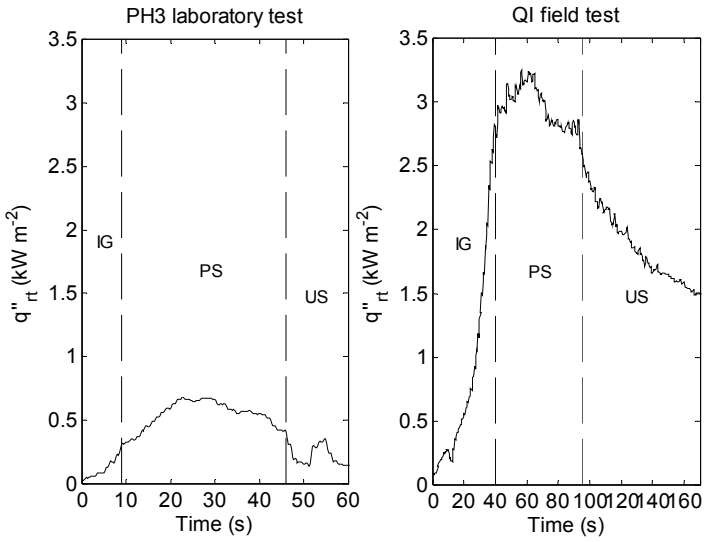

Figure 7.6 Heat flux transducer data for a laboratory test and a field test. Phases of flame behavior are differentiated (IG: ignition; PS: pseudo-stationary; US: unstable).

Time domains of around 5-10 s were selected for each test following the criterion of a flame tilt of approximately zero.

Figure 7.7 shows an example of the type of results obtained with Method 1. The data are from the QI field test. The figure shows the evolution of the emissivity values calculated for several elements of the matrices. The amount of data available decreased as the column number increased. This indicates that the assumption of thermodynamic symmetry was not completely fulfilled as the distance between the compared elements increased. Plots of the emissivity distribution within the area covered by the radiating panels were also extracted by applying Method 1. Figure 7.8 shows contour plots of the emissivity distribution for a laboratory test and a field test. There was no particular trend in the distribution of the emissivity values, but the contours were smaller and covered a wider range in the field test than in the laboratory test. This was probably due to a more turbulent flame. White regions of the plot indicate unavailable data. These regions were located either at the bottom or the right side of the contour plots. The unavailable data at the bottom of the plot are explained by the presence, before the fire, of branches blocking the view of the elements of the matrices representing the radiating panels. The unavailable data on the right side can be explained by the lack of symmetry between the associated elements, which led to the computation of invalid emissivity values.

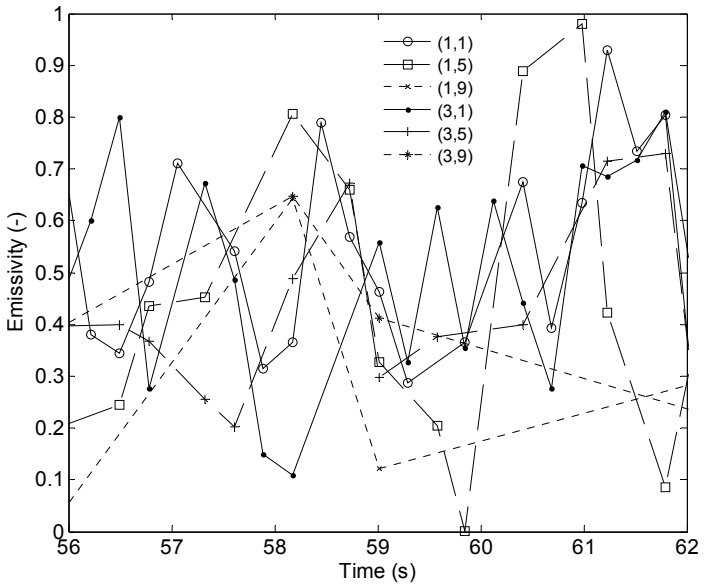

Figure 7.7 Changes over time in the emissivity values associated with several elements of the matrices considered to compute flame emissivity according to Method 1. Element notation: (row, column).

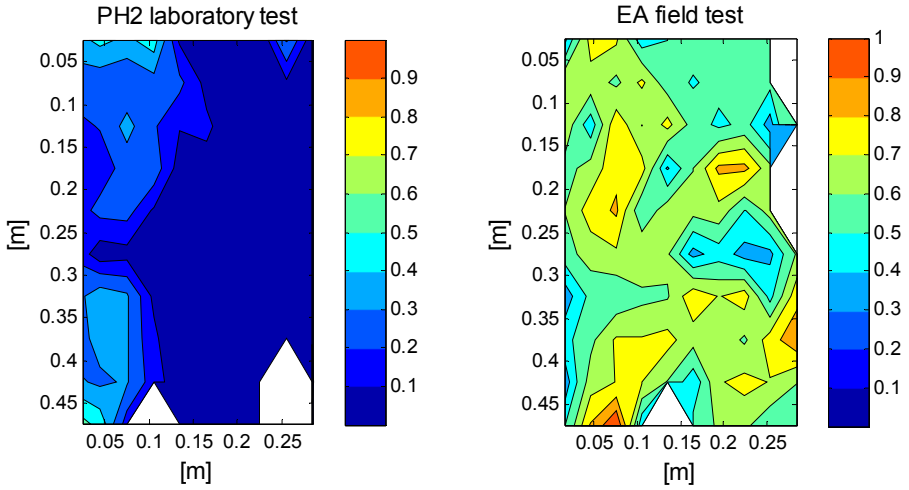

Figure 7.8 Mean emissivity distribution for a laboratory test and a field test in the time domain used to compute emissivity by applying Method 1. White areas indicate unavailable data.

Figure 7.9 shows results corresponding to Method 2. The figure shows an example of the temperature values extracted from the IR images based on the emissivity value entered as an object's emissivity in the ThermaCAM™ Researcher 2001 software (ε_f or ε_b in Eq. (11)). The three images were taken at

the same time instant during the PH3 laboratory test. The horizontal line represents the interface between the flame and the fuel bed. The results for three emissivity values (0.1, 0.2 and 1) are shown. Since flame temperatures are normally near 1100K (see Table 7.1 or the results in [17]), based on the values displayed in Figure 7.9, the flame emissivity associated with this test could be expected to be around 0.10-0.20. In fact, a value of 0.14 was computed for this test.

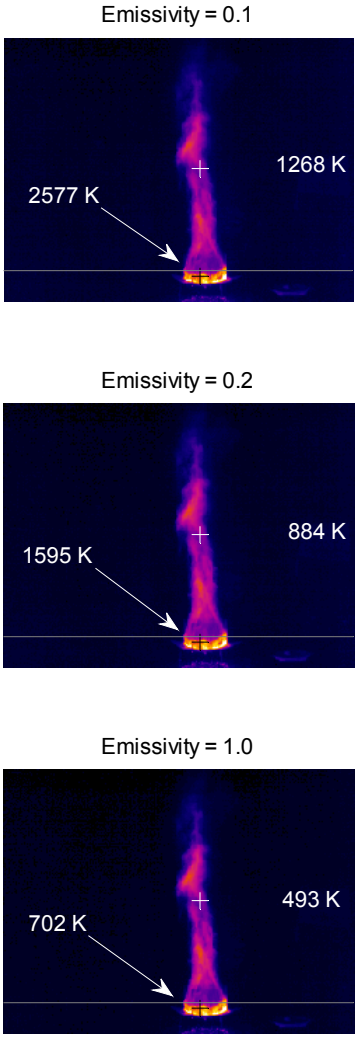

Figure 7.9 IR image of the PH3 laboratory test considering three different emissivity values: 0.1, 0.2 and 1. Temperature values are shown for two fire pixels (i.e. flame and fuel bed pixels). The horizontal line divides the burning fuel bed from the flame.

Figure 7.10 shows flame emissivity values obtained by applying both Method 1 and Method 2 and taking flame thickness into account. The median emissivity values obtained with Method 1 were represented against $\delta_{f_{rp}}$, whereas the emissivity values obtained with Method 2 were represented against the mean

flame thickness (δ_{fm}) because the entire flame, rather than one specific area, was studied with that method. Table 7.3 shows mean flame thickness values and standard deviations (SD). Note that SDs were higher for flame thickness values corresponding to Method 2. This variability was expected since the entire flame, from the base to the tip, was considered to compute an average flame thickness value. The data presented in Figure 7.10 were fitted to a model equivalent to the one shown in Eq. [7.3]. The extinction coefficient obtained from the Method 1 data had a value of 0.48 and an R-square value of 0.86, indicating satisfactory fitness. The extinction coefficient obtained from the Method 2 data had a value of 0.72 and an R-square value of 0.99, indicating very good fitness.

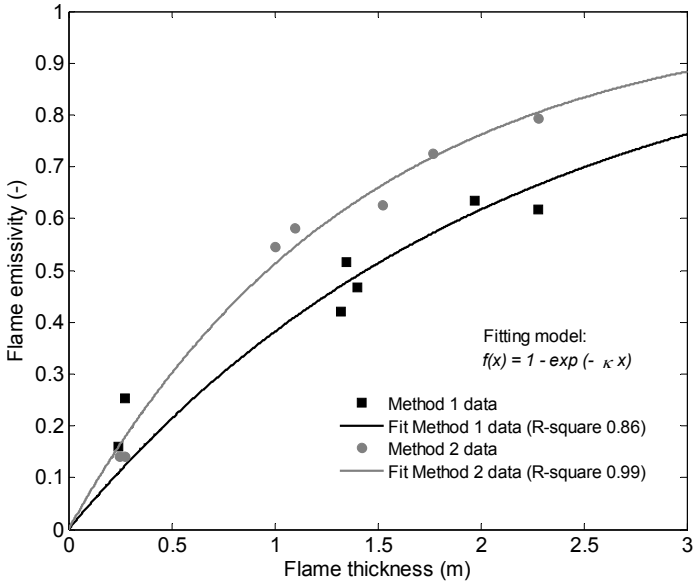

Figure 7.10 Flame emissivity vs. flame thickness. Experimental data obtained in this study and exponential fit.

In the tests for which the fuel had previously been treated with a retardant product (EA ret1 and EA ret2), ignition was more difficult and the flames were narrower than those observed in the EA test, which was performed with the same fuel (*Erica arborea*), but untreated (see Table 7.3). However, the emissivity values associated with these two tests followed the same trend as the data computed for the rest of the tests; this result was observed for both methods. Consequently, at the tested concentration level the retardant product did not modify flame emissivity and radiation continued being dominated by soot although ammonia, which is a major decomposition product of the retardant used in this study, has an absorbing band within the spectral range of

the IR camera (at 10.5 μm) and the concentration of water vapor theoretically increased.

Figure 7.11 shows flame emissivity data obtained by some of the authors mentioned in the review section (Section 2), as well as experimental data and exponential fit results obtained by applying both methods. These data have been plotted against flame thickness (or, as in [22], against the side of the fuel bed). As in this study, data from the authors presented in Figure 7.11 were fitted to exponential models to obtain extinction coefficient values. The only exception was the study by Dupuy et al. [17], because all of the data they obtained were in a very narrow range of flame thicknesses. They used a theoretical approach to obtain extinction coefficient values for soot.

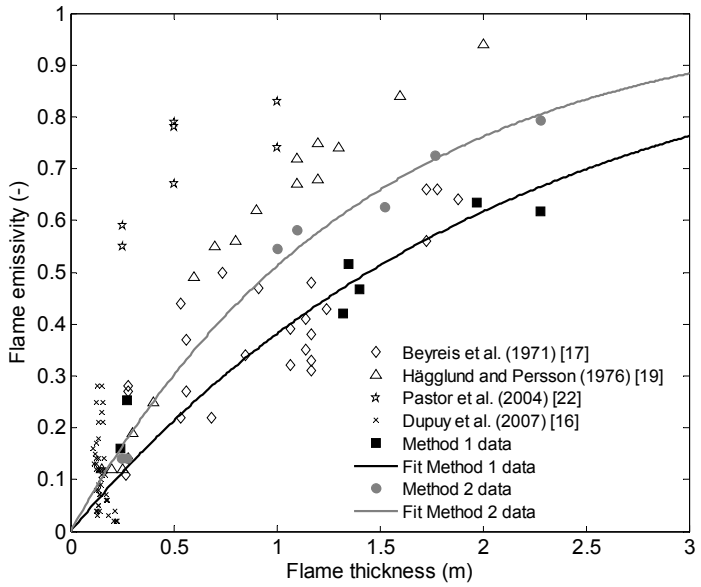

Figure 7.11 Flame emissivity vs. flame thickness. Data obtained by other authors and data points and exponential fits for the data of this study.

The fitting results obtained in this study seem to correlate well with data obtained by Beyreis et al. [18]. These authors obtained an extinction coefficient of 0.51, which falls between the two values obtained here (0.48 for Method 1 and 0.72 for Method 2). High variability in values obtained by Beyreis et al. [18] may be due to the fact that maximum temperature values obtained with a unique thermocouple were employed to determine emissivity. Hägglund and Persson [16] obtained an extinction coefficient of 1.03, which is 43% higher than the one obtained in this study by applying Method 2. Differences between emissivity values determined by [16] and values obtained in this study may be

due to several reasons, i.e. due to the fact that measurements were taken in different spectral ranges, due to the assumption taken in this study that flames were soot dominated or even due to the fact that flame emissivity values reported by [16] were highly dependent on flame temperature, a variable which is also very difficult to precisely determine when measured by thermocouples. The extinction coefficients obtained by Pastor et al. [22] were much higher than those calculated in this study (332% higher than the one obtained in this study by applying Method 2). This significant difference may be due to the fact that they used a blackbody that was at ambient temperature and radiation data from an IR camera working in the 623-1773K temperature range. Measurements taken with and without the blackbody behind the flame were probably numerically similar, resulting in very high emissivity values. Experimental emissivity values obtained by Dupuy et al. [17] had a mean value of 0.11 and a relative standard deviation (RSD) of 63.6%. This high RSD is due to the fact that the authors computed emissivity values at different flame heights. Their mean emissivity value would fit the curves obtained in this study.

The two methods used in this study to compute flame emissivity can be compared in terms of type of results. For Method 1, the evolution of the emissivity can be observed at different points of the flame and the method itself is sensitive to the assumption of symmetry. Method 2 is easy to implement but can only obtain a mean emissivity value for the entire flame. The fitted model obtained from data extracted by applying Method 2 was better than the model fitted with data extracted by applying Method 1 (i.e. it had a higher R-square value). The extinction coefficient obtained by applying Method 1 was 33.3% smaller than the one obtained by applying Method 2. This difference may be explained by taking into consideration that the infrared camera used in this study was only sensitive to radiation in the spectral range from 7.5 to 13 μm, whereas the transducer measured total (including all wavelengths) heat fluxes. Flame emissivity values turned out to be higher with Method 2 to compensate for the energy contribution not sensed by the infrared camera. However, the difference between both extinction coefficients cannot be considered large, since theoretically this coefficient can take values from 0 to infinite, and values as high as 6.2 [17] have been reported for forest fuel flames.

According to the results obtained in this study, flame emissivity values close to that of a blackbody (0.90) are only attained for flame thicknesses of 4.8 m and 3.2 m for Method 1 and Method 2, respectively. These results contradict the conclusion of Hägglund and Persson [16], who determined that 2-m-thick forest fuel flames had an emissivity in excess of 0.9. However, they are in agreement

with the results of Beyreis et al. [18], who found an emissivity of 0.9 for a flame thickness of 4.5 m.

7.6 Conclusions

The concept of flame emissivity is usually employed to solve radiative heat transfer problems in forest fires propagation. To characterize the emission of flames a kind of equivalent medium assumption has to be made since flame emission is produced by a varying semitransparent volume.

In this study, the experimental methods developed to date to compute the emissivity of forest fuel flames were reviewed. Two particular methods were developed to compute emissivity values from flames generated during the combustion of branches and leaves of typical Mediterranean forest fuels. One of these two methods (Method 2) represents an improvement of the approach used by Thomas [19], since it differentiates between the two radiating sources of the fire (flame and burning fuel bed). The other method (Method 1) represents a modification in terms of set-up of the flame transmission method also used in [17,21-22]. An IR camera sensitive at the spectral range from 7.5 to 13 μm was used to apply both methods. Several assumptions had to be made to apply and compare both methods, such as a grey medium assumption for sooty flames and homogeneity for the equivalent medium representing the flames.

The emissivity values obtained here were exponentially correlated against flame thickness. Two different extinction coefficients were obtained: 0.48 for Method 1 and 0.72 for Method 2. Despite this difference, both sets of data showed the same trend as the experimental values of Beyreis et al. [18], who obtained flame emissivity values by using a methodology not dependent on the spectral range of measurement. According to our results, flames thicker than 3.2 m would exhibit an emissivity value close to that of a blackbody (0.9). Moreover, the emissivity of the flame was unaffected by the presence of a long-term retardant product in the fuel at a concentration level of 0.75 l of dilution (15% v/v) per kg of fuel.

Nomenclature

$bb1$	blackbody 1
$bb2$	blackbody 2
F_f	view factor between the flame and the transducer according to Eq. [7.5]
$F_{(i,j)k}$	view factor between the cell (i, j) of the k-th image of the IR sequence and the heat flux transducer (-)
i	rows of the temperature matrix (from 1 to 240)
I_0	radiation intensity at the origin of the radiation path (W m^{-2})
I_{bb1}	radiation emitted by $bb1$ in the absence of flame (W m^{-2})
I_{bb2}	radiation emitted by $bb2$ in the absence of flame (W m^{-2})
I_f	radiation intensity of the flame according to Eq. [7.6]-[7.8] (W m^{-2})
I_{f+bb1}	radiation emitted by the flame plus the part of radiation emitted by $bb1$ that is transmitted by the flame (W m^{-2})
I_{f+bb2}	radiation emitted by the flame plus the part of radiation emitted by $bb2$ that is transmitted by the flame (W m^{-2})
I_δ	radiation intensity at the end of the radiation path (W m^{-2})
j	columns of the temperature matrix (from 1 to 320)
k	number of the image of the IR sequence
m	columns of the study area (from 1 to 10)
n	rows of the study area (from 1 to 10)
P	row of the temperature matrix at the interface between the flame and the fuel bed

OS	object signal
$OS_{bb673_{(n,m)}}$	OS mean value associated with the (n,m) element of the study area limited by the radiating panel at 673K in the absence of flame
$OS_{bb573_{(n,m)}}$	OS mean value associated with the (n,m) element of the study area limited by the radiating panel at 573K in the absence of flame
$OS_{f+bb673_{(n,m)}}$	OS mean value associated with the (n,m) element of the study area limited by the radiating panel at 673K for the k-th image of the IR sequence
$OS_{f+bb573_{(n,m)}}$	OS mean value associated with the (n,m) element of the study area limited by the radiating panel at 573K for the k-th image of the IR sequence
q''_{rt}	radiation heat flux received by the transducer (W m^{-2})
T_f	flame temperature according to Eq. [7.4]-[7.6] (K)
$T_{(i,j)k}$	temperature of the cell (i,j) of the k-th image of the IR sequence (K)
$(V_{bb})_{T=T_f}$	radiometer output for blackbody source at flame temperature (V)
V_f	radiometer output for flame radiation (V)

Greek symbols

α_f	absorptivity of the flame (-)
δ	radiation path (m)
δ_f	flame thickness (m)
δ_{f_m}	mean flame thickness (m)

$\delta_{f_{rp}}$	thickness of the flame at the region covered by the radiating panels (m)
κ	extinction coefficient (-)
κ_f	flame extinction coefficient (-)
ε_b	emissivity of the burning fuel (-)
ε_f	flame emissivity (-)
$\varepsilon_{(n,m)k}$	emissivity associated with the (n, m) element of the k-th image of the IR sequence (-)
σ	Stefan-Boltzmann constant ($5.67 \cdot 10^{-8}$ W m^{-2} K^{-4})
τ_a	atmospheric transmissivity (-)
τ_f	flame transmissivity (-)

References

1. Albini FA. A model for fire spread in wildland fuels by radiation. Combust Sci Technol 1985;42:229-58.

2. Morvan D, Dupuy JL. Modeling of fire spread through a forest fuel bed using a multiphase formulation. Combust Flame 201;127:1981-94.

3. De Mestre NJ, Catchpole EA, Anderson DH, Rothermel RC. Uniform propagation of a planar fire front without wind. Combust Sci Technol 1989;65:231-244.

4. Linn R. A transport model for prediction of wildfire behavior. PhD thesis, New Mexico State University, USA; 1997. Also published as Los Alamos National Laboratory Report number LA-13334-T.

5. Simeoni A, Santoni PA, Larini M, Balbi JH. Reduction of a multiphase formulation to include a simplified flow in a semi-physical model of fire spread across a fuel bed. Int J Therm Sci 2003;42:95-105.

6. Morvan D, Dupuy JL. Modeling the propagation of a wildfire through a Mediterranean shrub using a multiphase formulation. Combust Flame 2004;138:199-210.

7. Sullivan AL, Ellis PF, Knight IK. A review of radiant heat flux models used in bushfire applications. Int J Wildland Fire 2003;12:101-10.

8. Portiere B, Morvan D, Larini M, Loraud JC. Wildfire propagation: a two-dimensional multiphase approach. Combust Explo Shock Waves 1998;34:139-50.

9. Catchpole WR, Catchpole EA. The second generation US firespread model. Final report of RMRS-94962-RJVA, 2000. Joint research venture of the US Forest Service and ADFA.

10. Pappa A, Mikedi K, Tzamtzis N, Statheropoulos M. Chemometric methods for studying the effects of chemicals on cellulose pyrolysis by thermogravimetry-mass spectrometry. J Anal Appl Pyrol 2003;67:221-35.

11. Tzamtzis N, Karma S, Pappa A, Statheropoulos M. On-line monitoring of pine needles combustion emissions in the presence of fire retardant using a

'thermogravimetry (TG)-bridge/mass spectrometry method'. Anal Chim Acta 2006;573-574:439-44.

12. King NK. The influence of water vapour on the emission spectra of flames. Combust Sci Technol 1973;6:247-56.

13. Siegel R, Howell JR. Fundamentals and properties for radiation in absorbing, emitting, and scattering media. In: Thermal Radiation Heat Transfer (Eds. Prescott M, Ormes CV) Taylor and Francis, USA; 1992.

14. Sato T, Kunimoto T, Yoshi S, Hashimoto T. On the monochromatic distribution of the radiation from the luminous flame, Bulletin of the Jpn Soc Mech Eng 1969;12:1135-43.

15. Drysdale D. An Introduction to Fire Dynamics, John Wiley and Sons, New York; 1997.

16. Hägglund B, Persson LE. An experimental study of the radiation from wood flames. Försvarets Forskningsanstalt Huvudenhet, FoU-brand, Stockholm; 1974.

17. Dupuy JL, Vachet P, Maréchal J, Meléndez J. Thermal infrared emission-transmission measurements in flames from a cylindrical forest fuel burner. Int J Wildland Fire 2007;16:324-40.

18. Beyreis JR, Monsen HW, Abbasi AF. Properties of wood crib flames. Fire Technol 1971;7:145-55.

19. Thomas PH. Rates of spread of some wind-driven fires. Forestry 1971;44:155-75.

20. Knight IK, Sullivan AL. A semi-transparent model of bushfire flames to predict radiant heat flux. Int J Wildland Fire 2004;13:201-7.

21. Den Breejen E, Roos M, Schutte K, De Vries JS, Winkel H. Infrared measurements of energy release and flame temperatures of forest fires. In: 'Proceedings of the 3rd International Conference on Forest Fire Research' 16-20 November, Luso, Portugal; 1998.

22. Pastor E, Rigueiro A, Zárate L, Giménez A, Arnaldos J, Planas E. Experimental methodology for characterizing flame emissivity of small scale forest fires using infrared thermography techniques. In: 'Proceedings of the 4th International Conference on Forest Fire Research' 18-23 November, Luso, Portugal; 2002.

23. Vélez R. (coordinator). Métodos y medios para la modificación de los combustibles. In: La Defensa contra Incendios Forestales. Fundamentos y Experiencias (Ed. Grace AG) McGraw-Hill, Madrid; 2000.

24. Anderson HE. Aids to determining fuel models for estimating fire behavior. USDA Forest Service General Technical Report INT-122; 1982.

25. Qian C, Saito K. Measurements of pool-fire temperature using IR technique. In: Proceedings of Combustion Fundamentals and Applications (Joint Technical Meeting) (Ed. Gore JP) San Antonio, USA; 1995.

26. Muñoz M. Estudio de los parámetros que intervienen en la modelización de los efectos de grandes incendios de hidrocarburo: geometría y radiación térmica de la llama. PhD Thesis, Universitat Politècnica de Catalunya, Spain; 2005.

27. Toolkit IC2 Dig 16. Developers Guide 1.00 AGEMA 550/570 (AGEMA file format) file description; FLIR Systems AB Publication number: 557 344 version B.

28. Telisin HP. Flame radiation as a mechanism of fire spread in forests. In: Heat Transfer in Flames (Eds. Afgan NH, Beer JM) John Wiley and Sons, New York; 1974.

29. Corlett RC. Velocity distribution in fires. In: Heat Transfer in Fires (Ed. Blackshear PL) John Wiley and Sons, New York; 1974.

CHAPTER 8

Conclusions

In this PhD work an independent critical ability has been exercised to asses the present state of use of long-term retardants in Catalonia and the present state of knowledge in the area of long-term retardants effectiveness evaluation.

Existing techniques have been applied to investigate to what extent key characteristics of fire behavior (i.e. rate of spread, fuel consumption, fire intensity, flame length and flame angle) diminish due to the presence of long-term retardants under upslope or wind-aided conditions.

In this work we have taken a novel approach to the question of fire behavior under the presence of long-term retardants. Specifically, we have studied the influence of long-term retardants on several input parameters required in fire spread models (i.e. heat of combustion, char yield and flame emissivity).

Moreover, two new methodologies have been implemented to calculate the rate of spread of propagating flame fronts and the flame emissivity. Additionally, a

new technique has been successfully applied to treat analytical samples of forest fuel with long-term retardants commercialized as liquid concentrates.

Specifically, the main conclusions of this PhD work are the following:

1. Catalan fire chiefs and assistant chiefs interviewed in this study have a good opinion on the effectiveness of long-term retardants.

2. Fire attack strategies with long-term retardants are not clearly differentiated from general aerial attack strategies and Catalan fire chiefs and assistant chiefs use direct attack tactics with long-term retardants. Therefore, the added value of long-term retardants in comparison with foams is normally disregarded.

3. A bibliographic review has shown that nowadays there are no mathematical models able to predict the fire behavior of flame fronts propagating under the effect of long-term retardants. However, a huge amount of work has been done on the relative effectiveness of long-term retardants.

4. Results obtained from laboratory propagation tests carried out on fuel beds with a retardant-treated strip have shown that, for a retardant-concentration of 0.2 kg of dry retardant product per kg of fuel and a fuel bed bulk density of 7.5 kg m^{-3}, the fire intensity is reduced by a factor of 0.8 whatever the intensity of the front before the retardant-treated strip provided it is less than 1800 kW m^{-1}.

5. At the laboratory-scale, the behavior of fires propagating through a retardant-treated strip under upslope or wind-aided conditions is similar, in terms of rate of spread, fuel consumption and fire intensity reduction, to fire behavior under no-slope/no-wind conditions.

6. A new methodology based on the use of a multiple view projective geometry technique and an infrared camera has been developed to determine in laboratory tests the flame front position and the rate of spread of the propagating fronts.

   This methodology represents an improvement with respect to the methodology of using the breakage of woolen strings stretched across the fuel bed to mark when the fire reaches a particular location.

Maximum and mean rate of spread values can be calculated due to the fact that the flame front profile is detected. This new methodology is easy to extrapolate to field tests. It is neither dependent on the dimensions of the plots nor on the fuel loading nor on the bulk density of the vegetation. The only requirement to implement this methodology is to have four spatial references on a flat surface.

7. For analytical tests, a new methodology to treat forest fuel with long-term retardants commercialized as liquid concentrate has been satisfactorily implemented. It entails generating a powder from the liquid concentrate by dehydrating it and by milling the solid resulting after dehydration.

8. Results obtained from analytical tests carried out in a pyrolytic furnace have shown that the char yield generated after treatment of *Pinus halepensis* needles with two commercial retardant products (Fire-Trol 931 and Fire-Trol 934) fits a rational increasing model.

9. Terms and methodologies usually employed to characterize the heat of combustion of forest fuels have been reviewed. The suitability of using the heat of combustion of the volatiles for retardant-treated samples has been stressed. Results on the heat of combustion of the volatiles of *Pinus halepensis* needles treated with Fire-Trol 931 and Fire-Trol 934 have shown that the heat of combustion of the volatiles averages a reduction of 18% with respect to the heat of combustion of the volatiles of the untreated sample if the retardant concentration in the samples ranges from 10% to 20% w/w.

10. Experimental work carried out at two different scales (laboratory and open-field) has been successful in generating flames representative of forest fires. Open-field data have been collected from burning fuel piles with a diameter of 2.5 m, larger than those found in the literature.

11. Two different methodologies have been developed to compute the flame emissivity during the combustion of forest fuel. Both are based on the use of infrared technology. Experimental data on flame emissivity have been compared with results obtained by other authors. The exponentially increasing relationship between flame emissivity and flame thickness has been confirmed and it has been obtained that flame

emissivity is near the blackbody's one (0.9) only if the flame has a thickness greater than 3.2 m.

12. Experimental data obtained from fire tests carried out with retardant-treated fuel suggest that the flame emissivity is independent of the presence of retardants.

The overall conclusion of this study is that the presence of retardants reduces fire intensity primarily by reducing the amount of heat released per unit mass of fuel during flaming combustion, rather than by affecting the intrinsic radiative properties of the flames.

Since, according to the results obtained in this work, the char yield and the heat of combustion of the volatiles vary due to long-term retardants, an important issue that should be pursued in the near future is to evaluate fire spread models sensitivity to changes in these two parameters.

APPENDIX A

Computing the rate of spread of linear flame fronts by thermal image processing *

Rate of spread (ROS) is one of the most significant parameters in the description of forest fire behavior, since it is directly related to fire intensity [1] and flame front geometry [2] and, thus, to the levels of danger associated with its propagation. In forest fire emergency management, knowing this parameter is crucial. Therefore, a great deal of scientific research is devoted to this field, which centers either on mathematical modeling [3] or on experimental assessment for the validation of models.

Various methods can be used to experimentally assess the ROS, and their success depends on the extent to which straightforward implementation, reliability, precision, feasibility of extrapolation to other experimental scenarios (small scale, field scale and real scale) and cost come together.

Historically, very simple conceptual procedures have been used to experimentally determine the ROS. These are based on calculating the time that the front takes to cover certain known distances, by means of the integration of

* The content of this Appendix was published as: Pastor E, Àgueda A, Andrade-Cetto J, Muñoz M, Pérez Y, Planas E. Computing the rate of spread of linear flame fronts by thermal image processing. Fire Safety J 2006;41:569-79. See the first page of this article in the Appendix B.

several warning systems within the experimental scenario. Thus, a known linear arrangement of warning elements of an acoustic, mechanical, electrical or simply visual nature, which go off and give a signal during the passage of a fire front, makes it easy to calculate the ROS immediately. One of the most commonly used systems consists in the equidistant positioning of cotton or nylon threads perpendicular to the fire spread direction, in such a way that when the fire spreads it burns through them along its path. By recording the moment at which each thread breaks and by knowing its position, the rate of spread is calculated as the derivative of the distance in relation to time. This system is applicable to experimental fires on a laboratory scale, but it is difficult to extrapolate to field experiments, as it is restricted to those areas in which the features of the landscape and the fuel cover allow the threads to be fixed and observed. It is often difficult to obtain wholly reliable measurements of the ROS because of impaired visibility due to such factors as smoke formation, safety distances and vegetation structure. Moreover, this method only serves to measure the ROS from the most advanced sector of the front, which is the maximum ROS value, since this is the part that breaks the thread and, therefore, determines the point in time to be recorded. Thus, in those cases in which the fire deviates substantially from its linearity, this measurement is not representative of the spreading of the whole fire front.

In order to overcome some of these drawbacks, a very similar technique is often used in which the fixed parameter is not the position of the marker but the time. This procedure consists in throwing numbered metal sticks into the flame front at known time intervals [4]. Once the fire has passed, the distances between the successive markers are measured in order to match them with the time they were thrown and thus obtain the ROS. Nevertheless, this technique also has shortcomings, such as its dependency on the accuracy of the throwing and on whether the markers are actually found.

These types of methods are not technically complex, nor do they entail very high costs. However, their precision and feasibility decrease drastically when they are extrapolated to more complex experimental scenarios. Therefore, they are considered to be totally unfeasible for real forest fire emergencies.

During recent years, in reply to these weaknesses, new techniques have appeared based on discrete or continuous fire monitoring by image acquisition with either IR or video cameras. These techniques are becoming widespread in the field of forest fires due to their high precision and versatility with regard to experimental scenarios [5-6]. They are based on the detection of the fire front

position by remote sensing; therefore, they are applicable in the most extreme experimental conditions and even in real forest fires. Moreover, rapid advances in technology have made these equipments less costly and therefore more accessible to widespread use. Nonetheless, its use undoubtedly involves technical complexities at all stages (such as the calibration of the equipment in accordance with the experimental scenario and the final computation of the ROS), which means that these techniques are not often used to compute ROS, or that the results may be difficult to optimize once they have been obtained.

Within this group of technologies, the use of IR thermography is perhaps the most paradigmatic, since its potential is huge and the quality of the data that may be extracted is high. This technique allows the fire front position to be detected even in those situations in which the fire spreads accompanied by thick smoke and is therefore invisible to the human eye. Moreover, it allows valuable information about the fire temperature profile [7-8] and the fire intensity to be extracted. However, this technique is one of the most difficult to implement.

Therefore, the main objective of this work was to develop a simple and very practical method for computing the ROS of a flame front from a sequence of images recorded by an IR camera. The procedure was initially applied to laboratory forest fires, on a flat fuel bed with known dimensions. In the following sections, all the steps are detailed and the technical criteria and the mathematical tools needed for its practical implementation are provided. Finally, technical guidelines for the correct extrapolation of this method to experimental scenarios on a large scale are provided.

A.1 Description of the method

Methods for determining ROS that are based on forest fire monitoring by cameras involve a preliminary step during which the technical conditions for image acquisition are set and then the computation and processing of the images acquired, in order to reach the final ROS value.

Thus, several considerations must first be taken into account in order to select the correct position and calibration parameters of the equipment. In the case of video cameras, this is not a complex procedure, but in IR thermography, certain variables that have a significant influence on the correct functioning of this technology must be identified.

A.1.1 Prior tunings

Suitable parameters must be selected initially to ensure that the IR equipment works correctly. The following items must be taken into consideration:

- Geometric parameters: The first condition that must be taken into account is the position of the camera relative to the target. This decision is not always easy, above all in the case of mobile targets such as fire fronts. It must be determined whether the target will be recorded in a perpendicular or parallel direction, and in the latter case, whether it is better to record the target as it approaches the sensor or as it moves away from it. This decision is often dictated by environmental conditions, but whatever the case, the effects must be assessed, since the IR radiation captured by the sensors strongly depends on the relative position of the emitter and the receiver sources. However, once the direction is ascertained, the distance between the sensor and the target must be considered, as it determines the pixel dimension of the images recorded and the optics of the system.

- Environmental parameters: The ambient temperature and relative humidity must be known in order to work with the IR cameras. These variables, together with the distance between the sensor and the target, are needed to estimate the atmospheric transmissivity, which is a key parameter in determining the radiation from the fire that is absorbed by the atmosphere.

- Thermometric parameters: Some attention must be paid to the spectral range that the IR camera can detect, since in certain experimental scenarios it may condition the sensitivity of the camera and the accuracy of the measurement. Finally, the emissivity value of the target must be taken into account; this parameter must be chosen correctly if true values are to be obtained for temperature and heat power [9].

This stage prior to the method for evaluating the ROS is determined by the features of the experimental scenario and by the thermography equipment available. Moreover, the parameters involved are more or less important depending on the use that is ultimately made of the thermal images recorded. Thus, the adequate selection of environmental and thermometric parameters is essential for an accurate study of forest fire temperature profiles, while the fine-tuning of these parameters is not an indispensable requirement for computing the ROS.

Once the above-mentioned parameters have been set, the conditions related to the image acquisition process, i.e. hardware and software requirements, must be considered. At present, recording sequences of thermal images with the IR cameras available on the market may be computer controlled. The minimum advisable hardware requirements are a Pentium III at 1 GHz with 128 Mb, although this depends on the IR device used; concerning software requirements, an IR camera-controlling driver with an image acquisition and communications package is needed. Generally, this tool, together with a specific code for thermal image processing, is provided by the manufacturer.

The method developed for computing the ROS makes use of the ThermaCAM™ Researcher 2001 software for data acquisition, since that is the code that is available commercially. This code allows thermal images to be easily converted into intelligible information for Matlab, which is one of the most commonly used mathematical tools in the field of engineering, due to its versatility and computational capacity; and was used in this study to compute the ROS.

A.1.2 Computing the rate of spread

In general, the first issue one must consider when using the majority of these ROS calculation methods is finding the correspondence between the coordinate system of the image, which is expressed in pixels, and the real coordinate system, which is expressed in meters or centimeters. This correspondence makes it possible to locate the real position of the flame front, since its position in the images is known. Once this issue is solved, it is necessary to detect the flame front's position as a function of time in order to ascertain an ROS value.

The calculation method designed involved two steps. The first was to develop a function to compute a matrix of correspondences between the pixels in the image and their position in the real plane. In the second step, another function was defined to detect the position of the flame front as a function of time. Both functions were developed using Matlab; they were named 'homografia.m' and 'velocitat.m' respectively [10]. Their structure and the items considered during their definition are stated below. Nevertheless, before going into any detail, the most important criteria related to the design of the two functions must be taken into account. These criteria are as follows:

- The technique used to compute the point correspondence matrix demands that the flame front move forward on a flat surface (whether sloped or not) of known dimensions. Despite this restriction, the

technique was selected because of its simplicity. The extrapolation of this technique to more complex scenarios is tackled later in this appendix.

- As has already been mentioned, by using the ThermaCAM™ Researcher 2001 software, it is possible to store varied data of an image in a Matlab matrix format file. Since the computational space for images is three times higher than for simple matrices, only the temperature matrix (one of the matrices stored in the Matlab file) was used to detect the flame front's position. This matrix, which is of the same size as the corresponding image, contains the temperature of the corresponding pixel in each cell. Other matrices in the Matlab file contain operational data on the camera, such as the exact time at which the image was recorded.

A.2 Calculating the homography matrix

In general, when flame fronts are filmed, either in a laboratory or in an open field, images cannot be recorded from a completely perpendicular position above the advancing flame front's surface. For this reason, a projective vision of the scene is always recorded. This means that filmed surfaces show a geometrical distortion and, thus, the first step in computing the ROS is to determine the correspondence between the points on the recorded image and the real plane.

To solve this issue, a multiple view projective geometry technique was used, and what is known as the planar homography matrix H, was determined. Homography is the biunivocal geometric transformation between two planes or of a plane with itself, which transforms in such a way that every straight line on a plane corresponds to a straight line on the other plane and a point on the first straight line corresponds to a point on the other straight line. Therefore, the H matrix is the one that relates the pixels of the images to their position on the real surface.

If we begin by studying a flat surface, we only need to know the correspondence between four points in the image and their real position to compute the H matrix. If the dimensions of the real surface on which the flame front advances are known, the four vertices can be selected.

If the reference system used is centered on one of the four vertices, the coordinates of the other vertices will be in accordance with the dimensions of the study area and the point of origin selected. In a two-dimensional Euclidian

space (R^2), and for this case study, the coordinates of these four points can be expressed as shown in Figure A.1. Given the fact that the plane on which they are located has a certain perspective, these points are in the two-dimensional projective space P^2. When working in this space, points are represented by a 3 x 1 vector of homogeneous coordinates. A vector has homogeneous coordinates when its last component is exactly 1. Therefore, when writing a vector's coordinates, this last component must be appended.

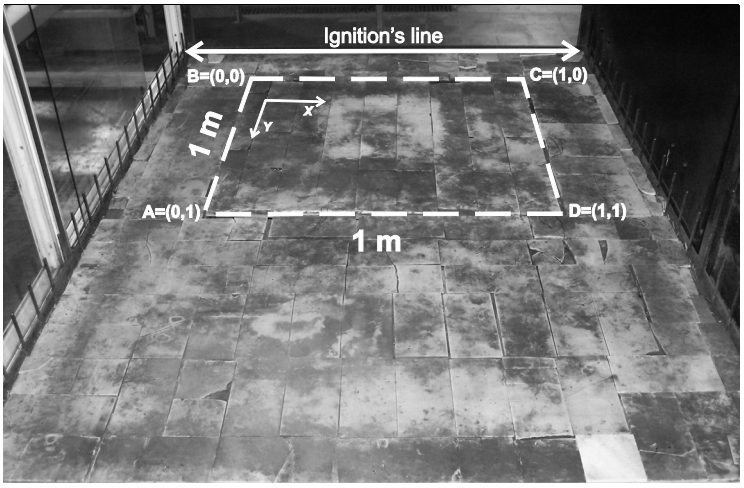

Figure A.1 Sketch and dimensions of the area of study (real surface marked with a dotted line).

The H matrix is calculated by applying the simple direct linear transformation (DLT) algorithm, which is described in detail in [11]. Given that:

- X_i' is a homogeneous column vector that contains the coordinates of the vertex i (for $i = 1, \dots, 4$) of the real surface (values are expressed in meters), and
- X_i is a column vector that contains the coordinates of the vertex i (for $i = 1, \dots, 4$) on the image (values are expressed in pixels),

in accordance with the example shown in Figure A.2, vectors X_i' and X_i take the values shown in [A.1] and [A.2].

$$X_1' = \begin{pmatrix}0\\1\\1\end{pmatrix}, X_2' = \begin{pmatrix}0\\0\\1\end{pmatrix}, X_3' = \begin{pmatrix}1\\0\\1\end{pmatrix}, X_4' = \begin{pmatrix}1\\1\\1\end{pmatrix} \quad [A.1]$$

$$X_1 = \begin{pmatrix}21\\186\\1\end{pmatrix}, X_2 = \begin{pmatrix}57\\72\\1\end{pmatrix}, X_3 = \begin{pmatrix}274\\78\\1\end{pmatrix}, X_4 = \begin{pmatrix}310\\194\\1\end{pmatrix} \quad [A.2]$$

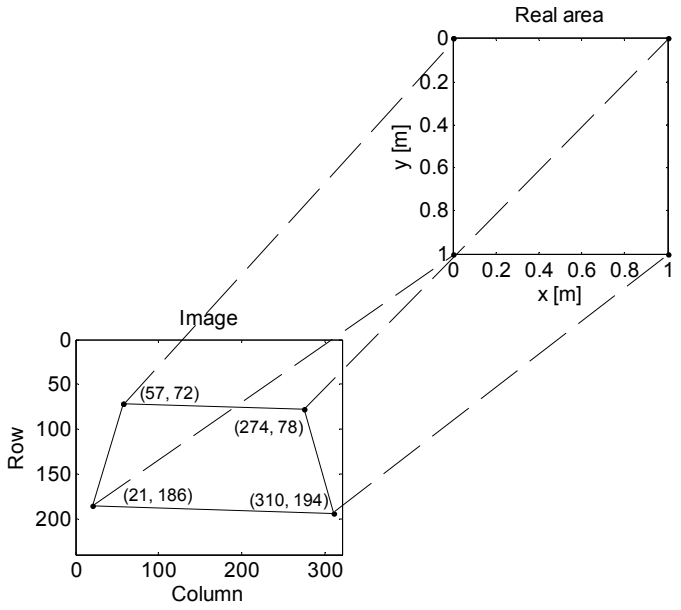

Figure A.2 Points correspondences necessary to compute homography.

For both sets of points, if they are written in a matrix format, Eqs. [A.3] and [A.4] may be written.

$$X' = [X'_1 \quad X'_2 \quad X'_3 \quad X'_4] = \begin{bmatrix} 0 & 0 & 1 & 1 \\ 1 & 0 & 0 & 1 \\ 1 & 1 & 1 & 1 \end{bmatrix} \tag{A.3}$$

$$X = [X_1 \quad X_2 \quad X_3 \quad X_4] = \begin{bmatrix} 21 & 57 & 274 & 310 \\ 186 & 72 & 78 & 94 \\ 1 & 1 & 1 & 1 \end{bmatrix} \tag{A.4}$$

In order to ensure that the resulting homography matrix does not depend on the coordinate system in which the points are expressed, both sets of points are normalized separately before the DLT algorithm is applied to compute H. The data normalization method consists in isotropically translating and scaling the coordinates, so as to bring the centroid of the set of all points to the origin and so that the average distance of each point from the origin is equal to $2^{1/2}$.

This normalization procedure transforms matrices X' and X' into $\hat{X}'$ and $\hat{X}$ respectively (see Eqs. [A.5] and [A.6] for this example). In Figure A.3, the xy coordinates of points X'_i and $\hat{X}'_i$ of matrices X' and $\hat{X}'$, and the xy coordinates of points $\hat{X}_i$ of matrix $\hat{X}$ are graphically represented. The xy coordinates of points X_i are not plotted in this figure because their inclusion would make it difficult to visualize the other points.

$$\hat{X}' = [\hat{X}_1' \quad \hat{X}_2' \quad \hat{X}_3' \quad \hat{X}_4'] = \begin{bmatrix} -1 & -1 & 1 & 1 \\ 1 & -1 & -1 & 1 \\ 1 & 1 & 1 & 1 \end{bmatrix} \tag{A.5}$$

$$\hat{X} = [\hat{X}_1 \quad \hat{X}_2 \quad \hat{X}_3 \quad \hat{X}_4] = \begin{bmatrix} -1.4681 & -1.1024 & 1.1024 & 1.4681 \\ 0.54356 & -0.61468 & -0.55372 & 0.62484 \\ 1 & 1 & 1 & 1 \end{bmatrix} \tag{A.6}$$

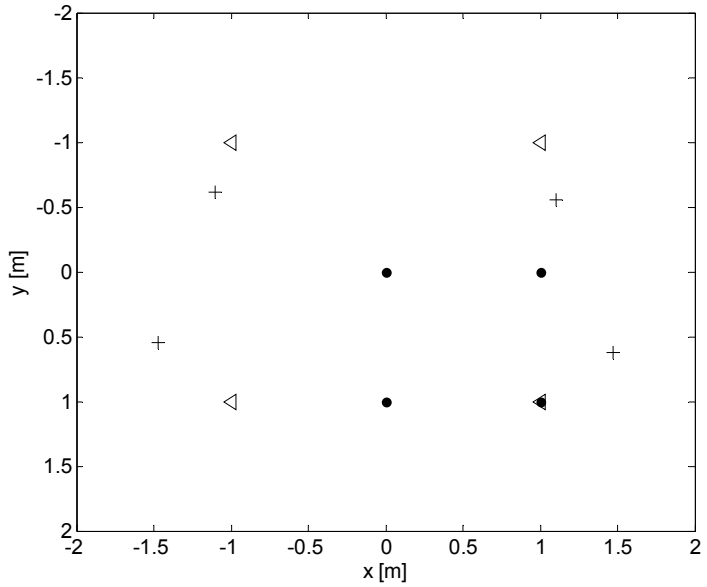

Figure A.3 *xy* coordinates of X_i' (circle), $\hat{X}_i'$(triangle) and $\hat{X}_i$ (cross) points.

Once the normalization is applied, the process of obtaining $\widehat{H}$ begins. The notation of $\widehat{H}$ is accompanied by a hood to make it clear that it will be necessary to denormalize it afterwards.

The DLT is given by the following expression (Eq. [A.7]).

$$\hat{X}_i' = \widehat{H}\,\hat{X}_i \tag{A.7}$$

This condition must be met by all four vertices previously quoted. Thus, the above expression may be written as shown in Eq. [A.8].

$$[\hat{X}_1' \quad \hat{X}_2' \quad \hat{X}_3' \quad \hat{X}_4'] = \begin{bmatrix} h_{11} & h_{12} & h_{13} \\ h_{21} & h_{22} & h_{23} \\ h_{31} & h_{32} & h_{33} \end{bmatrix} [\hat{X}_1 \quad \hat{X}_2 \quad \hat{X}_3 \quad \hat{X}_4] \tag{A.8}$$

The $\hat{X}_i'$ vectors and the vectors resulting from the $\widehat{H}\,\hat{X}_i$ multiplication are not equal since they were defined in homogeneous coordinates. They have the same direction but may differ in magnitude by a non-zero scale factor. Therefore, Eq.

[A.7] is not always valid. Nevertheless, by expressing this relation in terms of a cross vector product, a simple, linear solution may be found for $\widehat{H}$:

$$\hat{X}_i' \times \widehat{H}\,\hat{X}_i = 0 \qquad [A.9]$$

If the *j*-th row of the $\widehat{H}$ matrix is denoted by h^{jT} and the fact that $\widehat{H}$ is a 3 x 3 matrix is taken into account, we get Eq. [A.10].

$$\widehat{H}\,\hat{X}_i = \begin{bmatrix} h^{1T} \\ h^{2T} \\ h^{3T} \end{bmatrix} \hat{X}_i = \begin{pmatrix} h^{1T}\,\hat{X}_i \\ h^{2T}\,\hat{X}_i \\ h^{3T}\,\hat{X}_i \end{pmatrix} \qquad [A.10]$$

in which the superscript "T" included in the notation of h^{jT} indicates that it is a row vector. Moreover, if we write $\hat{X}_i' = \begin{pmatrix} X_i' \\ Y_i' \\ W_i' \end{pmatrix}$, the cross product may be given explicitly as shown in Eq. [A.11].

$$\hat{X}_i' \times \widehat{H}\,\hat{X}_i = \begin{pmatrix} y_i'\ h^{3T}\,\hat{X}_i - w_i'\ h^{2T}\,\hat{X}_i \\ w_i'\ h^{1T}\,\hat{X}_i - x_i'\ h^{3T}\,\hat{X}_i \\ x_i'\ h^{2T}\,\hat{X}_i - y_i'\ h^{1T}\,\hat{X}_i \end{pmatrix} = 0 \qquad [A.11]$$

Since $h^{jT}\hat{X}_i = \hat{X}_i^T h^j$ and $h^j = \left(h^{jT}\right)^T$, for $j = 1, \ldots, 3$, the previous vector may be written in the form of a set of three equations in the entries of $\widehat{H}$ (see Eq. [A.12]).

$$\begin{bmatrix} 0^T & -w_i'\ \hat{X}_i^T & y_i'\ \hat{X}_i^T \\ w_i'\ \hat{X}_i^T & 0^T & x_i'\ \hat{X}_i^T \\ -y_i'\ \hat{X}_i^T & x_i'\ \hat{X}_i^T & 0^T \end{bmatrix} \begin{pmatrix} h^1 \\ h^2 \\ h^3 \end{pmatrix} = 0 \qquad [A.12]$$

Eq. [A.12] takes the form $\hat{A}_i\, h = 0$, where $\hat{A}_i$ is a 3 x 9 matrix and h is a column vector with 9 cells. The vector h is made up of the entries of the $\widehat{H}$ matrix (see Eq. [A.13]).

$$h = \begin{pmatrix} h^1 \\ h^2 \\ h^3 \end{pmatrix} = \begin{pmatrix} h_{11} \\ h_{12} \\ h_{13} \\ h_{21} \\ h_{22} \\ h_{23} \\ h_{31} \\ h_{32} \\ h_{33} \end{pmatrix} \qquad [A.13]$$

Matrix $\hat{A}_i$ is computed for each of the four vertices, and then a new 12 x 9 matrix $\hat{A}$ is created with the entries of all four matrices (see Eq. [A.14]).

$$\hat{A} = \begin{bmatrix} \hat{A}_1 \\ \hat{A}_2 \\ \hat{A}_3 \\ \hat{A}_4 \end{bmatrix} \qquad [A.14]$$

To find the values for the entries in $\widehat{H}$, the overdetermined set of equations $\hat{A}\, h = 0$ must be solved. A least squares solution for this set of equations may be computed by decomposing $\hat{A}$ into singular values. Specifically, if $\hat{A} = U\, D\, V^T$ and D runs diagonally and has positive diagonal entries, which are arranged in descending order along the diagonal line, then h, the singular vector associated to the smallest singular value of $\hat{A}$, and is given by the last column of V.

As a last step, the matrix H is obtained by denormalizing the matrix $\widehat{H}$.

The 'homografia.m' function makes it possible to obtain H automatically, as has been explained in preceding paragraphs, independently of the real surface size and of the thermographic camera position. Nevertheless, if the configuration is different from that described in this work and one wishes to use the same function for the determination of H, the X' matrix must be changed. In addition, the image file name must be replaced with the one corresponding to a recorded image of the own facility.

This matrix is necessary for calculating the rate of spread of the flame front, as explained in the following paragraph.

A.3 Calculating the rate of spread

The images obtained with the thermographic camera allow us to ascertain the temperature corresponding to each pixel in the image, which at the same time corresponds to a given point on the real surface under study. In order to obtain the temperature distribution on the real surface, the area is considered to be a matrix of points, and each of these points will have a corresponding position. From the inverse of the homography matrix obtained from the 'homografia.m' function, the position in the coordinate system associated to the image can be obtained. The temperature value stored in each one of these positions is what is introduced in the matrix corresponding to the surface under study.

In order to determine the position of the flame front at each point in time, it is necessary to establish a search criterion within the temperature matrix

corresponding to the surface under study. To simplify this task, the matrix was normalized according to Eq. [A.15]:

$$\hat{T}_k = \frac{(T_k - T_{min})}{(T_{max} - T_{min})} \quad [A.15]$$

This normalization makes it possible to obtain a new matrix with values ranging between 0 and 1.

In the normalized matrix of temperatures, the search for the front position is carried out each column at a time, starting from the last line that physically corresponds to the surface side, which is parallel to the ignition line and burns last (see Points A and D in Figure A.1). In this way, errors in the localization of the flame front, which stem from the presence of heat points that do not belong to the flame front, are avoided.

The limit value of the normalized temperature from which it is considered that a given point belongs to the flame front corresponds to the input parameter *m* and can be fixed by the user. In the subsequent paragraph some practical recommendations on the most adequate values for *m* are given.

For each point in time, the mean position of the flame front and the most advanced position are determined. In this way, the function can calculate two values for the spread rate: a maximum and a mean value. The first value indicates the evolution of the most advanced part of the flame front at each point in time, which is assumed to be similar to the spread rate obtained from other measurement methods, such as the equidistant threads. The second value gives qualitative information about the linearity of the flame front: if it differs greatly from the maximum value, this means that the initial geometry of the flame front has undergone significant modification.

For the calculation of the mean spread rate, it was necessary to define another input variable, *cents*, which determines the moment at which the 'velocitat.m' function must finalize the search for the flame front position. The *cents* value is a limit value defined as the number of points on the flame front that have reached the final position on the surface under study (Line AD in Figure A.1). The more irregular the flame front profile, the greater the influence of this parameter on the final value of the spread rate. In these cases, if the *cents* value is too high, the 'velocitat.m' function can account reiteratively for those points on the flame front that have reached their final position some moments before, but which continue to burn in the form of incandescent combustion.

Figure A.4 shows an example of the results obtained after the execution of the 'velocitat.m' function. Besides the mean and most advanced position of the flame front as a function of time (Figure A.4A), a graph with the evolution of the flame position and the geometry of the flame front profile as a function of time is also included (Figure A.4B). Due to the generic nature of the function developed, another input variable was defined, *int*, which allows the interval of images between each profile on the flame front to be selected.

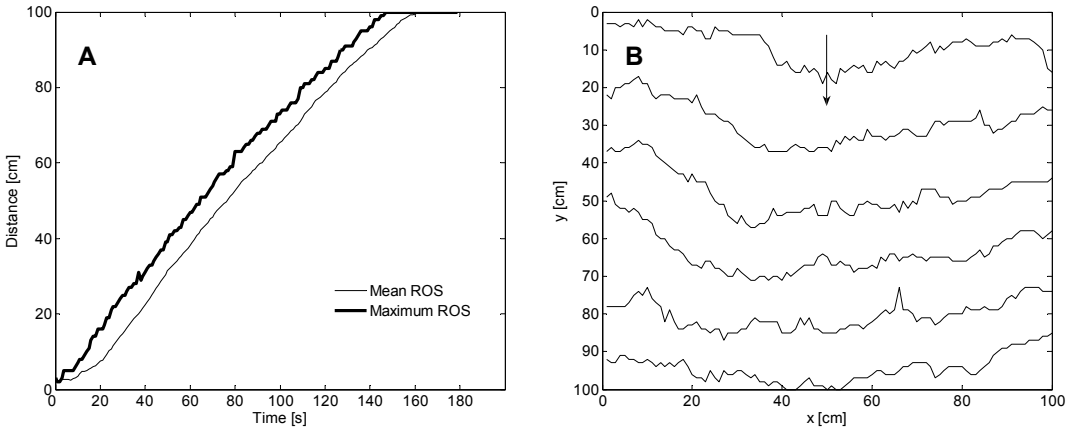

Figure A.4 Graphical results of 'velocitat.m' function: A) Covered distance vs. Time; B) Front profile evolution (every 24 seconds); the arrow of the figure indicates the direction of propagation.

A.4 Example

In order to show the validity of the method developed, the 'homografia.m' and 'velocitat.m' functions were applied to several thermographic image sequences that had been recorded during various tests performed in a combustion table at the Centre for Technological Risk Studies (CERTEC) at the Polytechnic University of Catalonia (UPC). In the following paragraph, the main features of the facility and the tests carried out are described. The values assigned to the input variables are also provided, and special attention is paid to parameter *m*. Finally, the results obtained with the method proposed were compared to the results obtained with the traditional threads method.

A.4.1 Description of the installation

The combustion table used in the experimental set-up had 4.8 m^2 useful burning surface and was equipped with a thermographic camera, a video camera, several thermocouples, a weighting system with a floating surface (1 m x 1 m) and a balance. The thermographic camera was able to record the flame front

approaching the sensor. During the tests the camera was centered in relation to the flame front length. It was placed at a height of 2.30 m from the bottom and at a distance of 2.70 m from the central point of the floating surface. In this position, the radiation reaching the thermographic camera came, on the one hand, from the radiation emitted by the incandescent fuel bed, which is transmitted by the flames, and, on the other hand, from the emission of the flames.

In Table A.1, several adjustments that were made on the thermographic camera are shown. Technical specifications of this camera are shown in Table 7.4.

Table A.1 Prior adjustments to take into account when working with the thermographic camera.

Mean distance between the camera and the object	2.70 m
Temperature	15°C – 20°C
Relative humidity	50-70 %
Emissivity	0.9

Concerning the direct relation of some of the values shown in Table 1 to the ROS calculation and the criterion used in the determination of the flame front position, the ROS will be more accurate as the temperature values given by the camera are more precise. Thus, the adjusted parameters selected are consistent. In the experimental conditions presented here, the fuel bed can be considered a black body and the emissivity of the flame front, which is characterized by yellow flames between 15 and 20 cm wide, can be taken as being near to 0.5 [9]. The difference between these two radiation contributions, the greatest of which is the fuel bed, is shown in the thermographic images because the flame contour is completely diluted (Figure A.5A). The emissivity of the whole is nearer to that of the black body than to that of the flames. Thus, a value of 0.9 was assigned to the emissivity of the whole, as this is the most suitable value for obtaining precise temperature values.

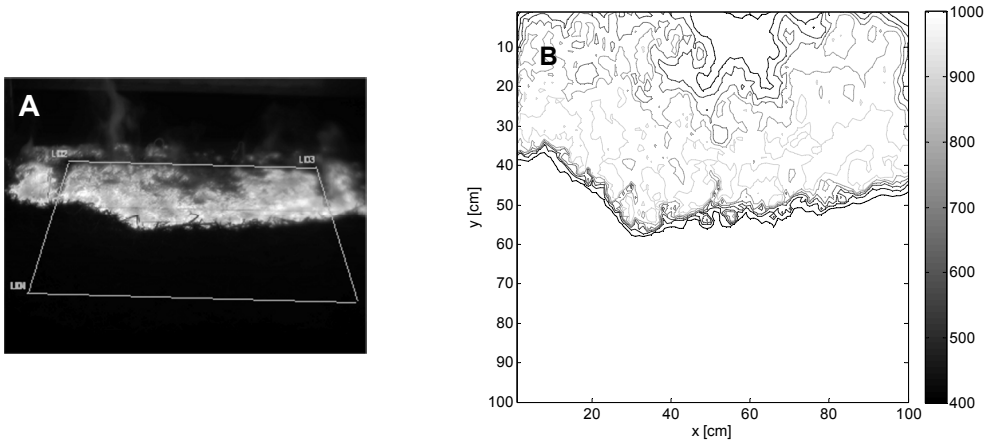

Figure A.5 A) IR image of a laboratory test; B) Temperature isolines plot of the same time instant of the laboratory tests.

Concerning the mean distance between the camera and the flame front (2.70 m) and the optics of the camera, the pixel size is less than 4 mm, which allows an optimal resolution in obtaining the flame front contour.

Finally, the values for ambient temperature and relative humidity were measured and entered in the ThermaCAM™ Researcher as input parameters for each test. Using these values, the software automatically calculates the atmospheric transmissivity and corrects the temperature values accordingly.

In Figure A.5A, an image recorded during the execution of a test can be seen. The quadrilateral that appears in this image indicates the position of the floating study surface. Finally, Figure A.5B is a temperature isoline map of the surface under study, after the *H* homography matrix has been applied to the temperature matrix corresponding to the IR image in Figure A.5A.

By way of summary, the image sequences used in this study correspond to tests executed without the presence of wind and slope. The tests consist in burning forest fuel beds by creating a linear flame front. In [12], the facility, the experimental method and the diverse tests carried out are described in more detail.

A.4.2 Calculation considerations

In this practical case, data were only taken from the position of the flame front within the study area or floating surface (Figure A.1). To avoid calculation errors and to reduce the operation time, the initial and final files, which corresponded to images in which it could clearly be seen that the flame front

was still not in the area under study or it had already passed it, were eliminated manually.

In order to execute the 'velocitat.m' function, it was necessary to set a numerical value for the input parameters *m, int* and *cents,* according to the characteristics of the experimental test.

In the case of parameter *m*, a detailed study was carried out of the differences generated in the results of the ROS when different values are assigned to it. By superimposing *m* isoline maps on the infrared images, it was verified visually that the values of *m* that were closest to the front position were between 0.1 and 0.3. According to Eq. [A.15], a value of 0.3 for *m* was obtained by considering the maximum and minimum temperatures to be equal to 1000 K and 300 K respectively (temperatures observed in the analysis of several sequences used in this study) and the instantaneous temperature for every element (T_k) in the order of 500 K, a value that corresponds to the ignition temperature of wheat straw [13], the fuel used in these tests.

The *int* parameter took different values depending on the specifications of the experimental test corresponding to the sequence of images analyzed. For tests in which the fire advanced faster (approximately 1 cm s^{-1}), a value equal to 10 images between every contour profile front was used, while in tests in which the fire advanced more slowly (approximately 0.3 cm s^{-1}), a value equal to 25 images was used.

The *cents* parameter was set at a value equal to 50 points in all cases. Thus, it was assumed that the computed value of the front mean position was representative of the propagation of the whole of the front, while half of the points had reached their final position on the surface under study. Nevertheless, in cases in which the flame front loses its linearity completely, it would be advisable to use a lower value for the *cents* parameter.

A.4.3 Results threads vs. 'velocitat.m'

The maximum rate of spread obtained using the method described and the one obtained with the traditional method of threads were compared for different image sequences. In general, the values obtained by applying the 'velocitat.m' function are slightly higher than those computed for the threads (Figure A.6). Nevertheless, the mean value of the differences obtained using one method or the other is less than 6%, a significantly low error rate that is the result of the different nature of the methods. The cases in which this difference is most

significant correspond to tests in which there are no time references for some of the threads, or in those cases in which the front had lost its linearity practically from the start of its course.

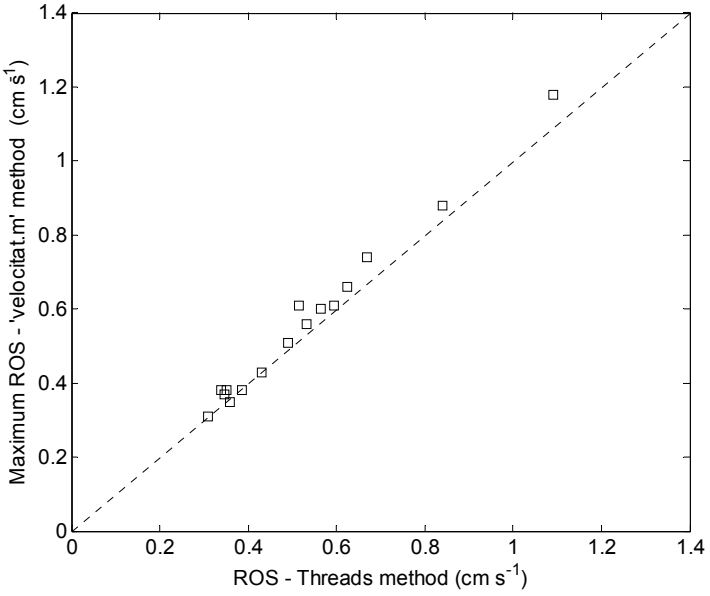

Figure A.6 ROS threads method vs. ROS 'velocitat.m'.

A.5 Extrapolating the method to other scenarios

The method developed using the functions described in the preceding sections is directly applicable to other laboratory devices for fires, since the data required are easy to obtain in any small-scale experimental scenario. Thus, the homography computation function only needs information on the geometry of the fuel bed located on a plane. As far as the rate of spread computation function is concerned, it was defined in a flexible manner, making it possible to change characteristic input parameters depending on the fire scenario.

Most of the work that lies ahead involves adapting the functions described to experimental fires that take place in real scenarios. In these kinds of situations, if the filming is terrestrial, two problems can generally be found. First of all, human figures appear in the IR images that make the flame front difficult to visualize completely. These figures are usually the silhouettes of fire-fighters advancing towards the fire to control its propagation. This difficulty could be overcome by interpolation methods. In most cases, however, the slope of the terrain is not uniform, which strictly precludes the application of the DLT algorithm, since the terrain is made up of different planes. A reasonable solution

could be the discretization of the land in a specific number of planes, and consequently, in the same number of homography matrixes. Topographical maps of the surface under study would be required for this latter case in order to fix planar patches to the terrain for the computation of the various homographies, one per patch.

As for thermographically determining factors, ambient temperature, relative humidity, absolute distance between camera and object and emissivity of the radiation source are necessary parameters in any experimental scenario. Under experimental conditions in a laboratory, all these data can easily be obtained, except for emissivity. In order to obtain a suitable value for this parameter, specially in those cases in which the thermography equipment uses a spectral range that is sensitive to the selection of this value and there is an overlapping of the sources of radiation, it is necessary to consider, on the one hand, the specific weight of each of these contributions and, on the other, the thickness of the flame. Whatever the case, if this information is not available, reasonable estimates of the parameters are sufficient to obtain equally valid values for the ROS. In experimental conditions on a field scale, estimating the emissivity is simpler, since for thick, intense flames such as those observed in prescribed burnings or real fires, the emissivity is very near to unity [14]. Nevertheless, the distance at which the thermography equipment is positioned in relation to the flame front can be a limiting factor in these scenarios. As the distance between the object and the camera increases, the atmosphere attenuates the fire radiation and the spatial resolution diminishes (the pixel size increases). The first effect can be corrected by a transmittance factor. The ThermaCAM™ Researcher 2001 software has a built-in model that computes it according to atmospheric parameters (temperature and relative humidity). Concerning the spatial resolution, the larger the distance between the object and the camera, the less the number of pixels included into the study area. Therefore, the number of pixels can be too low to suitably represent the evolution of the fire and the computed ROS may have an underestimated value. Nevertheless, since the size of the resulting pixel for a fixed distance depends also on the optics of the camera, this effect can be solved by attaching lenses with an adequate field of view to the equipment.

A.6 Conclusions

A method for the fast and accurate calculation of the ROS by processing infrared images was presented in this Appendix.

Matlab was used to develop the necessary functions to implement this method, so that it can be freely used and directly applied to the calculation of the ROS by means of thermography in a laboratory. The design criteria for the functions were simple and appropriate; it was demonstrated that a normalized DLT algorithm is an appropriate method for calculating the projection of the plane of the image onto the plane of the area under study. Likewise, the selection criterion of the front position by temperature is valid and robust. The practical application and the comparison with the classical method for determining the ROS in a laboratory through the observation of broken equidistant and parallel nylon threads in the advance of the front were successful.

This method is easily applicable to other experimental scenarios that are more complex than the ones described in this study, such as prescribed burnings or real forest fire emergencies. The guidelines for correct extrapolation have been discussed and compiled and it remains as future work to implement all of them as an extension to the functions described.

Nomenclature

$\hat{A}_i$	matrix of equation coefficients contributed from the i-th correspondence
$\hat{A}$	matrix of equation coefficients built from the matrix rows $\hat{A}_i$ contributed from each correspondence
A, B, C, D	vertices of the area of study
cents	maximum number of points of the flame front that have reached the final position on the surface under study
D	diagonal matrix with positive diagonal entries, which are arranged in descending order along the diagonal line
DLT	direct lineal transformation
h	column vector containing the elements of the $\widehat{H}$ matrix
h^j	column vector of the j-th row of the $\widehat{H}$ matrix
h^{jT}	j-th row vector of the $\widehat{H}$ matrix
H	planar homography matrix
$\widehat{H}$	normalized planar homography matrix
i	i-th vertex of the area of study
int	interval of images between each profile on the flame front plot
j	j-th row of the matrix $\widehat{H}$
k	k-th element of the temperature matrix
m	limit value of inclusion in the flame front
P^2	two-dimensional Projective space
R^2	two-dimensional Euclidian space
ROS	rate of spread

T_k	temperature of the k-th element of the temperature matrix
T_{min}	minimum temperature of the temperature matrix
T_{max}	maximum temperature of the temperature matrix
$\hat{T}_k$	normalized temperature value of the k-th element
U	unitary matrix which contains the eigenvalues of $\hat{A}\ \hat{A}^T$
V	unitary matrix which contains the eigenvalues of $\hat{A}^T \hat{A}$
X_i'	homogeneous column vector that contains the coordinates of the vertex i of the real surface
X_i	column vector that contains the coordinates of the vertex i on the image
$\hat{X}_i'$	homogeneous column vector that contains normalized coordinates of X_i'
$\hat{X}_i$	homogeneous column vector that contains normalized coordinates of X_i
X'	matrix that contains X_i' vectors
X	matrix that contains X_i vectors
$\hat{X}'$	normalized X' matrix
$\hat{X}$	normalized X matrix
α	inclination angle in relation to the horizontal working plane
( )	denotes a vector
[ ]	denotes a matrix

References

1. Byram G. Combustion in forest fuels. In: Forest Fire Control and Use (Ed. Davis KP) McGraw-Hill, New York, 1959;61-89.

2. Anderson HE. Fire spread and flame shape. Fire Technol 1968;4:51-8.

3. Pastor E, Zárate L, Planas E, Arnaldos J. Mathematical models and calculation systems for the study of wildland fire behaviour. Prog Energ Combust Sci 2003;29(2):139-53.

4. Rothermel RC, Rinehart GC. Field procedures for verification and adjustment of fire behaviour predictions. USDA Forest Service General Technical Report INT-142; 1983.

5. Gomez F, Merino L, Arrue B, Ollero A. Aerial monitoring and measurement of forest fires. Prog Biomed Optics Imaging 2002;4713:95-105.

6. Martínez-de Dios JR, Ollero A, Arrue BC. Sistema fuzzy-wavelet para monitorización visual. Aplicación a los incendios forestales. In: 'Actas del X Congreso Español de Tecnologías y Lógica Fuzzy (ESTYLF)' 20-22 September, Seville, Spain; 2000.

7. Aranda JM, Meléndez J, Briz S, De Castro AJ, López F. Measurements of laboratory forest fires with bi-espectral infrared imaging. In: 'Proceedings of the 4th International Conference on Forest Fire Research' 18-23 November, Luso, Portugal; 2002.

8. Morandini F, Simeoni A, Santoni PA, Balbi JH. A model for the spread of fire across a fuel bed incorporating the effects of wind and slope. Combust Sci Technol 2005;177(7):1381-1418.

9. Pastor E, Rigueiro A, Zárate L, Giménez A, Arnaldos J, Planas E. Experimental methodology for characterizing flame emisivity of small scale forest fires using infrared thermography techniques. In: 'Proceedings of the 4th International Conference on Forest Fire Research' 18-23 November, Luso, Portugal; 2002.

10. Centre d'Estudis del Risc Tecnològic. Computing the rate of spread of linear flame fronts by thermal image processing. Source: http://certec.upc.es/articles/forestal/rateofspread.htm. Last modified: -. Visiting date: 08/09/2009.

11. Hartley R, Zisserman A. Multiple View Geometry in Computer Vision, Cambridge University Press, Cambridge; 2003.

12. Pastor E. Contribució a l'estudi dels efectes dels retardants en l'extinció d'incendis forestals. PhD Thesis, Universitat Politècnica de Catalunya, Spain; 2004.

13. Grotkjaer T, Dam-Johansen K, Jensen AD, Glarborg P. An experimental study of biomass ignition. Fuel 2003;82(7):825-33.

14. Sullivan AL, Ellis PF, Knight K. A review of radiant heat flux models used in bushfire applications. Int J Wildland Fire 2003;12(1):101-10.

APPENDIX B

Publications derived from this work

Publications arising as a consequence of the research undertaken for this PhD Thesis are included in Table B.1. In this table the title of the papers (already published or under review after submission), the year of publication (whenever possible) and the impact factor of the corresponding journal during the year of publication or during the last year available in the database of the ISI Web of Knowledge are included. The first page of the published papers is included afterwards (see Figures B.1-B.3).

Table B.1 Summary of publications derived from this work. Note: the impact factor has been extracted from the database of the ISI Web of Knowledge; in parentheses there is the year to which the impact factor is referred. Manuscripts under revision are differentiated by xxxx at the year of publication.

Different scales for studying the effectiveness of long-term forest fire retardants		
Journal:	*Year of publication:*	*Impact factor:*
Progress in Energy and Combustion Science	2008	8.000 (2008)
Characterization of laboratory-scale fires propagating under the effect of a long-term retardant		
Journal:	*Year of publication:*	*Impact factor:*
Combustion Science and Technology	xxxx	0.877 (2008)
Characterization of the thermal degradation and heat of combustion of *Pinus halepensis* needles treated with ammonium-polyphosphate-based retardants		
Journal:	*Year of publication:*	*Impact factor:*
Journal of Thermal Analysis and Calorimetry	2009	1.630 (2008)
Experimental study of the emissivity of flames resulting from the combustion of forest fuels		
Journal:	*Year of publication:*	*Impact factor:*
International Journal of Thermal Sciences	xxxx	1.683 (2008)
Computing the rate of spread of linear flame fronts by thermal image processing		
Journal:	*Year of publication:*	*Impact factor:*
Fire Safety Journal	2006	0.481 (2006)

Progress in Energy and Combustion Science 34 (2008) 782–796

Contents lists available at ScienceDirect

Progress in Energy and Combustion Science

journal homepage: www.elsevier.com/locate/pecs

Different scales for studying the effectiveness of long-term forest fire retardants

Alba Àgueda, Elsa Pastor, Eulàlia Planas *

Centre d'Estudis del Risc Tecnològic (CERTEC), Universitat Politècnica de Catalunya, ETSEIB, Diagonal 647, pav. G, planta 1. 08028 Barcelona, Catalonia, Spain

ARTICLE INFO

Article history:
Received 7 November 2007
Accepted 24 June 2008
Available online 28 August 2008

Keywords:
Forest fires
Long-term retardants
Diammonium phosphate
Ammonium sulfate
Pyrolysis
Rate of spread

ABSTRACT

The effectiveness of long-term retardants used in forest fire fighting has been studied at three different scales. In this paper, retardant effectiveness experiments conducted since 1965 are examined and reviewed. These experiments include studies carried out with analytical instrumentation as well as studies involving laboratory and field flame-spread tests. Special attention is paid to the work performed with diammonium phosphate (DAP) and ammonium sulfate (AS). The experimental methodologies and the results obtained are reviewed in detail. A lack of effort in the modeling of fire behavior under the effect of these products is evidenced and recommendations for further work are made.

Contents

1. Introduction

Wildland fires occur in vegetative fuels and involve high-temperature gaseous combustion reactions (flaming) and/or low-temperature solid combustion reactions (smoldering). The rate at which forest fires spread is determined by the rate at which heat released is transferred from the burning matter to unburnt matter. The mechanisms of heat transfer are radiation, conduction and convection.

A forest fire consists of different parts: head, flank, rear, spot fires, etc. Fire-spread models have focused on the characteristics of the head fire, which is the fastest moving section. Nevertheless, any fire front can be described by the rate of spread (ROS), the geometrical characteristics of the flames (length, depth and angle) and the fire intensity. Fire intensity is the rate of energy release per unit time per unit length of fire front. Numerically, it is equal to the product of the available fuel, the heat yield and the ROS.

Three types of wildland fires are distinguished according to the vegetation layer in which they are burning: ground, surface and crown fires. The organic material beneath the surface ground litter is consumed in ground fires and they burn by smoldering combustion. The term surface fire refers to a fire that burns

* Corresponding author. Tel.: +34 934016675; fax: +34 934017150.
E-mail address: eulalia.planas@upc.edu (E. Planas).

0360-1285/$ - see front matter © 2008 Elsevier Ltd. All rights reserved.
doi:10.1016/j.pecs.2008.06.001

Figure B.1 First page of the work: Àgueda A, Pastor E, Planas E. Different scales for studying the effectiveness of long-term forest fire retardants. Prog Energ Combust 2008;34:782-96.

J Therm Anal Calorim
DOI 10.1007/s10973-009-0134-0

Characterization of the thermal degradation and heat of combustion of *Pinus halepensis* needles treated with ammonium-polyphosphate-based retardants

A. Àgueda · S. Liodakis · E. Pastor · E. Planas

Abstract The thermal degradation behavior of *P. halepensis* needles treated with two ammonium-polyphosphate-based commercial retardants was studied using thermal analysis (DTG) under nitrogen atmosphere. Moreover, for the same experimental material, the heat of combustion of the volatiles was estimated based on the difference between the heat of combustion of the fuel and the heat contribution of the charred residue left after pyrolysis. The heat of combustion of the volatiles was exponentially related to the retardant concentration of the samples. In the range of retardant concentrations from 10 to 20% w/w the mean reduction percentage of the heat of combustion of the volatiles, with respect to untreated samples, was 18%.

Keywords Bomb calorimeter · Char · Forest fires · Heat of combustion · Long-term retardants · Thermal analysis · Volatiles

List of symbols

APP	Ammonium polyphosphate
DTG	Differential thermogravimetry
DR	DTG peak decomposition rate (10^3 s^{-1})
EHC	Effective heat of combustion (MJ kg^{-1} fuel consumed)
FT1	Fire-Trol 931
FT4	Fire-Trol 934
HC	Heat of combustion (MJ kg^{-1})
HHC	High heat of combustion (MJ kg^{-1})
HY	Heat yield (MJ kg^{-1})
$(\Delta h_c/r_0)$	Heat of combustion released per kg of oxygen consumed (13.1 MJ kg^{-1})
$\Delta h_{dsp\,H_2O}$	Heat of desorption of bound water in the fuel (MJ kg^{-1})
$\Delta h_{v\,H_2O}$	Latent heat of vaporization of water at 100 °C (MJ kg^{-1})
LHC	Low heat of combustion (MJ kg^{-1})
$\dot{m}_{O_2,\infty}$	Oxygen mass flow at ambient conditions (kg s^{-1})
$\dot{m}_{O_2}$	Instantaneous oxygen mass flow (kg s^{-1})
PH	*Pinus halepensis*
$\dot{q}$	Heat rate (kW)
Q_{inc}	Heat loss due to incomplete combustion (MJ kg^{-1})
Q_{rad}	Heat loss due to radiation losses (MJ kg^{-1})
R_{550}	Percentage of residual mass at 550 °C to initial mass at 150 °C (% w/w)
PT	DTG peak temperature (°C)
X_c	Char yield (% w/w)
X_H	Percentage of hydrogen (% w/w)
X_r	Retardant concentration (% w/w)
X_w	Moisture content on a dry basis (% w/w)

Subscripts/superscripts

c	Charred residue
f	Fuel
r	Retardant
vol	Volatiles
1, 2, 3	Peak number in DTG graphs

A. Àgueda · E. Pastor · E. Planas (✉)
Centre d'Estudis del Risc Tecnològic (CERTEC),
Universitat Politècnica de Catalunya, ETSEIB,
Diagonal 647, pav. G, planta 2, 08028 Barcelona, Catalonia, Spain
e-mail: eulalia.planas@upc.edu

S. Liodakis
Laboratory of Inorganic and Analytical Chemistry,
Department of Chemical Engineering, National Technical
University of Athens (NTUA), 9 Iroon Polytechniou Street,
157-80 Athens, Greece

Journal : Large 10973 | Dispatch : 2-6-2009 | Pages : 9
Article No. : 134 | LE | TYPESET
MS Code : JTAC-D-08-00009 | CP | DISK

Figure B.2 First page of the work: Àgueda A, Liodakis S, Pastor E, Planas E. Characterization of the thermal degradation and heat of combustion of *Pinus halepensis* needles treated with ammonium-polyphosphate-based retardants. J Therm Anal Calorim; DOI: 10.1007/s10973-009-0134-0.

Available online at www.sciencedirect.com
ScienceDirect
Fire Safety Journal 41 (2006) 569–579
FIRE SAFETY JOURNAL
www.elsevier.com/locate/firesaf

Computing the rate of spread of linear flame fronts by thermal image processing

E. Pastor[a], A. Àgueda[a], J. Andrade-Cetto[b], M. Muñoz[a], Y. Pérez[a], E. Planas[a,*]

[a]*Centre for Studies on Technological Risk (CERTEC), Universitat Politècnica de Catalunya, ETSEIB, Diagonal 647, Pav.G, Planta 2, 08028 Barcelona, Catalonia, Spain*
[b]*Centre de Visió per Computador (CVC), Universitat Autònoma de Barcelona Edifici O, Bellaterra 08193, Spain*

Received 3 October 2005; received in revised form 13 March 2006; accepted 2 May 2006
Available online 22 August 2006

Abstract

This work proposes a new thermal image processing method for computing the rate of spread (ROS) of forest fires. It is based on an application for linear flame fronts that are generated on flat surfaces with known dimensions. In the first step of the method, the correspondence between the points of the thermal image obtained and the real plane is calculated by means of a direct linear transformation (DLT). Subsequently, the position of the flame front is determined by applying a threshold-value-searching criterion within the temperature matrix of the target surface. The design principles for the implementation of this method in the laboratory are described in depth, as well as the considerations that must be taken into account if the method is to be correctly extrapolated to more complex experimental scenarios, such as prescribed burnings or real forest fire emergencies.

Keywords: Forest fire; Homography; Thermography; Rate of spread

1. Introduction

Rate of spread (ROS) is one of the most significant parameters in the description of forest fire behaviour, since it is directly related to fire intensity [1] and flame front geometry [2] and, thus, to the levels of danger associated with its propagation. In forest fire emergency management, knowing this parameter is crucial. Therefore, a great deal of scientific research is devoted to this field, which centres either on mathematical modelling [3] or on experimental assessment for the validation of models.

Various methods can be used to experimentally assess the ROS, and their success depends on the extent to which straightforward implementation, reliability, precision, feasibility of extrapolation to other experimental scenarios (small scale, field scale and real scale) and cost come together.

Historically, very simple conceptual procedures have been used to experimentally determine the ROS. These are based on calculating the time that the front takes to cover certain known distances, by means of the integration of several warning systems within the experimental scenario. Thus, a known linear arrangement of warning elements of an acoustic, mechanical, electrical or simply visual nature, which go off and give a signal during the passage of a fire front, makes it easy to calculate the ROS immediately. One of the most commonly used systems consists in the equidistant positioning of cotton or nylon threads perpendicular to the fire spread direction, in such a way that when the fire spreads it burns through them along its path. By recording the moment at which each thread breaks and by knowing its position, the rate of spread is calculated as the derivative of the distance in relation to time. This system is applicable to experimental fires on a laboratory scale, but it is difficult to extrapolate to field experiments, as it is restricted to those areas in which the features of the landscape and the fuel cover allow the threads to be fixed and observed. It is often difficult to obtain wholly reliable measurements of the ROS because of impaired visibility due to such factors as smoke formation, safety distances and vegetation structure. Moreover, this method only

*Corresponding author. Tel.: +34 93 401 17 36; fax: +34 93 401 71 50.
E-mail address: eulalia.planas@upc.edu (E. Planas).

0379-7112/$ - see front matter © 2006 Elsevier Ltd. All rights reserved.
doi:10.1016/j.firesaf.2006.05.009

Figure B.3 First page of the work: Pastor E, Àgueda A, Andrade-Cetto J, Muñoz M, Pérez Y, Planas E. Computing the rate of spread of linear flame fronts by thermal image processing. Fire Safety J 2006;41:569-79.